2017

STRIDE | Southeastern Transportation Research, Innovation, Development and Education Center

Final Report

Signal Timing Optimization with Consideration of Environmental and Safety Impacts, Part A

(Project # 2013-022S)

Authors: Mohhammed Hadi, Ph.D., Florida International University; Lily Elefteriadou, Ph.D., University of Florida, and students: Xuanwu Chen, Tao Wang, and Yan Xiao

June 2017

U.S. DOT DISCLAIMER

Acknowledgment of Sponsorship

This work was sponsored by a grant from the Southeastern Transportation Research, Innovation, Development, and Education Center (STRIDE) at the University of Florida. The STRIDE center is funded through the U.S. Department of Transportation's University Transportation Centers Program. Additional financial support was provided by the Florida Department of Transportation. The authors would like to thank STRIDE and FDOT for their support of university-based research in transportation, and especially for the funding provided in support of this project.

STRIDE Project 2013-022S

Signal Timing Optimization with Consideration of Environmental and Safety Impacts
Part A: Estimation of Environmental Impacts

Mohammed Hadi, Ph.D., P.E.; Florida International University
Lily Elefteriadou, Ph.D.; University of Florida
Xuanwu Chen, Ph.D., Tao Wang, Ph.D., and Yan Xiao, Ph.D., PE; Florida International University

Southeastern Transportation Research, Innovation, Development, and Education Center
Gainesville, FL
June 2017
http://www.stride.ce.ufl.edu

TABLE OF CONTENT

LIST OF TABLES

TABLE PAGE

LIST OF FIGURES

FIGURE PAGE

ABSTRACT

This study aims at developing models that relate pollutant emissions to macroscopic mobility measures, which can be estimated using macroscopic/mesoscopic analysis tools or can be measured using sensors in the real world. Such models can be used in signal optimization tools to allow the optimization of signal timings based on emission, combined with other measures. These models can also be used as part of sketch planning tools, analysis models, and real-world data analytical tools to allow for the assessment of environmental impacts of advanced transportation and demand management (ATDM) strategies.

Two sets of emission estimation models were developed in this study, one based on microscopic simulation and one based on real-world trajectory data collected as part of the Federal Highway Administration Next Generation Simulation (NGSIM) program data. Both simulated and real-world trajectory data were input to the MOtor Vehicle Emission Simulator model (MOVES) operating mode distribution analysis procedure to calculate emissions. Macroscopic mobility measures were also extracted from these trajectory data and related to the emission outputs from MOVES using regression analyses. It is found that the significant factors in the regression models to estimate pollutant emissions are Vehicle-Miles Traveled (VMT), total vehicle delay, stop delays, and/or number of stops, depending on the estimated pollutants, when using simulation model trajectory data. The significant factors when using NGSIM trajectory data are VMT, average speed, and number of stops. The developed emission models were tested using a simulated network as well as real-world roadway sections. The results show that the NGSIM-data-based model perform relatively better than the simulation-based models.

As an application of the developed emission estimation models, a method is further developed to extract macroscopic mobility measures from automated vehicle identification (AVI) or Automatic Vehicle Location (AVL) data, such as Inirx and Wi-Fi data, and use them as input to emission models to estimate the pollutant emissions at a signalized intersection. This approach can be used by transportation agencies to monitor environmental impacts based on real-world data in data analytic tools.

EXECUTIVE SUMMARY

At the present time, the main performance measures used in the assessment and optimization of signal timing have been mobility measures such as travel time, delays, stops, queue lengths, and throughput with limited consideration of environmental and safety impacts. Consideration of these measures is important, particularly with the increased emphasis on performance measurement and management of transportation systems. Performance measurement requires the consideration of a wide array of measures; which should be mapped to agency goals and objectives. This STRIDE 2013-022S research project has been conducted to evaluate, develop, and recommend signal timing methods for simultaneous assessment of environmental and safety performance impacts, in combination with mobility measures.

As a part of the project deliverables, this document focuses on pollutant emission estimation. This includes developing models that relate pollutant emissions to macroscopic mobility measures, which can be estimated using macroscopic/mesoscopic analysis tools or can be measured using sensors in the real world. Such models can be used in signal optimization tools to allow the optimization of signal timings based on emission, combined with other measures. These models can also be used as part of sketch planning tools, analysis models, and real-world data analytical tools to allow for the assessment of environmental impacts of advanced transportation and demand management (ATDM) strategies.

EMISSION ESTIMATION MODEL DEVELOPMENT

This study first derived emission and energy consumption estimation models based on emission estimates from the MOVES operating mode distribution analysis procedure and performance measures from an artificial microscopic simulation network. The MOVES operating mode distribution analysis procedure is believed to be the most accurate tool among the MOVES

procedures for emissions estimation and can use vehicle trajectories from simulation or real-world as input. Models with various combinations of independent variables were tested, and the study selected two models as the final models. The first model is based on the combination of vehicle miles traveled (VMT) and the total vehicle delays. The second model is based on a combination of VMT, vehicle delays, stop delays, and number of stops.

The two models were tested using a simulated real-world arterial in microscopic simulation. Both of them showed acceptable performance for most of the investigated cases. However, it is recognized that the both the model development and evaluation were based on microscopic simulation. Questions have been raised about the validity of the vehicle trajectories from microscopic simulation models, particularly as they relate to vehicle acceleration and deceleration. Thus, the models developed based on simulation were tested utilizing real-world data collected as part of the Next Generation Simulation (NGSIM) program funded by the Federal Highway Administration (FHWA). It was found that in this testing, the developed model with VMT and total vehicle delays as independent variables produced reasonable estimations and the percentage errors were within acceptable ranges. However, the second model, which is based on VMT, total vehicle delays, total stop delays, and number of stops, did not perform well. This could be because this second model require estimating variables that requires trajectories with accurate acceleration and deceleration estimates. The quality of the trajectories in microscopic simulation is expected to affect the accuracy of the second model.

A further effort was made to utilize the real-world trajectory data (NGSIM) data to develop emission and energy consumption estimation models utilizing a similar procedure as that used for simulation-based models, mentioned above. The independent variables included in the final estimation models are VMT, average speed, and number of stops. The performance of the NGSIM-

data-based estimation models were compared to the simulation-based estimation models and the emission estimation models developed by University of South Florida (USF) for a use-case real-world roadway segments. The comparison results indicate that the NGSIM data-based models perform better than the other models.

EMISSION ESTIMATION BASED ON VEHICLE DATA

The models developed as described in the previous section can be used as part of analysis, modeling, and signal optimization tools; as is described in Part B document of this final report. Another possible application is to use these models as part of data analytic tools, if data can be used to estimate the independent variables of the models, which are macroscopic measures of traffic flow. This study develop and evaluate a method to estimate the required macroscopic measures (that is, VMT, average speed, and number of stops) from real-world data and use them in emission estimation. The use of two types of real-world data were examined in this study: third party vendor automatic vehicle location (AVL) data (from Inrix data) and automatic vehicle identification (AVI) data based on Wi-Fi technology combined with historical turning movement counts. The average speed was obtained based on individual vehicle travel speed estimated from Inrix trajectory data or Wi-Fi matched vehicle data. The number of stops was retrieved by comparing the vehicle arriving time at the study intersection with signal timing data. The developed method was applied to the intersection located at SW 8th St. and SW 107th Ave in Miami, FL and the emission estimation results show that both Inrix and Wi-Fi data produce similar estimates of emissions. The developed method provides a new approach for transportation agencies to assess environmental impacts based on real-world data.

CHAPTER 1

INTRODUCTION

BACKGROUND

Transportation agencies are increasingly realizing the importance of performance measurement and management. This realization has become even greater with the signing of the Moving Ahead for Progress in the 21st Century Act (MAP-21) legislation on July 2012. MAP-21 creates a streamlined, performance-based, and multimodal program to address various issues facing the transportation system. Thus, performance measures will become even more important in the coming years.

Signal control is expected to impact various performance measures. For example, Skabardonis (2011) analyzed the impacts of signal control improvements, utilizing results from a large number of real-world projects. That study found that the average measured savings for coordinated signal control were a 7.4 percent reduction in travel time, 16.5 percent reduction in delay, and a 17 percent reduction in stops. However, the main performance measures used in assessment and optimization of signal timing continues to be travel time and/or delays, with limited considerations of environmental and safety measures. Existing signal timing control software does not allow the user to select signal timing parameters based on these impacts. The consideration of such additional measures is important, particularly with the increased emphasis on performance measurement and management of transportation systems. This requires consideration of a wide array of measures mapped on to agency goals and objectives, and to identify issues associated with the region or specific system under consideration.

The Highway Safety Manual reports that the impacts of most signal timing adjustments on crashes are unknown. A review of literature conducted for this project has identified only a few studies on the subject. For example, previous studies on safety performance have confirmed that clearance interval length has impacts on red-light running and dilemma zones (Zimmerman and Bonneson, 2005). Also regarding dilemma zones, it has been suggested that signal optimization tools can evaluate and optimize the number of "dilemma zone" vehicles, presumably based on whether large platoons of vehicles were expected to arrive during the yellow interval. Another study found that traffic signal coordination can reduce the number of crashes by 23% (Moore and Lowrie, 1976).

Recent work appears to have focused on utilizing surrogate performance measures to assess safety impacts. Sabra et al. (2010) examined the relationship between signal timing and safety surrogate measures, including the frequency of rear-end, angle, and lane-change conflicts. This analysis was performed using the Surrogate Safety Assessment Methodology (SSAM), developed for the Federal Highway Administration (FHWA) combined with the Synchro and VISSIM tools. Results indicated that the demand to capacity ratio, cycle length, left-turn phase type, phase sequence, detector extension, and offsets have a significant influence on safety. Interestingly, the impacts of phase-change interval on safety were found to be marginal. Sabra et al. (2010) also proposed a multi-objective optimization to adjust signal timing parameters in a real-time adaptive system, with the purpose of minimizing the number of conflicts, as well as traffic delays. Case studies for two simple intersections were conducted. Stevanovic et al. (2012) commented that the use of Synchro to optimize signal timing in a Sabra et al. (2010) may not produce the best signal timing when is evaluated in VISSIM. Therefore, their study applied the SSAM, VISSIM, and VISSIM-based Genetic Algorithm (GA) in signal timings optimization to optimize signal timing

parameters, with the goal of minimizing the total number of conflicts. These results indicated that there is a trade-off between safety and efficiency of the traffic stream.

On the other hand, a limited number of studies on environmental impacts of signal control can be found in the literature. Pandian et al. (2009) reported that fleet speed, acceleration/deceleration speed, queuing time, queue length, traffic flow rate, traffic composition, and ambient conditions greatly affect vehicle exhaust emissions near intersections. Coensel et al. (2012) investigated the impacts of traffic signal coordination, traffic intensity, and signal parameters on noise and air pollutant emissions. This research used the Paramics microsimulation model, combined with Imagine (software for estimation of noise impacts) and VERSIT+ (software for estimating air pollutants). These results showed that high-quality platoon progression can reduce air pollutants by 10-40% in some scenarios. Green splits and traffic intensity were shown to have the largest impacts on emissions, but cycle lengths were found to not significantly influence emissions. Mitra and Pravallika (2013) developed an integrated optimization model to study the relationship between congestion levels, emissions, and traffic compositions. Synchro was used for estimating mobility measures, and the MOBILE module was applied for emissions estimation. Guo and Zhang (2013) also used VISSIM to explore relationships between intersection mobility and environmental impacts. Li et al. (2004) defined a performance index of signal timing as a function of vehicle delay, fuel consumption, and emissions at intersections. Optimization was conducted to minimize this performance index, finding the optimal cycle lengths and green times, but constrained by minimum green times for pedestrians to cross.

Yang and Ju (2011) developed a multi-objective traffic signal optimization method using a cell transmission model. The objective was to minimize total delay, fuel consumption, and vehicle exhaust emissions. Zhang et al. (2013) also used a cell transmission model in the

optimization of signal timing including cycle length, offsets, green splits and phase sequences, with a bi-objective function to minimize traffic delay and emissions. A cell-based, Gaussian plume air dispersion model was used to estimate emissions.

Skabardonis et al. (2012) proposed an analytical model to estimate vehicle activity along signalized arterials. Required inputs for this model included only loop detector data and signal settings. The output of this model is an estimation of time spent per driving mode, which can then be used to estimate vehicle emissions. The study results showed that optimized signal offsets can significantly reduce emissions. Liao (1995) proposed a signal optimization model based on the Analytical Fuel Consumption Model (AFCM), which accounts for fuel consumption in three components: idle mode, acceleration from stop to pass the stop line, and stochastic effects of vehicle movements. Comparisons against TRANSYT-7F and Synchro showed that the proposed model was more effective in producing signal timing that can reduce fuel consumption and CO_2 emissions.

PROBLEM STATEMENT

The above review indicates that a number of studies have been conducted to incorporate fuel consumption and emissions, and to a significantly lesser degree safety, in signal timing analysis and optimization. These studies vary in terms of their objective functions, underlying models, and optimized signal timing parameters. No studies have considered a signal timing optimization that would simultaneously address mobility, fuel consumption, emissions and crashes. Despite the availability of some studies on these subjects, no guidelines and tools are available to traffic engineers, to assist in their evaluation and optimization of signal control based on these measures.

RESEARCH GOAL AND OJBECTIVES

The goal of this research project is to evaluate, develop, and recommend signal timing methods for simultaneous assessment of environmental and safety performance impacts, in combination with mobility measures. The specific objectives are

1. to evaluate state-of-knowledge with regard to signal timing impacts on emissions and safety and the methods used in assessing these impacts,
2. to examine the implementation of such methods in existing signal timing evaluation and selection,
3. to assess trade-offs between the different measures (mobility, emission, and safety) when selecting signal timing plans,
4. to provide recommendations regarding the utilization of environmental and safety performance measures in assessing and selecting signal timing plans, and
5. to incorporate and test these recommendations in the assessment and optimization of signal timing based on evaluation and optimization tools and based on real-world data.

As a part of this project, this document (Part A of the final report of this project) focuses on developing emission estimation models based on macroscopic mobility measures and estimation these measures based on analysis data and real-world data.

DOCUMENT ORGANIZATION

This report documents the research efforts that are related to the incorporation of emission and fuel consumption impacts in signal timing optimization. It is organized into four chapters. Chapter 1 introduces the research background, describes the problems to be solved, and sets the goal and objectives to be achieved. Chapter 2 presents an extensive literature review of emission

estimation. Chapter 3 discusses the development of emission estimation models based on simulation and real-world data. Chapter 4 demonstrates the emission estimation using real-world data based on macroscopic data as part of performance measurement efforts.

CHAPTER 2

LITERATURE REVIEW

This chapter presents a detailed review of the state-of-the-art of the estimation of emission impacts that are associated with signal timing optimization.

EMISSION ESTIMATION

Few studies have investigated the relationships between signal timing settings and their environmental impacts. Environmental impacts caused by traffic signals have gained more attentions in the 21st century with the efforts mainly focusing on fuel consumption and/or pollutant emissions, while a very limited number of studies investigated the effects of traffic signal on noise pollution (De Coensel, et al., 2012; Ellenberg and Bedeaux, 1999; Desarnaulds et al., 2004).

Only a small portion of the relevant literatures is based on field studies. For example, Unal et al. (2003) conducted an empirical analysis before and after signal timing and coordination changes that was done using on-road tailpipe emission measurements and found measurable reductions in emission with signal coordination. Midenet and his research team applied a multi-camera system that can automatically calculates vehicle idle time and stop rates per vehicle trip (Midenet et al., 2004). While calibrating the emission profiles measured on test benches, a studied adaptive real-time control strategy, CRONOS, showed a 4% reduction in CO_2 emission in the peak hours. Rakha and his co-authors used Global Positioning System (GPS) equipped vehicles to collect second-by-second speed measurements and calculate delays, energy consumptions, emissions, and safety impacts based on these measurements (Rakha et al., 2000). Congestion was found to be reduced by increasing the mainline average speed by 6 percent with coordinating traffic

signal timings across jurisdictional boundaries. However, CO emissions was found to increase by 1.2 percent.

Due to the difficulties in the collection of emission data in the field, most of the studies that relate traffic signal timing to environmental impacts have been based on modeling. The majority of the scholars seek answers by utilizing various models to estimate emission, which can be categorized into analytical models and microscopic simulation-based models.

Relationships between vehicle emissions and/or fuel consumptions and various traffic mobility performance measures such as speed, travel time, delay, and stops were developed utilizing analytical models. For instance, Liao and Machemehl (1996) proposed an analytical model, referred to as the Analytical Fuel Consumption Model (AFCM), to estimate fuel consumptions at signalized intersections and concluded that there is a significant difference between the optimal cycle length for fuel consumptions and that for delays. The paper indicated that optimization based on fuel consumption usually leads to longer cycle lengths compared to delay minimization. Ahn (1998) developed a series of multivariable nonlinear regression models and artificial neural network models for vehicle emissions and fuel consumptions utilizing the Oak Ridge National Laboratory (ORNL) data. Speeds and acceleration rates were used in these models in order to estimate emissions and fuel consumptions. These models were applied in the INTEGRATION microscopic simulation model (Rakha et al., 2000). Reductions in fuel consumptions and emission rates were found when good real-time signal coordination was implemented.

Frey et al. (2001) developed a macroscopic traffic-flow-based approach and a microscopic traffic-and-engine-based approach to estimate emission based on on-road tailpipe emission measurements. Li and his colleague optimized signal cycle length and green time based on a

Performance Index (PI) function to reduce vehicle delays, fuel consumption, and emission at signalized intersections (Li et al., 2004). Applying pre-defined weights (4:3:3) for the three measurements (average delay, fuel consumption, and exhaust emission) in the PI function, the researchers found that there is an optimal cycle length when the signal cycle length increases from 20 to 200 seconds. Skabardonis et al. (2012) estimated the emissions at saturated signalized intersections by identifying the vehicle activity distribution, i.e. the distribution of the time spent per driving mode that is used as an input to a developed analytical model. The model utilizes system loop detectors and signal settings as inputs. The paper also proved that coordinated signal control significantly reduces vehicle emissions on the test arterial. Mitra and Pravallika (2009) observed that LOS B is the most favorable traffic flow conditions for minimizing the impacts of fuel consumption, emission, and delays at the intersection. Although not directly related to traffic signal timing, Kim and Choi (2013) identified two critical acceleration rates to categorize aggressive acceleration and extreme aggressive acceleration. Emissions were found to increase rapidly once the acceleration rates pass these two critical values respectively.

Other researchers use microscopic simulation-based models to evaluate emissions and/or fuel consumption at intersections. A study analyzed the impacts of signal control improvements achieved by optimizing signal timings in TRANSYT-7F, a macro-simulation-based signal optimization model, and drew a conclusion that the average measured savings for coordinated signal control are a 7.4 percent reduction in travel time, 16.5 percent reduction in delay, and a 17 percent reduction in stops (Skabardonis, 2011). Stevanovic et al. (2009) optimized traffic signal to minimize fuel consumption in a micro-simulation environment that integrated VISSIM, the Comprehensive Modal Emission Model (CMEM), and a VISSIM-based Genetic Algorithm Optimization of Signal Timings (VISGAOST). The study found that approximately 1% to 1.5%

of fuel consumption can be reduced compared to the traditional traffic signal optimization based on delay. Park et al. (2009) evaluated fuel consumptions and emissions at signalized intersections using the Virginia Tech Microscopic energy and emission model (VT-Micro) based on the individual vehicular trajectory data generated from the CORSIM micro-simulation model. Optimizations based on reducing queue time and reducing fuel consumption were compared and apparent trade-offs between the two objectives were noticed. Coensel and Botteldooren (2011) found that green waves can reduce air pollutant emissions by 10% to 40%, depending on traffic flow and signal timing settings. Traffic intensity and green split were found to have the largest influence on emissions. Another study used an activity-specific model approach, referred to as the Mobile Emission Assessment System for Urban and Regional Evaluation (MEASURE), to estimate the air quality benefits from improved signal coordination (Hallmark et al., 2000). The authors concluded that the reduction in Carbon Monoxide (CO) is more significant when estimating the emissions using MEASURE compared to the EPA's vehicle emission modeling software at that time (MOBILE5a, which in now replaced by EPA's MOVES). Liao (2013) stated that fuel-based signal optimization resulted in a more significant reduction in fuel consumption and CO2 emissions compared to the traditional delay-based signal optimization. Grumert et al. (2013) showed that the application of variable speed limit system leads to the reduction of both the fuel consumptions and emissions based on simulation results using a combination of the Simulation of Urban MObility (SUMO) tool and CMEM tool.

Simulation models utilization in estimating emission have attracted even more attention since the development of MOtor Vehicle Emission Simulator model (MOVES) by the EPA, because MOVES is capable of assessing emissions based on individual vehicle data, which can be obtained from simulation model outputs. MOVES was first released in 2004 and designated as the

official model for estimating air pollution emissions from cars, trucks, and motorcycles since 2010 in replacement of the MOBILE6.2 motor vehicle emission factor model.

MOVES has three scales of emission estimation: National, County, and Project scales. The most detailed level of analysis in MOVES estimates vehicle emissions by analyzing the second-by-second speed profiles of vehicle trajectories obtained from real-world data or micro-simulation models. Scholars and practitioners investigated the accuracy of the MOVES and interfaced it with various simulation models. Song et al. (2013) compared different car-following models built in various micro-simulation software packages. They identified the inaccuracies in the estimation of the vehicle specific power (VSP) distribution which can be input into MOVES. Chamberlin et al. (2012) compared EPA's Operating Mode Distribution Generator (OMDG) to provide inputs to MOVES with the Total On-Board Tailpipe Emissions Measurement System (TOTEMS) and showed that the OMDG performs better in the condition of no to low grade and high congestion level. Zhao and Sadek (2013) found that the sampling method is better than the aggregation methods in sampling average vehicle speed profiles for MOVES inputs. They stated that a few model runs with fewer sampled vehicles outperformed a method that uses a single model run with more samples.

Guo (2013) estimated the emissions generated at a single intersection utilizing a combination of SYNCHRO, VISSIM, and MOVES, and demonstrated that the CO2 and PM emissions have a positive linear relationship with delays; while NOx, SO2, and CO could be negatively correlated with delays in congested conditions. Guo and Zhang (2014) later investigated the relationship between mobility measures (i.e., total delay, stops per vehicle, and average speed) and environmental factors (i.e., CO2, CO, NOx, PM10, PM25, SO2, and Fuel) based on VISSIM microsimulation utilizingMultivariate Multiple Linear Regression (MMLR) analysis. Ghafghazi

and Hatzopoulou (2014) analyzed a traffic network with 576 intersections with VISUM, VISSIM, and MOVES. The research revealed that isolated traffic-calming measures actually induce higher emissions. Lin et al. (2011) integrated a mesoscopic simulation-based dynamic traffic assignment model, DynusT, and MOVES at the project-level. A Strategic Highway Research Program 2 (SHRP2) report suggested that signal control management is effective on reducing greenhouse gas (Meyer et al., 2013). This report provides a guideline to estimate greenhouse gas (GHG) emissions using MOVES and suggests that traffic signal timing and coordination should be considered as one of the potential GHG emissions reduction measures in long-range transportation planning, programming, corridor planning, and the National Environmental Policy Act (NEPA) project development and permitting process.

SUMMARY

Microscopic simulation models generally require more effort and expertise to develop and calibrate. Thus, it is useful to develop better analytical models to estimate emission that can be incorporated as part of traffic analysis in macroscopic and mesoscopic analysis and simulation, when optimizing signal timing based on emission, and when estimating emission based on real-world macroscopic traffic measurements collected using traffic monitoring systems. The development of MOVES and its release by EPA in 2010 provides the opportunity to develop detailed analytical models based on individual vehicle measures, as is done in this study.

CHAPTER 3

EMISSION ESTIMATION MODEL DEVELOPMENT

INTRODUCTION

In this study, analytical models were developed to estimate vehicle emissions at one and/or multiple intersections along an arterial street. The developed analytical models relate mobility performance measures to emissions based on the results of a microscopic simulation model, combined with the MOVES operating mode distribution approach. Since the most detailed level of analysis in MOVES is able to estimate emissions by analyzing the second-by-second vehicle speed profiles, vehicle trajectories that can be output from microscopic simulation models were extracted and input to MOVES in order to obtain the most accurate emission estimation.

EPA MOVES

As stated in Chapter 2, the EPA's MOVES model estimates emissions at three different scales: National, County, and Project scales. The National and County scales are usually applied to a large area such as a state or a county, but are not appropriate for the analysis of a small network, such as a corridor. The project scale in MOVES is more appropriate for smaller networks (Environmental Protection Agency, 2012). The project level is the finest level of vehicle emission estimation in MOVES. It has three different estimation methods: the average speed approach, drive schedule approach, and operating mode distribution approach. The average speed approach is the simplest of the three and is based on the average speed of the vehicles and the vehicle miles traveled by vehicle type. The drive schedule method uses second-by-second speed profiles of vehicles as an input to estimate emissions. The operating mode distribution approach estimates

emissions based on the Vehicle-Specific Power (VSP), vehicle speed, and vehicle acceleration. VSP calculation is in the form of the vehicle's tractive power $P_{trac.t}$ normalized to its weight m_{tonne} (Koupal et al., 2005). The operating mode distribution approach can be complex, and it consists of many factors, such as a third-order polynomial in speed, aerodynamic drag coefficient, cross-sectional frontal area of the vehicle, density of air, and so on. In MOVES, a simplified form of the VSP calculation is used as follows (Environmental Protection Agency, 2010).

$$VSP = \left(\frac{A}{M}\right) \cdot v + \left(\frac{B}{M}\right) \cdot v^2 + \left(\frac{C}{M}\right) \cdot v^3 + (a + g \cdot \sin\theta) \cdot v \quad (1)$$

where

A = the rolling resistance coefficient, *0.156461* kw·sec/m for passenger car;

B = the rotational resistance coefficient, *0.002002* kw·sec^2/m^2 for passenger car;

C = the aerodynamic drag coefficient, *0.000493* kw·sec^3/m^3 for passenger car;

M = fixed mass factor for the source type, *1.4788* metric ton for passenger car;

v = vehicle velocity (m/sec);

a = vehicle acceleration (m/sec^2);

g = acceleration due to gravity (9.8 m/sec^2); and

θ = road grade (fractional).

The model's coefficients can be obtained from Table 7-3 in the EPA's technical report (Environmental Protection Agency, 2010). VSP can be calculated based on real-world or microscopic simulation-generated vehicle records, including vehicle velocity, acceleration rate, and road grade at every time step during the study period for each vehicle. The combination of VSP, vehicle velocity, and vehicle acceleration can be used to categorize each vehicle at every time step into a different operating mode. This process involves assigning an operating mode identification number (OpModeID) to that vehicle at that time step based on the criteria tabulated

in the MOVES documentation (Environmental Protection Agency, 2005; TranSystems, and E.H. Pechan & Associates, Inc., 2012). The distribution of each operating mode is therefore calculated as the frequency of the corresponding OpModeID divided by the total number of vehicle records. These percentages can then be input into MOVES to estimate vehicle emissions.

Among the three approaches used at the MOVES project scale, the operating mode distribution can be considered as the basis for emission estimation, even when using the other two approaches. In the average speed approach, MOVES assigns a default drive schedule that includes a second-by-second speed profile to the input average speed and converts the default drive schedule to the corresponding operating mode distribution. In the drive schedule approach, MOVES converts the second-by-second profile to the operating mode distribution internally and estimates emission based on that distribution. In other words, MOVES estimates emission using the operating mode distribution in all three project scale approaches. The operating mode distribution approach is also believed to be the most accurate and comprehensive approach in the MOVES emission estimation. The average speed approach is too general to capture details, such as vehicle acceleration and deceleration, which have high impacts on emission. The drive schedule approach utilizes a second-by-second speed profile to represent detailed vehicle operations. However, the input drive schedule can only represent one or a limited number of similarly operating vehicles that disregard the variations in vehicle operating parameters. The operating mode distribution approach is the only MOVES approach that consider each individual vehicle performance in the network in an efficient manner.

METHODOLOGY

The models developed and evaluated in this study uses the project-level estimation in MOVES. The national scale and county scale are not appropriate for deriving the models of this study due to their low levels of details. Among the three project level approaches of MOVES, the operating mode distribution approach was selected because it accounts for the detailed vehicle operations for all vehicles in the network, as previously mentioned. Figure 1 displays a flow chart of the steps in developing the analytical models.

As shown in Figure 1, Step 1 was to run a microscopic simulation tool with different scenarios of a simple, artificial network. VISSIM version 6.00-16 was used for this purpose. The necessary information to quantify the operating mode distributions was then extracted from VISSIM vehicle records, including vehicle velocity and vehicle acceleration. The operating mode distributions were calculated using Equation 1 presented earlier and used as inputs to MOVES. In order to develop models that relate emission to macroscopic mobility performance measures, these measures were also extracted from the VISSIM runs and associated with the estimated vehicle emission (Step 2). Statistical relationships between vehicle pollutant emissions and different combinations of mobility performance measures were developed utilizing normal linear regression.

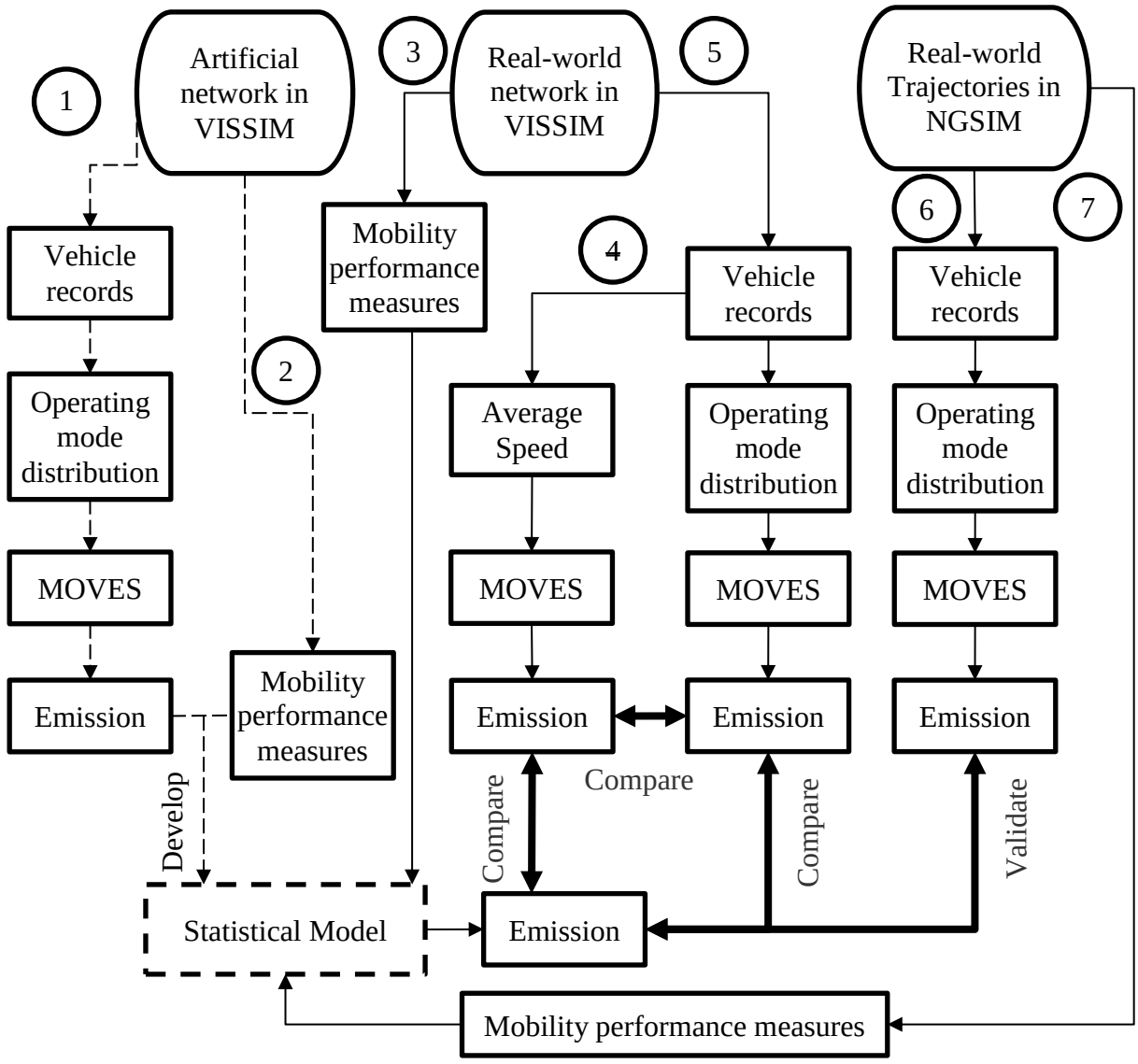

Figure 1. Steps of deriving the relationships between mobility performance measures and emissions.

The developed models were tested to examine their ability to estimate emission based on macroscopic traffic measures. The examination was done first, based on the simulation of a real-world urban arterial facility (Step 3, 4, and 5). The emission estimations for selected intersections on the facility using the developed statistical models were compared with the estimations that were

done using MOVES with inputs calculated from microscopic simulation results. Estimated emission quantities from three methods were compared, as follows: developed statistical models (Step 3), MOVES average speed approach (Step 4), and the MOVES operating mode distribution approach (Step 5). Next, the proposed statistical models were tested using real-world trajectories from the Next Generation Simulation (NGSIM) dataset (Steps 6 and 7). In this validation process, the estimated emission quantities based on the MOVES operating mode distribution approach using NGSIM trajectories (Step 6) were used to validate the emission estimations from the proposed statistical models with the independent macroscopic measures estimated based on the same NGSIM trajectories (Step 7).

The operating mode distributions used in this study were extracted automatically from VISSIM vehicle records and NGSIM dataset using a script written in Visual Basic®. The mathematical calculations and data processing were written in SQL (the Structured Query Language).

MODELS BASED ON SIMULATION

For the purpose of investigating the relationship between emission and other performance measures, a simple, artificial network with an isolated signalized intersection was simulated in VISSIM. The artificial network and example demands are shown in Figure 2. The geometry configuration of this artificial network is modified from the one presented in the report of Sabra et al. (2010). As can been seen from the figure, the east-west direction is the main street in this artificial network. The main street has two lanes and a 200-foot-long left-turn bay in each direction. The rightmost lanes on the main street are shared by the through and right-turning movements. The minor street which is in north-south direction has two lanes with no left-turn bay. The leftmost

lane on the minor street is shared by the through and left-turning movements and the rightmost lane is shared by the through and right-turning movements.

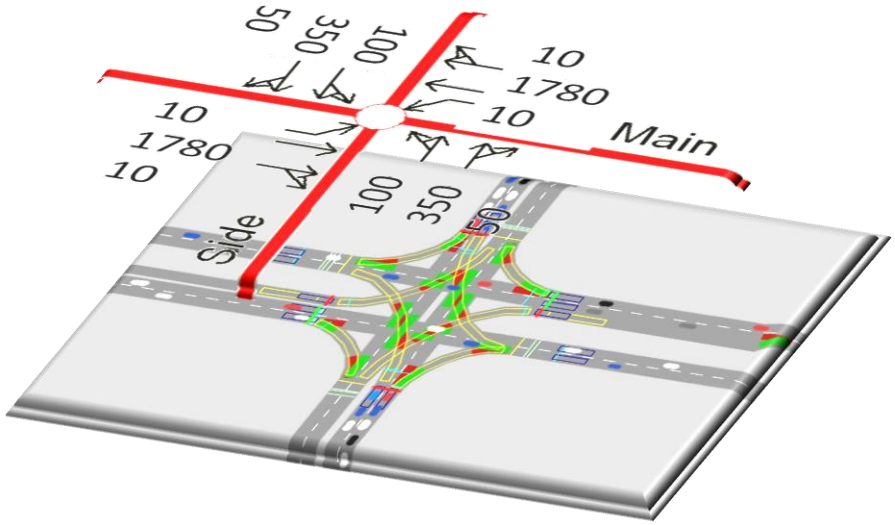

Figure 2. The base artificial network utilized in deriving the models.

The VISSIM model of the isolated signalized intersection was calibrated to the base saturation flow rate of 1,900 passenger cars per hour per lane according to the Highway Capacity Manual (HCM 2010) (Transportation Research Board of the National Academies, 2010). As a starting point, only passenger cars traveling along the eastbound through movement on the main street was studied. In order to eliminate the impacts from the left-turning and right-turning vehicles as well as to avoid the spill back from the intersection caused by those two movements, the left-turn and right-turn demands on the main street were kept zero. Table 1 summarizes the traffic scenarios which were utilized to generate different performance measures and vehicle profiles.

Table 1. Configurations of different traffic scenarios at the artificial isolated intersection.

Category	Information
Geometry	Main: Two lanes with left-turn bay and the right lane share right-turn and thought movement; 3200-ft link; 200-ft bay.
	Side: Two lanes; Left lane with shared left-turn and through; Right lane with shared right-turn and through; 3000-ft link.
Traffic volumes	Main: 600, 800. 1000, 1200, 1400, 1600, 1800, 1900, 2000 vph; though movement only.
	Side: 500 vph with 100 left-turn and 50 right-turn.
Speed	Main: 45 mph
	Side: 30 mph
	Side: Stop line. 30-ft loop detector. 3-s extension
Phasing	Main: Concurrent protected-only lead left-turns.
	Side: Concurrent phase with permitted-only left-turns.

Vehicle records and the associated mobility measures were extracted from VISSIM outputs. Other than the operating mode distributions and link inputs, the default values of the MOVES model were used in the analysis. The traffic signal in the artificial network is controlled by a pre-timed Ring-Barrier Controller (RBC) in VISSIM. Table 2 summarize the pre-time signal timing plans in different scenarios. Three signal timing plans with different cycle lengths were utilized. The combinations between various demands and the three signal timing plans are summarized in Table 3. Overall, twenty-five scenarios with different combinations of demands and signal timing plans were modeled in VISSIM.

Table 2. Signal timings in different traffic scenarios at the artificial isolated intersection.

Cycle Length	100 s	150 s	180 s
Main Street Left-turn Split	8	8	8
Main Street Through Split	60	80	100
Side Street Split	14	44	54
Yellow Interval	4	4	4
All Red Interval	2	2	2

Table 3. Combinations of various demands and signal timing plans at the artificial isolated intersection.

Cycle Length of Signal Timing Plans (s)	EB Demands (vph) / Corresponding v/c Ratio								
100	600	800	1000	1200	1400	1600	1800	1900	2000
	0.28	0.37	0.46	0.56	0.65	0.74	0.83	0.88	0.93
150	600	800	1000	1200	1400	1600	1800	1900	
	0.31	0.42	0.52	0.63	0.73	0.83	0.94	0.99	
180	600	800	1000	1200	1400	1600	1800	1900	
	0.30	0.40	0.50	0.60	0.70	0.80		0.95	

For each scenario, VISSIM was run five times with different seed numbers and the simulation results were input to MOVES. The average results of the five different MOVES runs for each scenario were employed as the final emission estimations. In this study, statistical models were developed to estimate vehicle pollutant emissions and energy consumption, including carbon monoxide (CO) in grams, oxides of nitrogen (NO_x) in grams, carbon dioxide equivalent (CO_2 Equivalent) in grams, and the total energy consumption in joules. In addition, the following mobility performance measures were extracted from the VISSIM model outputs for each scenario and used as potential independent variables in the regression models: total stop delays in hours (SD), total number of stops (S), total vehicle delays in hours (VD), volume-to-capacity ratio (VC), green occupancy ratio based on detectors at stop line (GOR), average queue length in feet (Q), number of stops in queue (QS), average speed in miles per hour (V), total vehicle miles traveled (VMT), and total vehicle hours traveled (VHT). It is worth mentioning that GOR, which is calculated as the stop bar detector occupancy divided by the duration time of the green phase, is proposed by Smaglik and others as a measure to quantify the operation of traffic signals (Smaglik et al., 2011).

Statistical relationships between performance measures and emission from various scenarios were developed using the R Software Package. It should be noted that not all of the above mobility performance measures will be available for use in estimating emission in all cases. For example, the available variables, when estimating emission based on real-world data, are different depending on the utilized traffic data collection technology. On the other hand, If the model is to be integrated with a macroscopic or mesoscopic model such as the HCM urban facility procedure, variables such as the green occupancy ratio are not available.

Multiple statistical models were tested to relate combinations of performance measures to emissions of pollutants, as listed above. A stepwise regression with a bidirectional elimination approach was utilized to find the best potential models for emission. The bidirectional elimination approach tests the model at each step by including and excluding different variables until no further improvement is possible. Other than the model selected by the stepwise regression, other regression models between emission and combinations of performance measures were also derived, and their coefficients were tested for significance. This was done because, as stated earlier, different applications may require models with different independent variables, depending on the availability of the information. The models that have both significant coefficients and high adjusted R-squared values are listed in Table 4 for CO emission, including the best model derived using the stepwise regression, which is model 1 in the table.

Table 4. Statistical Models between CO and Combinations of Performance Measures

Model Number	Variables*	Adjusted *R*-squared
1	INT[1], VMT[1], VD[3], S[1]	0.995
2	INT[1], VMT[1], VD[1]	0.992
3	VMT[1], VD[1]	0.991
4	INT[1], VMT[2], VD[1], SD[1], VHT[3]	0.999
5	INT[1], VMT[1], VD[1], SD[1]	0.999
6	VMT[1], VD[1], SD[1]	0.999
7	INT[2], VMT[1], VD[1], SD[1], S[1]	0.999
8	VMT[1], VD[1], SD[1], S[1]	0.999
9	VMT[1], VD[2], S[1], VD*S[1]	0.997
10	VMT[1], VD*VD[1], S[3]	0.997
11	INT[1], VMT[1], VD*VD[1]	0.995
12	VMT[1], VD*VD[1]	0.996

* INT = the intercepts in the statistical model.
VMT = total vehicle miles traveled (miles).
VD = total vehicle delays (hours).
S = number of stops.
VHT = total vehicle hours traveled (hours).
[1] independent variable is significant at 0.001 level.
[2] independent variable is significant at 0.01 level.
[3] independent variable is significant at 0.05 level.

As can be seen from Table 4, all qualified models have high adjusted R-squared values. In order to find the best models for emission estimation, these models were tested for accuracy using a real-world arterial network coded in VISSIM. The arterial network is shown in Figure 3, which is a segment of Glades Road in Boca Raton, Florida. The segment is about 2.5 miles long and has 9 signalized intersections. The base values for this accuracy assessment are assumed to be the emission estimations from a combination of microscopic simulation modeling and the MOVES operating mode distribution approach.

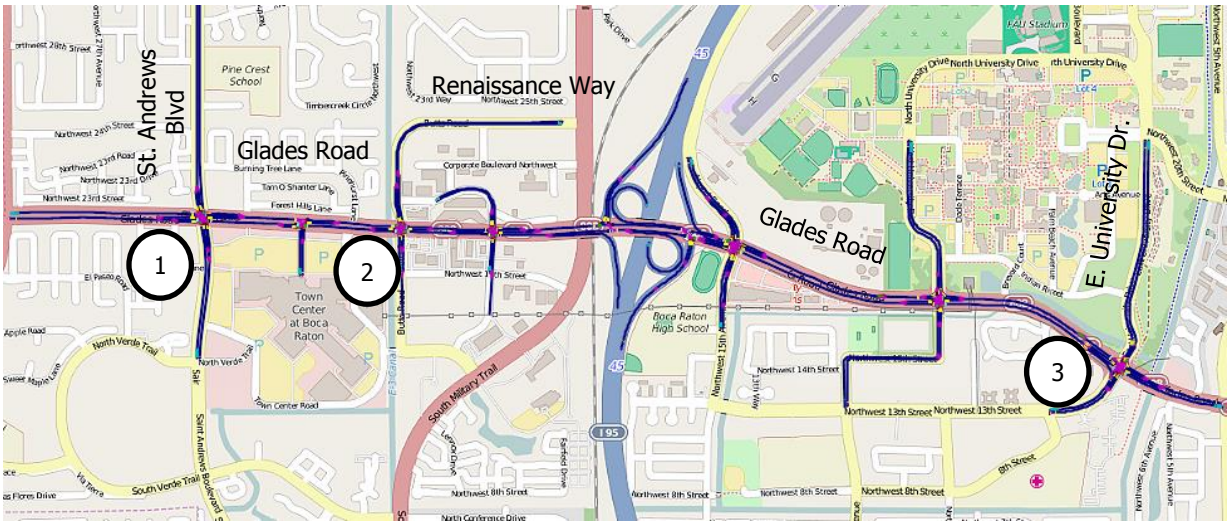

Figure 3. VISSIM network developed on Glades Road in Boca Raton, Florida.

The simulation model was calibrated and validated using the turning movement volume counts from point detectors in the AM peak period, as well as the travel times from the automatic vehicle identification technology (the SENSYS technology). This technology utilizes magnetometers installed immediately downstream of several critical intersections along the corridor. The estimated quantity of emissions based on the regression equations that relate emission to macroscopic mobility measures were compared to the MOVES estimates based on the operating mode distributions utilizing vehicle records extracted from the microscopic simulation model. Three intersections along the Glades Road were selected to test the proposed statistical model, as shown in Figure 3. The three intersections were: 1) the intersection of Glades Road at St. Andrews Boulevard; 2) the intersection of Glades Road at Renaissance Way; and 3) the intersection of Glades Road at East University Drive. These three intersections were selected as the SENSYS detection systems were installed there, which provides additional information for the study. The eastbound direction was analyzed in the evaluation since it is the peak direction in the AM peak period.

The Root Mean Square Error (RMSE) was calculated for all the candidate models in order to evaluate the performance of those models. For example, the best two models for carbon monoxide emission estimation with the least RMSE are represented in Equations 2 and 3.

$$CO = 2.504 \times VMT + 606.607 \times VD - 568.118 \times SD - 0.913 \times S \quad (2)$$

$$CO = 2.860 \times VMT + 179.560 \times VD \quad (3)$$

As can be interpreted from the equations, carbon monoxide emission increases as vehicle miles traveled increase. The CO emission also increases as vehicle delays increase. In contrast, the carbon monoxide decreases as the stopped delays or number of stops increases, given that the total vehicle delays are included in the equation. The relationships between vehicle miles traveled and vehicle delays in the above equations are logical and according to expectation. The relationship with the stopped delays, however, need to be explained as follows. As demonstrated by Frey and his co-authors; various types of emission, including CO emission, have higher emission rates during acceleration than in the cruise mode (Frey et al., 2002). The negative sign of the stopped delay in the equation is because the acceleration and deceleration effects are already accounted for by the total vehicle delays and the inclusion of stopped delay represent the portion of the delay that is in idle mode. For example, Equation 2 can be rewritten as Equation 4, where NSD indicates non-stopped delays or the time spent on acceleration/deceleration. The non-stopped delay (i.e., NSD) in Equation 4 indicates the time that vehicles spent on acceleration/deceleration, which is a part of the total vehicle delays in Equation 2. This equation indicates that most of the contributions to emission are due to acceleration/deceleration, and less contributions is due to stopped delays.

The negative sign for the number of stops indicates that for the same total delays, the lower number of vehicles that experience stops for the same non-stopped delays, the higher the level of emissions. This is logical, since this in turn indicates more frequent acceleration and deceleration per vehicle. In summary, Equation 2 indicates that emission is a function of VMT and acceleration/deceleration rate per vehicle. The two model forms in Equations 2 and 3 are recommended for use as the statistical models to estimate carbon monoxide emission at arterial signalized intersections, depending on the availability of the independent variable estimates.

$$CO = 2.504 \times VMT + 606.607 \times NSD + (606.607 - 568.118) \times SD - 0.913 \times S \quad (4)$$

The above discussion of regression model development focuses on carbon monoxide emission to illustrate the development of the models. The same forms seen in Equations 2 and 3 but with different parameters were derived to estimate other environmental impacts, including NO_x emission, CO_2 equivalent (CO_2equi) emission, and Total Energy Consumption (EC). The models derived for these environmental impacts are presented in Equation 5-10.

$$NO_x = 0.279 \times VMT + 27.89 \times VD - 22.76 \times SD - 0.034 \times S \quad (5)$$

$$NO_x = 0.293 \times VMT + 11.105 \times VD \quad (6)$$

$$CO_2\,equi = 252.994 \times VMT + 13442.284 \times VD - 9602.928 \times SD - 10.302 \times S \quad (7)$$

$$CO_2\ equi = 258.967 \times VMT + 6768.984 \times VD \quad (8)$$

$$EC = 3.512 \times 10^6 \times VMT + 1.867 \times 10^8 \times VD - 1.336 \times 10^8 \times SD - 1.433 \times 10^5 \times S \quad (9)$$

$$EC = 3.595 \times 10^6 \times VMT + 9.385 \times 10^7 \times VD \quad (10)$$

It is interesting to see that the signs of the variables in all models are the same, which confirms the trend previously observed when deriving the CO emission estimation model. In addition, the magnitudes of the coefficients in the total energy consumption (EC) models are much higher than those in the emission models, as the unit for energy consumption is joule and the unit for emissions is gram. The values of various coefficients in a model account for the relationship between the dependent and independent variables, as well as the scale of the independent variables. Different independent variables have different scales. Sensitivity analysis was conducted and it was determined that the dependent variable responded logically to changes in the independent variables.

The performance of the above models were tested for three intersections along Glades Road in Boca Raton, Florida, during the morning peak hour. The emissions estimated by the models versus those estimated based on microscopic model outputs were compared in terms of percentage errors as defined below.

$$Percentage\ Error = \frac{(Model\ Prediction - MOVES\ Estimation)}{MOVES\ Estimation} \times 100\% \quad (11)$$

The results of the comparison are presented in Figure 4(a) to Figure 4(d). The results indicate that the percentage errors of the models' estimations are within a reasonable range for various types of

vehicle emission and energy consumption. Both proposed models for each type of pollutant performed well. The model that considers VMT, vehicle delays, stop delays, and number of stops performed slightly better than the model with only VMT and vehicle delays.

An additional comparison was conducted between the performance of the developed models and the MOVES average speed approach for estimating emission using the MOVES operating mode approach as the basis. The errors in the CO and NO_x emission estimates based on the derived models are lower than those based on the average speed model. The developed statistical models' estimation of CO_2 equivalent emissions and total energy consumption were not better than the MOVES average speed approach, although the absolute values of the percentage errors of the estimates from the two approaches were within 10%.

The proposed models were also tested using a VISSIM model of three intersections of Glades Road with different signal timing settings. Figure 5 shows the percentage errors of the two proposed models and the MOVES average speed approach using the MOVES operating mode approach as the basis. In this scenario, coordination was disabled, and all intersections of Glades Road were running free-mode (i.e., fully-actuated) during the AM peak period. The two developed models performed better than the MOVES average speed approach for two of the three intersections: 1) the intersection of Glades Road at St. Andrews Boulevard, and 2) the intersection of Glades Road at East University Drive. At the intersection of Glades Road at Renaissance Way, the MOVES average speed approach had lower absolute values of the percentage errors when compared with the derived model based on the VMT and vehicle delays. Due to the short distance between that intersection and its upstream intersection in the eastbound direction, the vehicle delays increased dramatically when removing coordination. As a result, the model that is based on

only VMT and vehicle delays had high emission estimations. However, the model that includes the stop delays had more reasonable estimations of the emission and energy consumption.

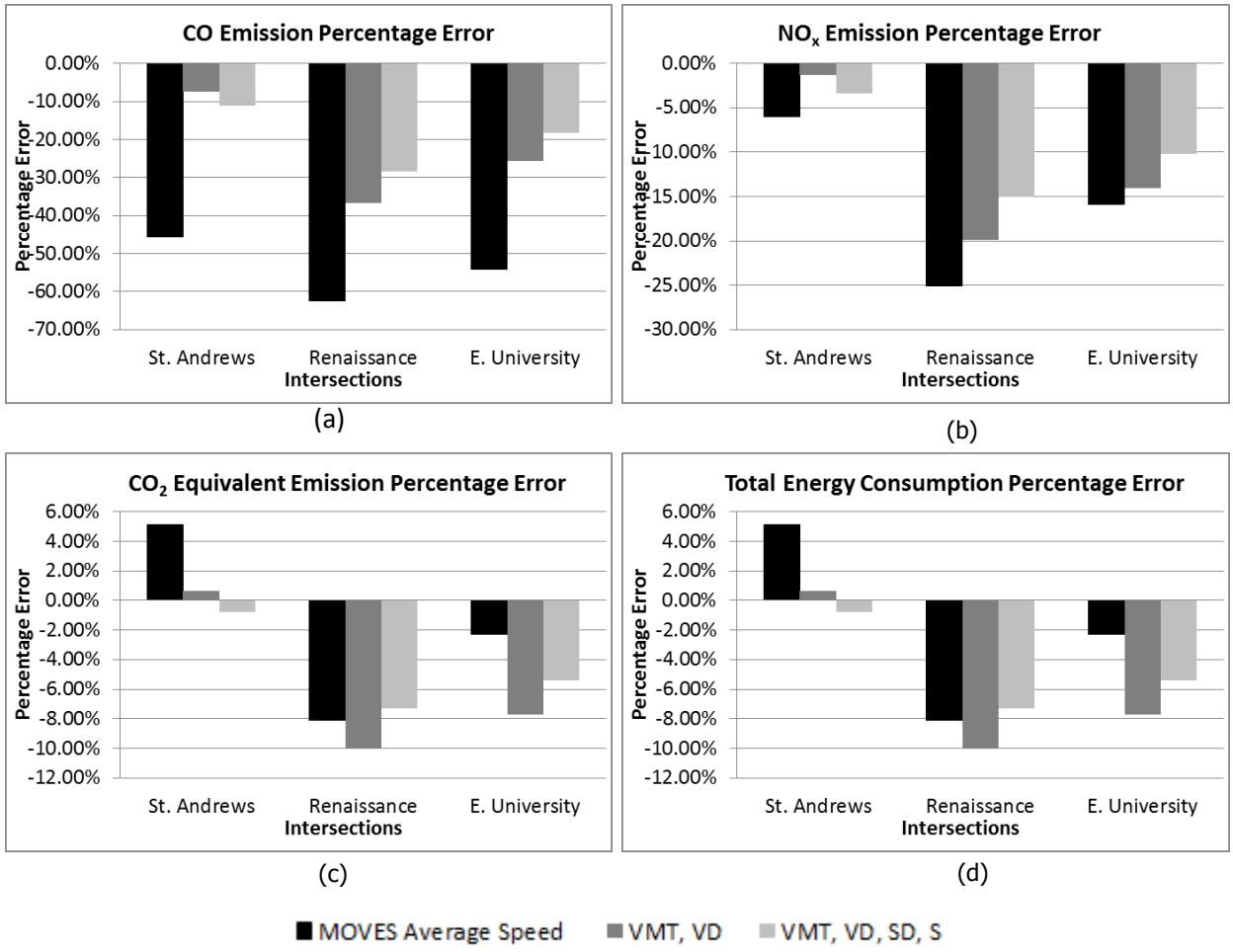

Figure 4. Percentage errors of different models for three intersections on Glades Road with coordination.

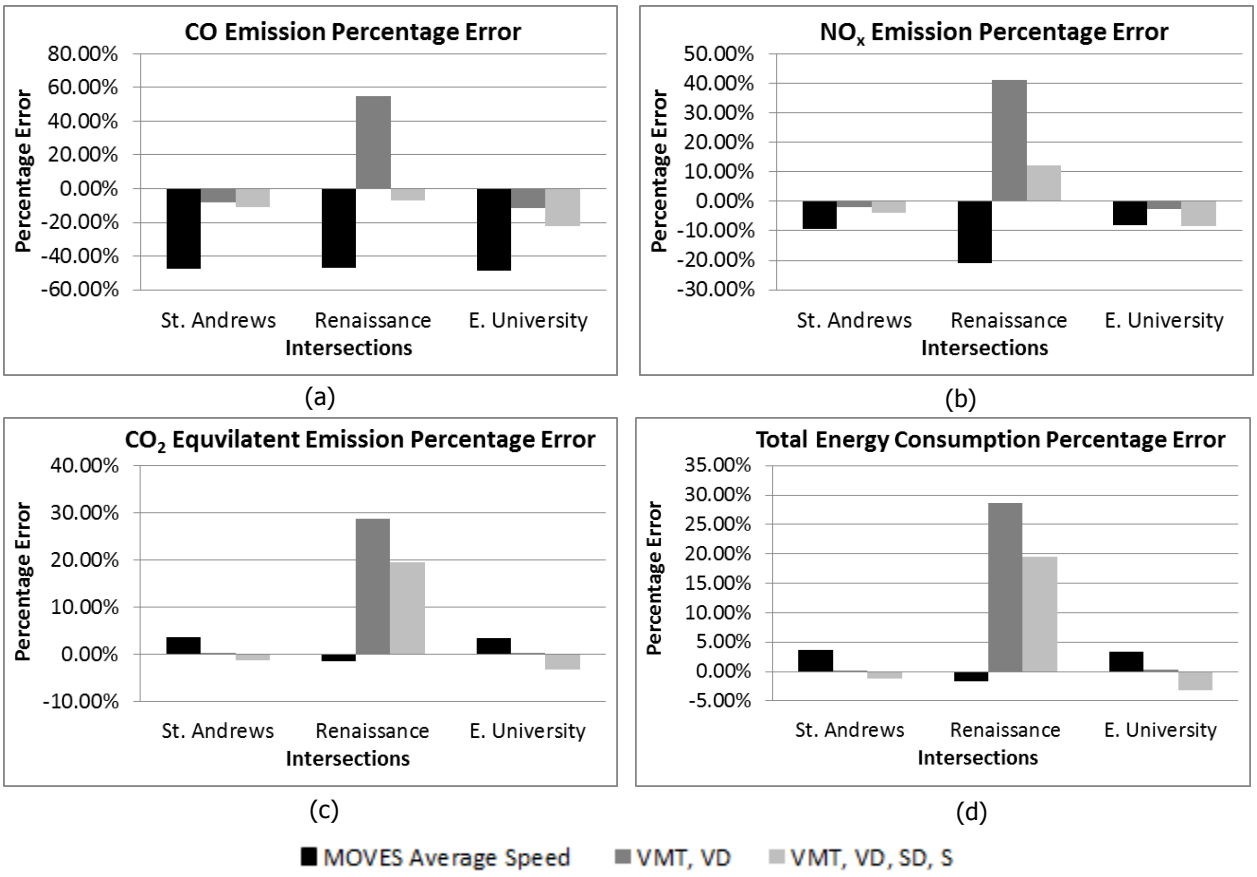

Figure 5. Percentage errors of different models for three intersections of Glades Road without coordination.

Based on the above discussion, the two proposed models seem to be reasonable when compared with emission estimates based on the MOVES operating mode approach with simulation results. However, questions have been raised about the validity of the vehicle trajectories from microscopic simulation models, particularly as they relate to vehicle acceleration and deceleration. This may have direct impacts on emission estimation based on the microscopic simulation models, such as the MOVES operating mode distribution approach (Hadi et al., 2011). Since both the model development and evaluation in this study were based on the outputs of microscopic simulation, and in order to further validate the emission and energy consumption models developed in this

study, field-collected vehicle trajectories from the Next Generation Simulation (NGSIM) program databases were used in a second set of model testing.

Vehicle trajectories from Peachtree Street in Atlanta, Georgia, obtained from 4:00 PM to 4:15 PM, were used to perform the validation. The analyzed street segment is approximately 2,100-feet long and has five intersections and two to three through lanes in each direction (Cambridge Systematics, 2007). It should be pointed out that Intersection 4 at the segment is a stop-controlled intersection, and the rest are signalized intersections. The segment is naturally divided into 6 sections by the five intersections (Cambridge Systematics, 2007) and Section 2 and Section 3 are the only two sections that have signalized intersections both upstream and downstream.

The vehicle trajectories from the site were filtered by the vehicle types and directions. Only passenger cars traveling either northbound or southbound on Peachtree Street were utilized, since the models developed in this study only accounted for passenger cars. The trajectories were processed to derive the operating mode distributions and input to MOVES to calculate emission and energy consumption using the operating mode distribution approach. The macroscopic performance measures, such as VMT, vehicle delay, stop delay, and number of stops were also calculated based on those trajectories. The developed statistical models took these macroscopic performance measures as input to estimate emission/energy consumption. These results were then compared to the estimates from the MOVES operating mode distribution approach, based on NGSIM vehicle trajectories. The comparison results are presented in Figure 6.

Four scenarios were utilized in the evaluation: 1) northbound traffic along the whole segment; 2) southbound traffic along the whole segment; 3) northbound traffic in Sections 2 and 3; and 4) southbound traffic in Sections 2 and 3. As shown in Figure 6, the first model that is based on VMT and total vehicle delays showed reasonable estimations in all four cases, and the

percentage errors were within acceptable ranges. However, the second model, which is based on VMT, total vehicle delays, total stop delays, and number of stops, did not perform well. This could be because the total stop delays and number of stops requires accurate vehicle trajectories, including accurate acceleration and deceleration estimates. The quality of the trajectories in microscopic simulation is expected to affect the accuracy of this second model, which accounts for acceleration and deceleration delays (see Equation 4). Thus, it is recommended to use the first model based on VMT and vehicle delays to estimate emission and energy consumption, if one of these two models is used.

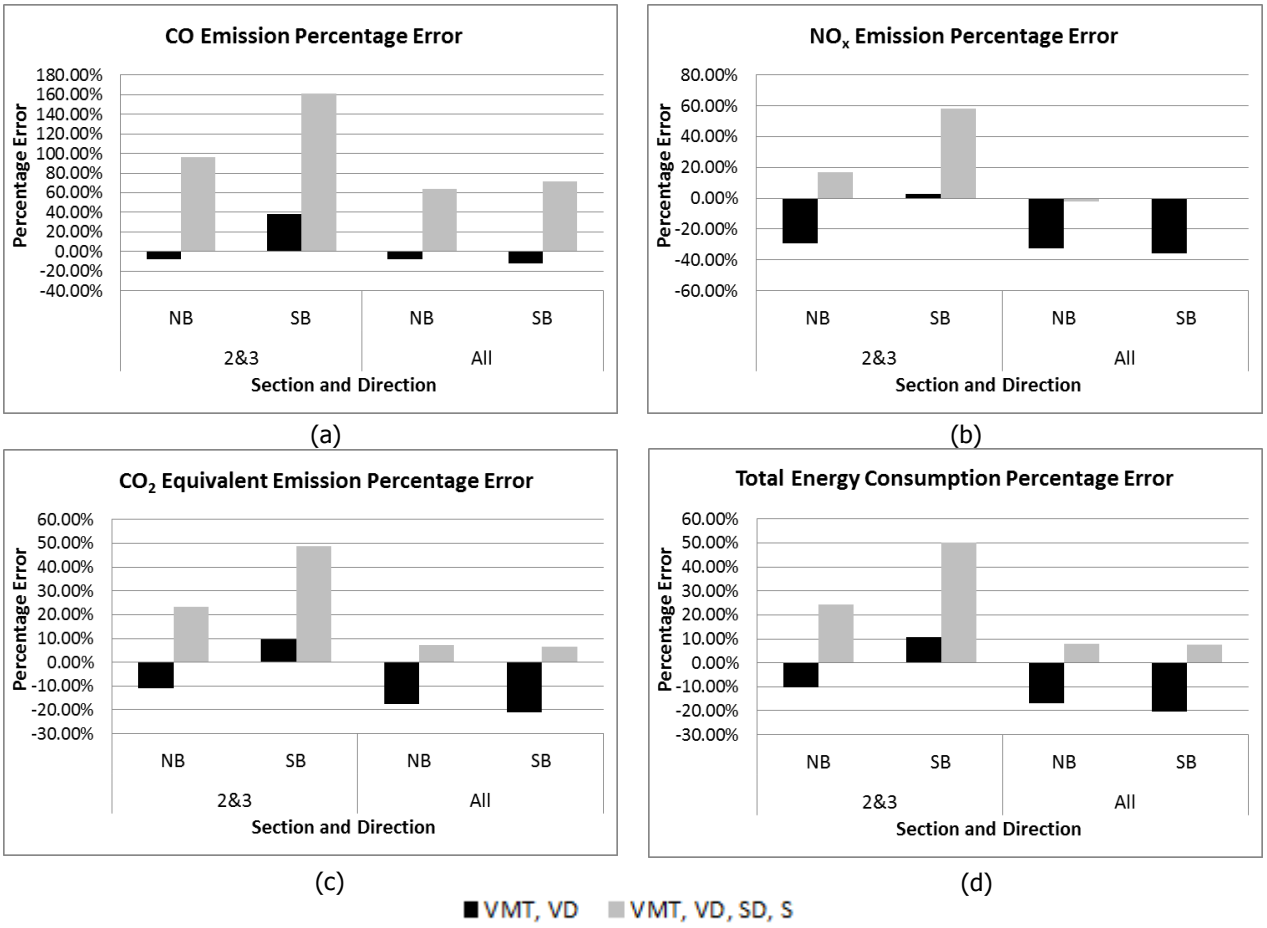

Figure 6. Percentage errors of different models at Peachtree Street using NGSIM data.

Although the first model that considers the VMT and total vehicle delays is shown to produce good results based on the above comparison, the second model has an advantage compared to the first model in that it includes the impacts of vehicle acceleration, deceleration, and idling on emission and energy consumption. The lower performance of the second model does not indicate that these additional variables should not be included but it implies that estimating these variables based on microscopic simulation may not be correct due to the discrepancy between the trajectories obtained from microscopic simulation and the real world. A further effort has been made to utilize the real-world trajectory data for the development of analytical models, similar to the ones described above, as discussed in the next section.

MODELS BASED ON NGSIM DATA

In order to account for the acceleration and deceleration characteristics of real-world trajectories, statistical models were developed based on NGSIM data from Lankershim Boulevard and NGSIM data from Peachtree Street. Two 15-minute interval data sets are available for each location, providing a total of four sets of data. In order to have adequate sample sizes for the statistics analysis, the data of the original 15-minute intervals were further divided into 5-minute intervals. The data was also disaggregated further by the segments between intersections, resulting in a total of 72 scenarios that can be used in the statistical analysis. Applying the same procedure as described in the previous section, the emission models developed from NGSIM data are presented below.

$$CO(g) = 10.8622 \times VMT(miles) + 3037.8036 \times \frac{1}{avgspeed(mph)} + 1.4861 \times \frac{Stops(\#)}{avgspeed(mph)} \quad (12)$$

$$NO_x(g) = 1.23458 \times VMT(miles) + 196.09465 \times \frac{1}{avgspeed(mph)} + 0.20111 \times \frac{Stops(\#)}{avgspeed(mph)} \quad (13)$$

$$SO_2(g) = 0.004392 \times VMT(miles) + 9.717131 \times \frac{1}{avgspeed(mph)} \quad (14)$$

$$EC(joule) = 7.223 \times 10^6 \times VMT(miles) + 1.084 \times 10^9 \times \frac{1}{avgspeed(mph)} + 2.388 \times 10^6 \times \frac{Stops(\#)}{avgspeed(mph)} \quad (15)$$

$$AtmCO_2(g) = 519.10 \times VMT(miles) + 77950.59 \times \frac{1}{avgspeed(mph)} + 171.60 \times \frac{Stops(\#)}{avgspeed(mph)} \quad (16)$$

$$CO_2Equi(g) = 519.10 \times VMT(miles) + 77950.59 \times \frac{1}{avgspeed(mph)} + 171.60 \times \frac{Stops(\#)}{avgspeed(mph)} \quad (17)$$

Those models were compared to other analytical models developed using MOVES in the previous effort described in this chapter and in a recent study by the University of South Florida, which as listed in Table 5. Among the five models tested, the VISSIM 1 and VISSIM 2 models were developed in this study from VISSIM trajectory data and VISSIM Measures of Effectiveness (MOE) as previously introduced. The USF 0 and USF 1 models were developed from VISSIM model trajectory data and Synchro MOEs by Guo and Zhang at USF (2014). The NGSIM model is the model developed in this study based on the NGSIM trajectory data and NGSIM-trajectory-extracted MOEs.

The aforementioned five models were tested based on the scenarios summarized in Table 6. It is worth pointing out that there is a stop-controlled intersection between Section 4 and Section 5 along the Peachtree segment. Consequently, the NB direction of Section 4 and the SB direction of Section 5 were excluded from this analysis. The ground truth environmental measures were estimated based on the MOVES operating mode approach with NGSIM Peachtree trajectory data.

Table 5. Emission Models Comparison

Model	Intercept	IV1	IV2	IV3	IV4	IV5	IV6
VISSIM 1	No	**VMT**	Total vehicle delay (**VD**)				
VISSIM 2	No	**VMT**	Total vehicle delay (**VD**)	Total stop delay (**SD**)	Total number of stops (**S**)		
USF 0	Yes	Total vehicle delay (**VD**)	Quadratic form of total vehicle delay ($\mathbf{VD^2}$)	Stops per vehicle (**SPV**)	Quadratic form of stops per vehicle ($\mathbf{SPV^2}$)	Average speed (**V**)	Intersection type (**I**=0)
USF 1	Yes	Total vehicle delay (**VD**)	Quadratic form of total vehicle delay ($\mathbf{VD^2}$)	Stops per vehicle (**SPV**)	Quadratic form of stops per vehicle ($\mathbf{SPV^2}$)	Average speed (**V**)	Intersection type (**I**=1)
NGSIM	No	**VMT**	Reciprocal form of average speed (**1/V**)	Quotient of total number of stops divided by average speed (**S/V**)			

IV1-OV5: Independent Variable 1 to Independent Variable 5

Table 6. Emission Models Testing Scenarios

Street	Date	Time	Section	Direction
Peachtree St.	Nov. 8, 2006	12:45 PM -1:00 PM	2	NB
				SB
			3	NB
				SB
			4	SB
			5	NB
		4:00 PM - 4:15 PM	2	NB
				SB
			3	NB
				SB
			4	SB
			5	NB

Six environmental measures were tested in our study: 1) Carbon Monoxide (CO); 2) Oxides of Nitrogen (NO_x); 3) Sulfur Dioxide (SO_2); 4) Total Energy Consumption (EC); 5) Atmospheric Carbon Dioxide ($AtmCO_2$); and 6) Carbon Dioxide Equivalent (CO_2Equi). In this study, all

environmental measures have the unit of gram except the EC which is in joules. The results from different models were converted to the units used in this study during the comparison.

The results are presented and discussed below. The percentage error used in the comparison of this study was calculated, as shown in Equation 11, given earlier. When applying that equation to this analysis, the model prediction references the results calculated using the five statistical models shown in Table 5 and the MOVES estimation reference the results from actual MOVES runs based on NGSIM trajectory data.

Figure 7 presents the percentage errors for the five models. It is clear that the models of USF 0 and USF 1 have large error percentages in all scenarios and they are much less close to the ground truth of CO emission amounts compared to the other three models. One potential explanation of the large discrepancies is that the USF study used different intersection layouts compared to the Peachtree segment and it considers the layout as one of the independent variables in their model (i.e., intersection type). The USF 0 model estimated environmental measures for intersection type zero with 2 lanes in Main Street and 1 lane in Minor Street, while the USF 1 model analyzed the intersection type one with 2 lanes in both the Main Street and Minor Street. On the other hand, the Peachtree segment in NGSIM data had different number of lanes in the entering and exiting approaches of each leg of the intersection at different locations.

Figure 7. Percentage errors of different models at Peachtree Street using NGSIM data.

In order to better compare the rest three models, Figure 8 illustrates the percentage errors of these models. As can be seen from this figure, the VISSIM 2 model has the largest percentage errors among the three models in most of the scenarios. The VISSIM 1 model and NGSIM model have lower of performance errors comparing to the VISSIM 2 model. It is difficult to conclude if the VISSIM 1 model or the NGSIM model performed better based on the figure. However, it appears that in general, the VISSIM 1 model seems to underestimate CO emissions since it does not consider the effect of the total number of stops. The Root Mean Square Error (RMSE) was calculated for the two models, respectively. Based on the results, the VISSIM 1 model has a RMSE of 273.7734 grams and the NGSIM model has 174.2596 grams for CO emission. Therefore, it can

be concluded that NGSIM CO emission model performs better than the other four CO emission model based on Peachtree scenarios.

Figure 8. CO comparison for 3 models.

Similar analyses were conducted on other five types of environmental measures. As was observed with the estimation of the CO emission, the USF 0 and USF 1 produced large percentage errors when estimating these remaining environmental measures as shown in Figures 9 to 18. Figures 10, 12, 14 and 18 present comparisons among VISSIM 1, VISSIM 2, and NGSIM models that clearly show that the NGSIM model had the closest predictions of SO_2 emission and atmospheric CO_2 emission. In addition, Table 7 presents the RMSE values for the 3 models: 1) VISSIM 1; 2) VISSIM 2; 3) NGSIM model. Except for SO_2 and atmospheric CO_2, which were not

included in VISSIM 1 and VISSIM 2 models, NGSIM models have the smallest RMSE values for all environmental measures predictions. Therefore, it can be concluded that the NGSIM model have the closest predictions to the ground truth environmental measures. In addition, Table 8 summarizes the adjusted R-squared values for VISSIM 1 and NGSIM models developed based on the 5-minute trajectory data. These values also show that the NGSIM models have better predictions than the VISSIM 1 models.

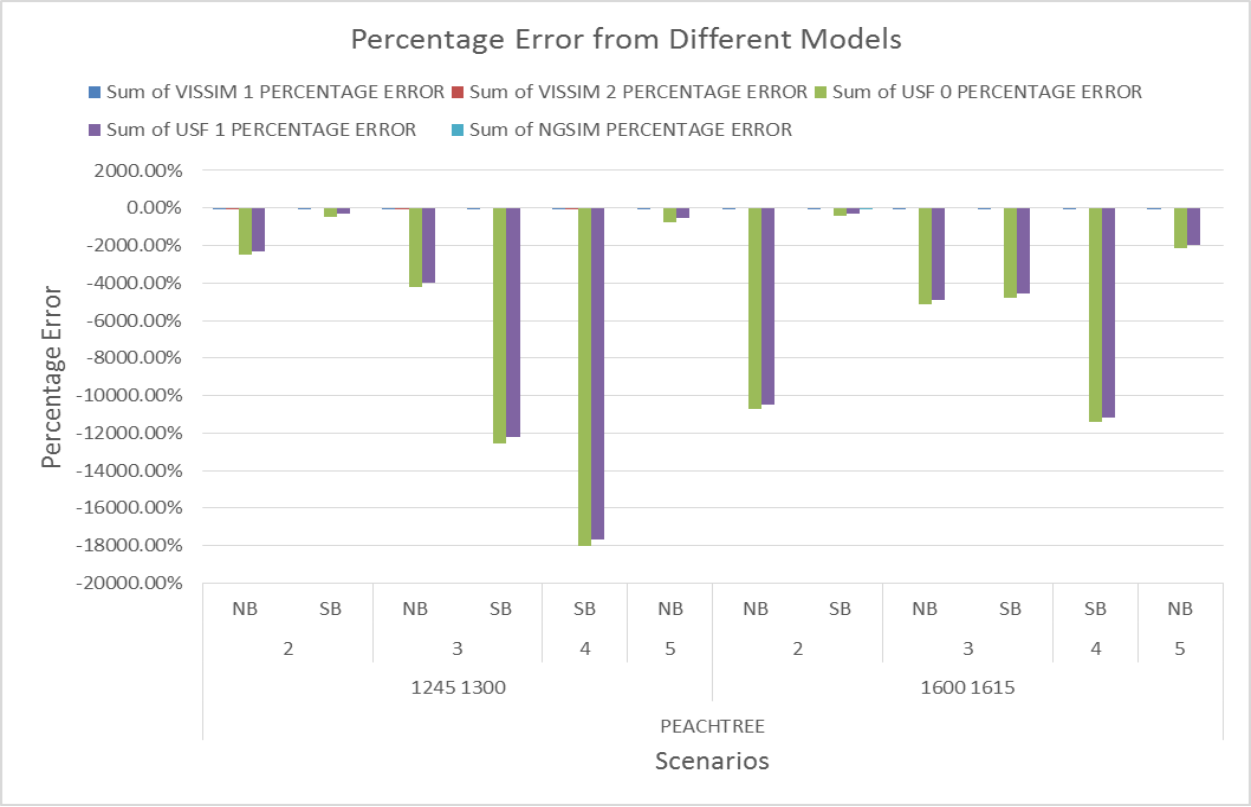

Figure 9. NO_x comparison for 5 models.

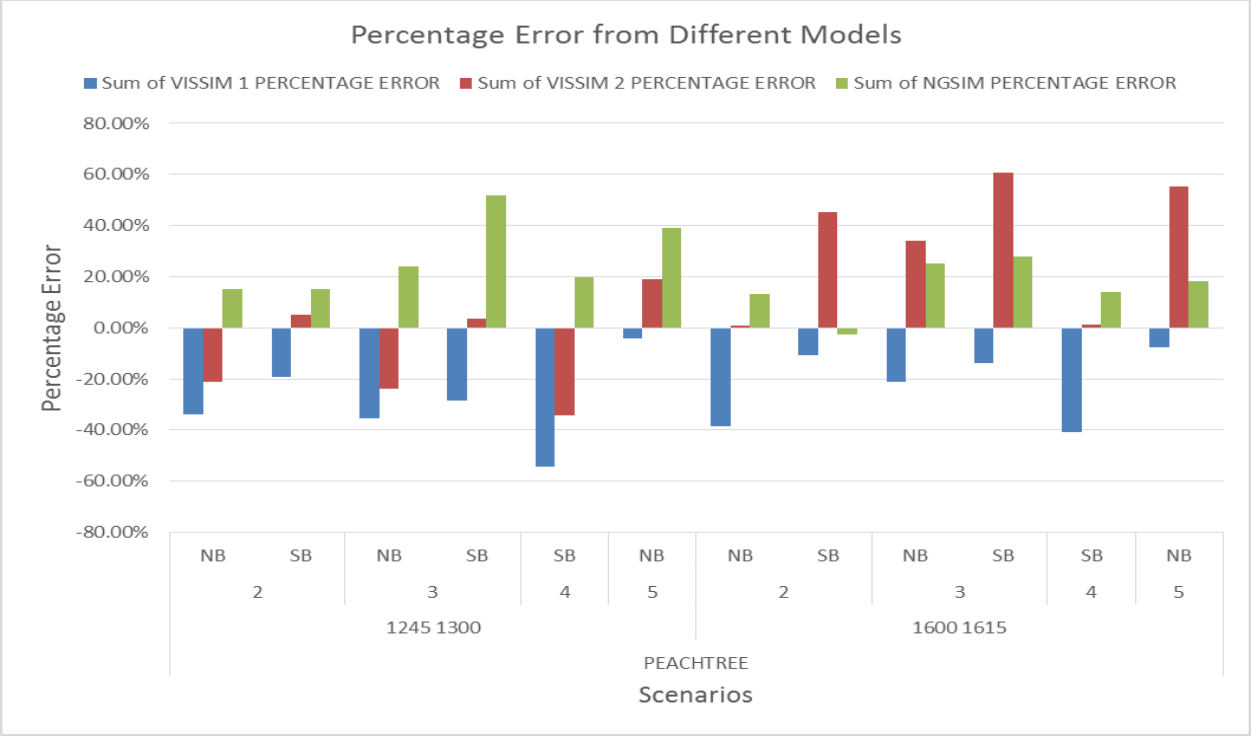

Figure 10. NO_x comparison for 3 models.

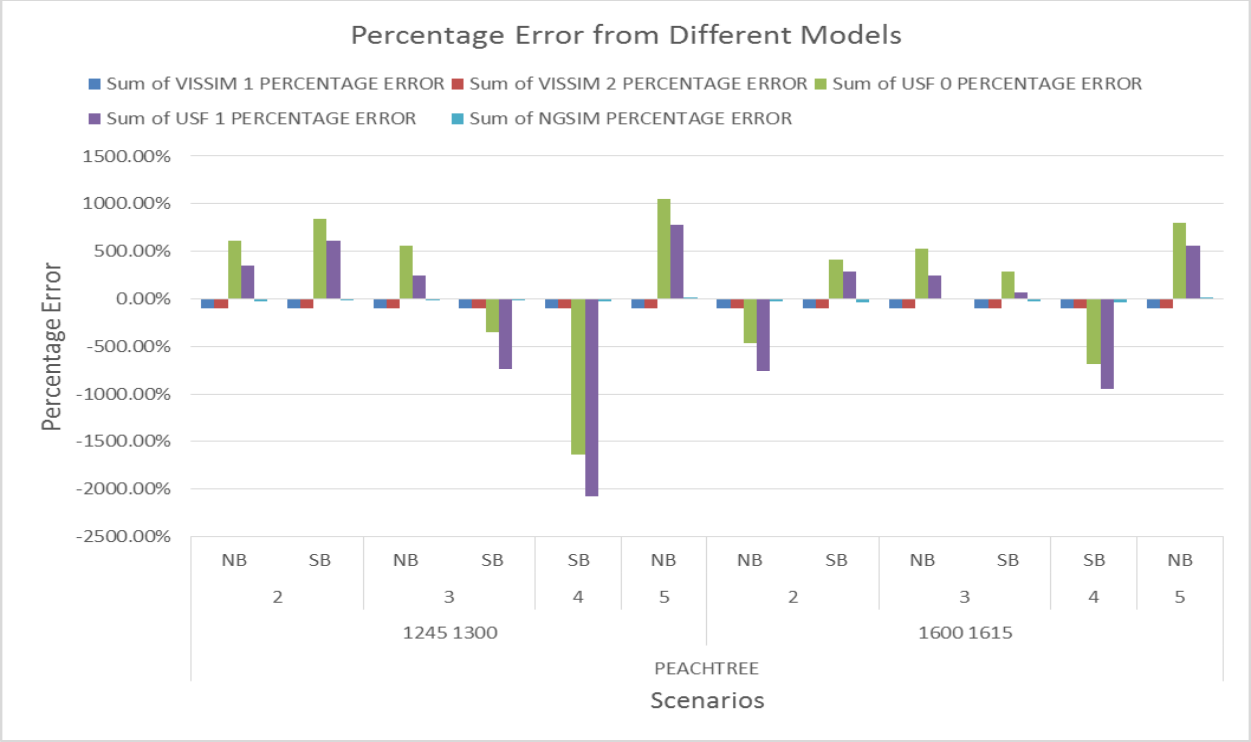

Figure 11. SO_2 comparison for 5 models.

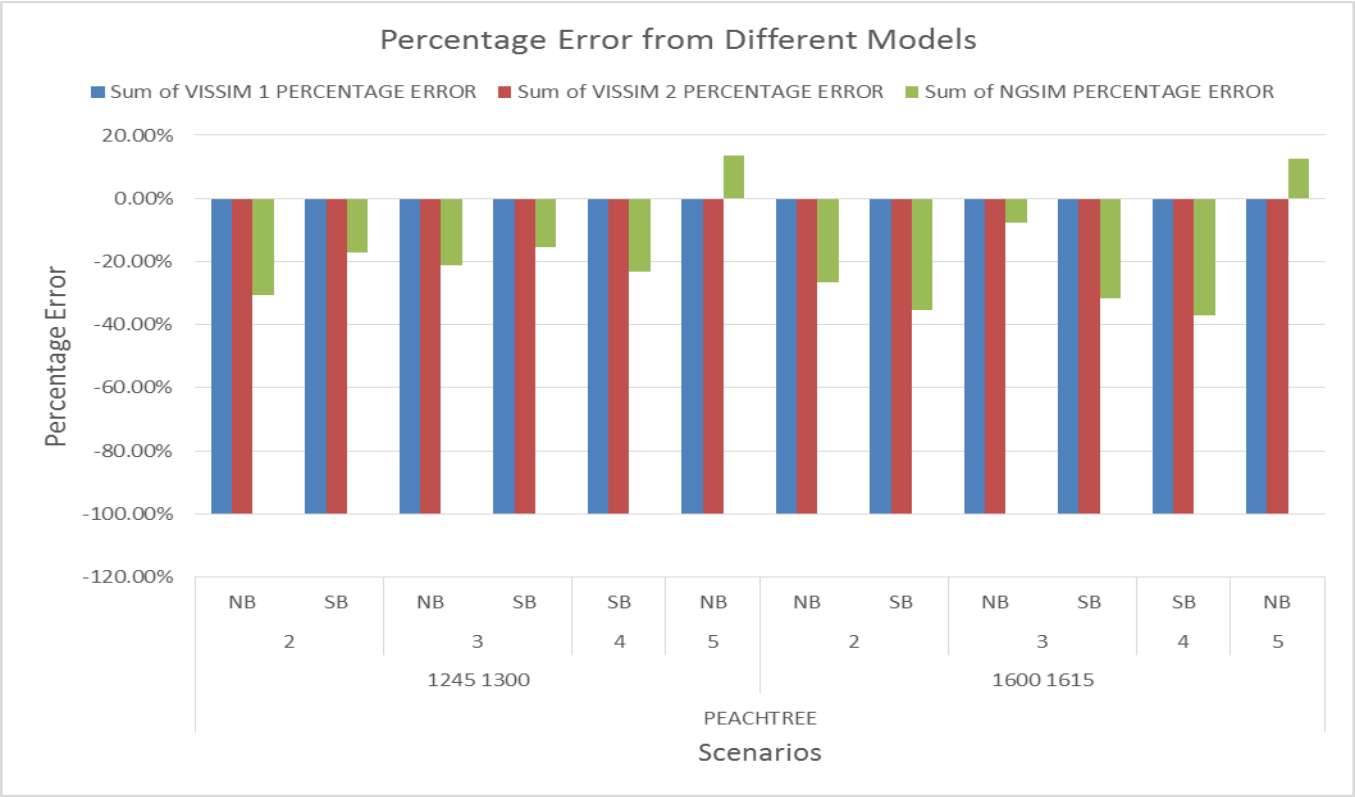

Figure 12. SO_2 comparison for 3 models.

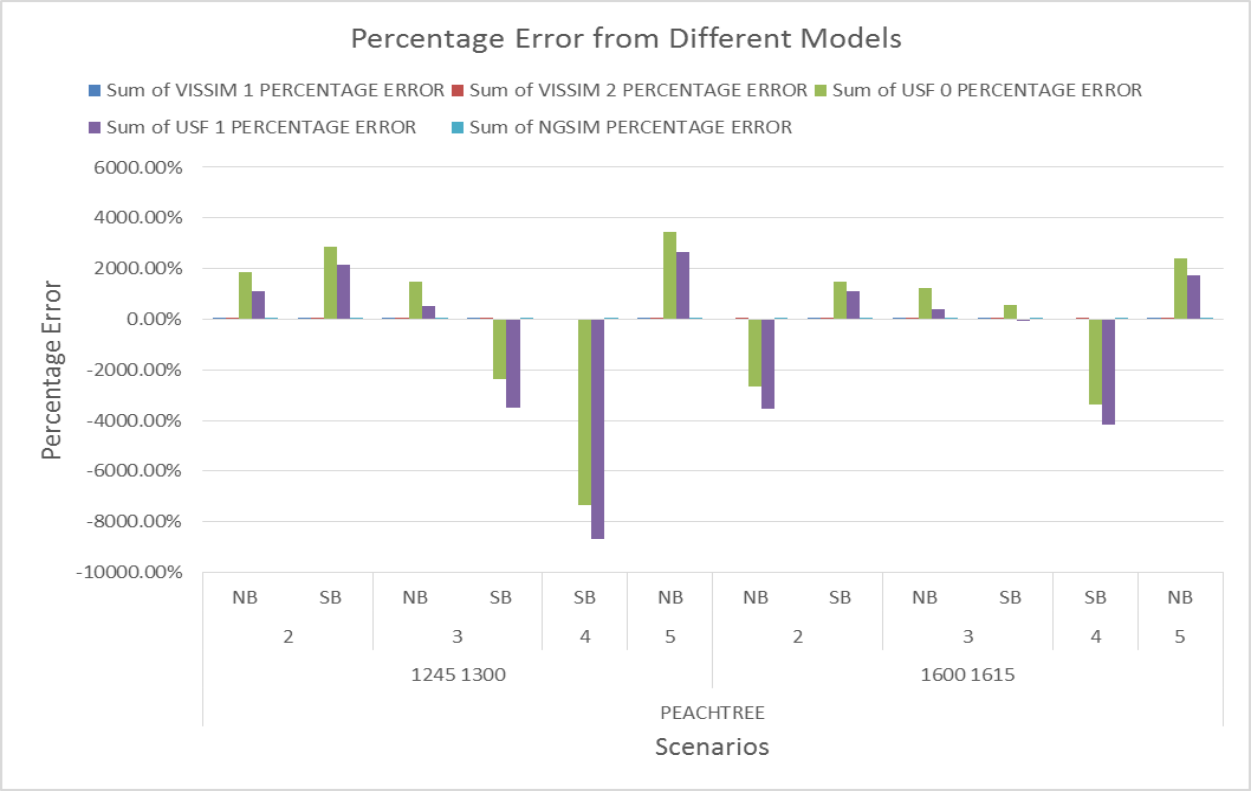

Figure 13. Total Energy Consumption comparison for 5 models.

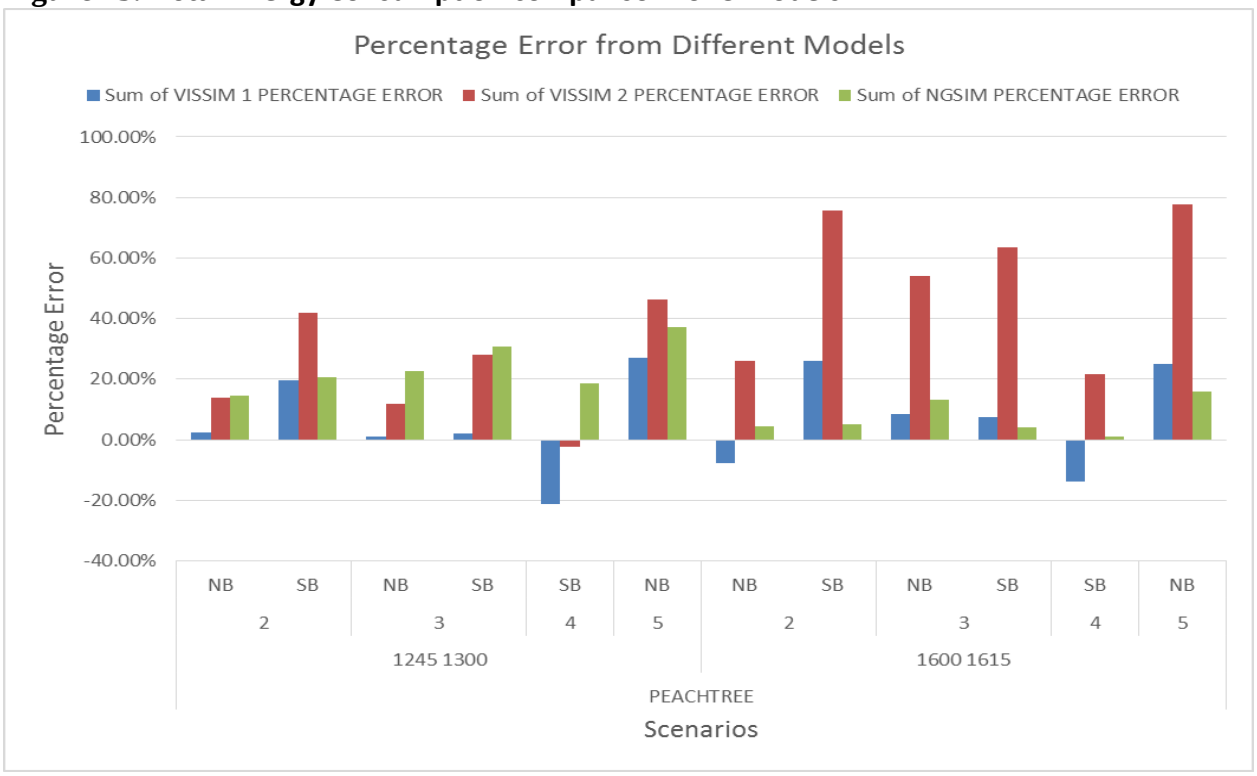

Figure 14. Total Energy Consumption comparison for 3 models.

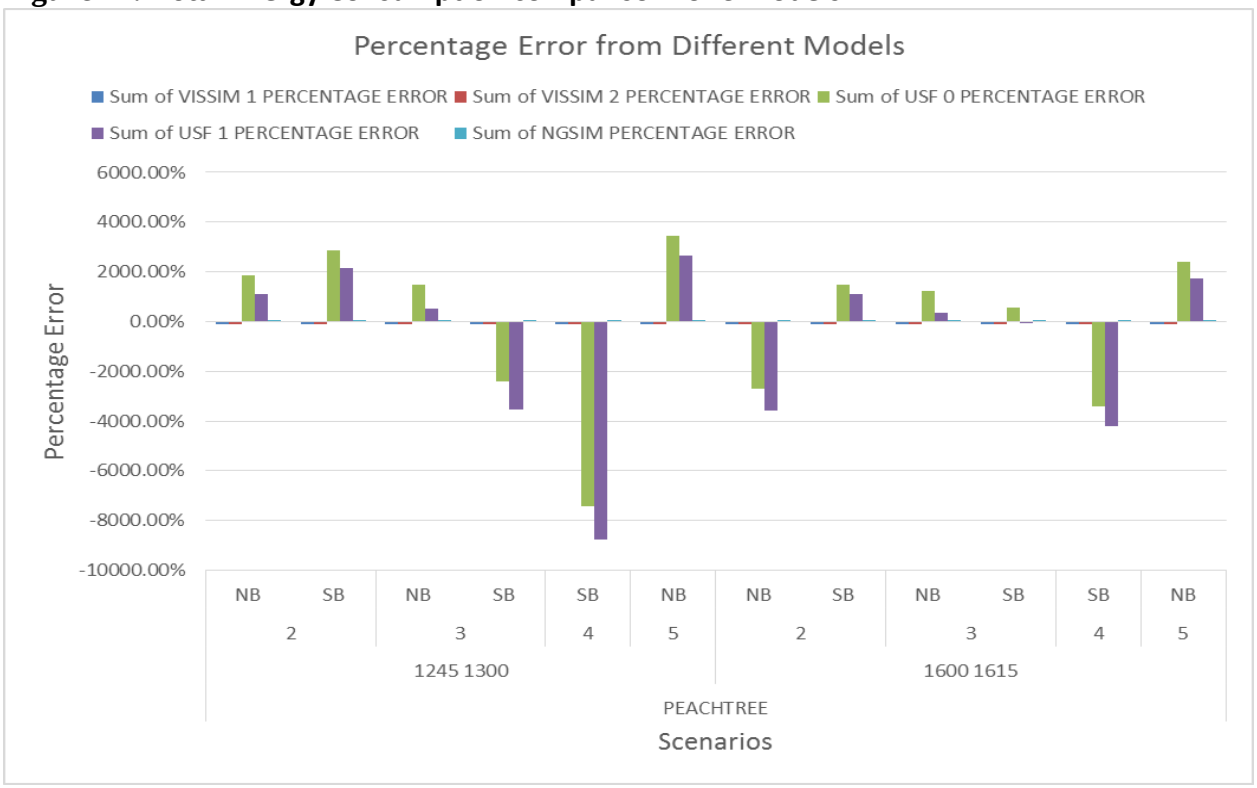

Figure 15. Atmospheric CO_2 comparison for 5 models.

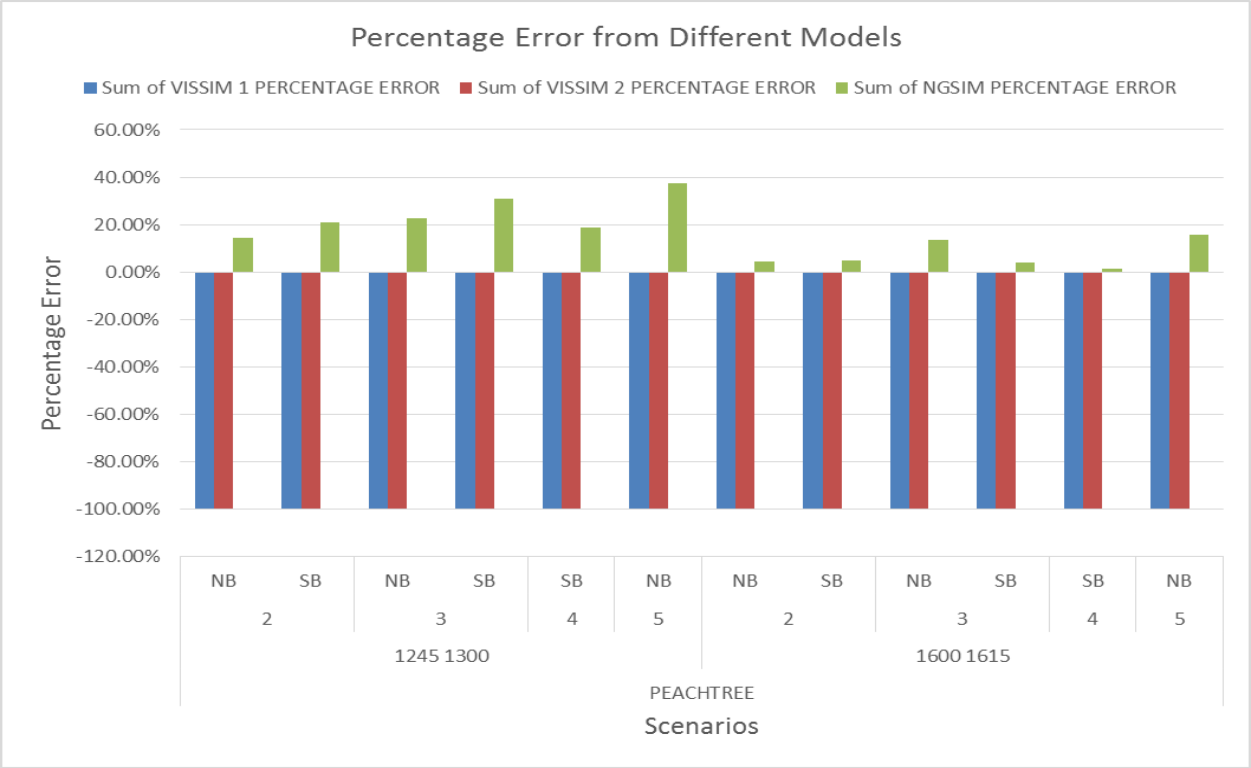

Figure 16. Atmospheric CO_2 comparison for 3 models.

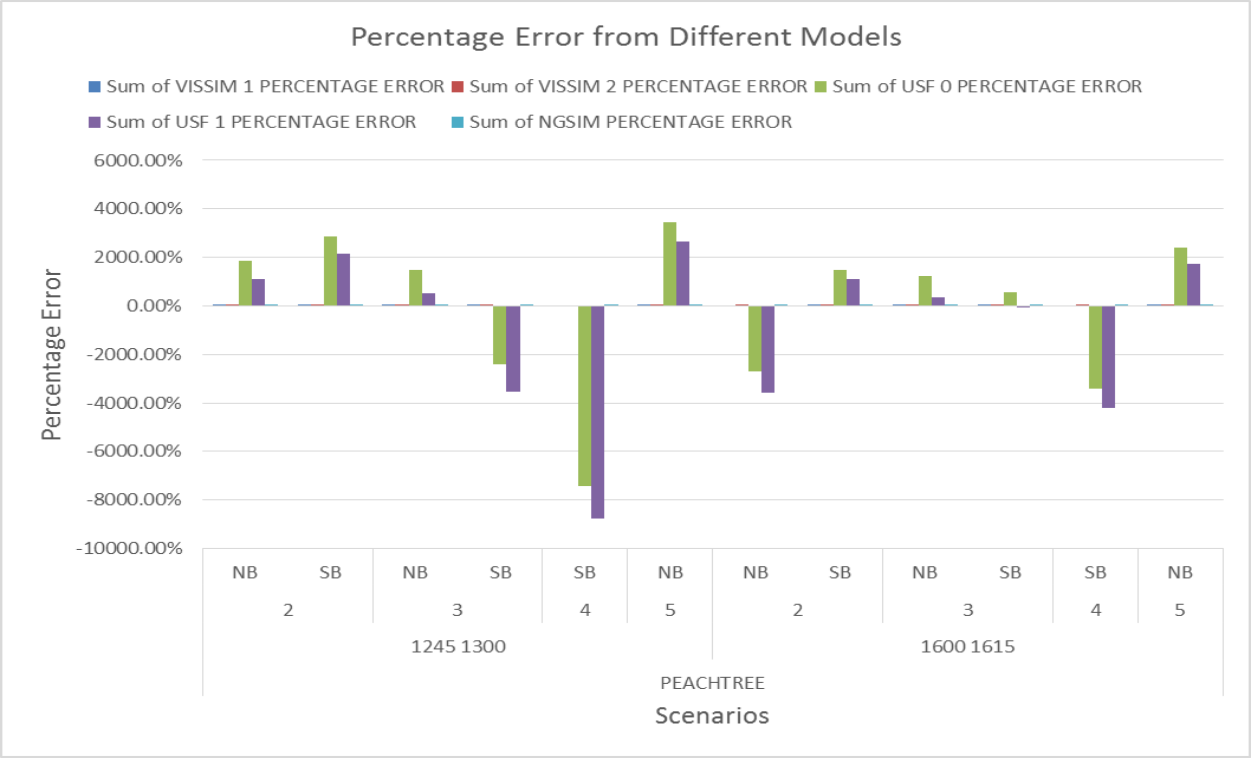

Figure 17. CO_2 Equivalent comparison for 5 models.

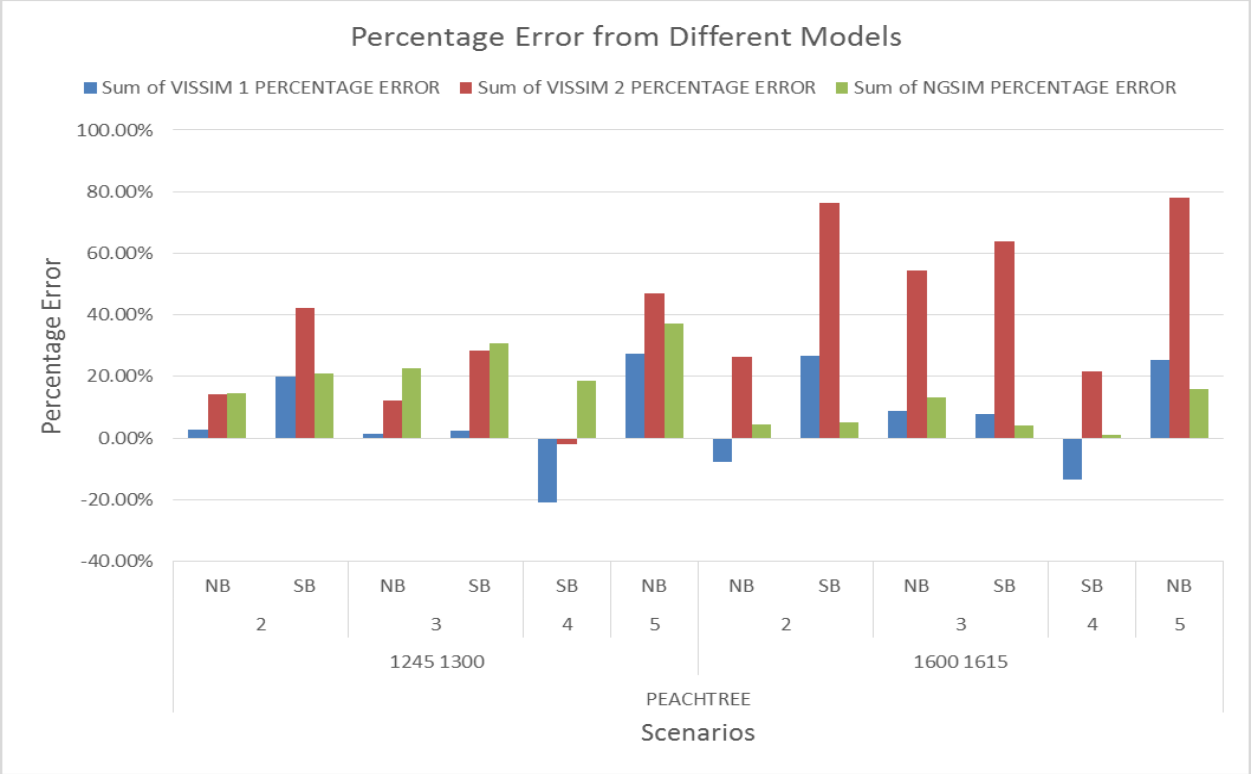

Figure 18. CO_2 Equivalent comparison for 3 models.

Table 7. RMSE Comparison for Three Models.

Emission	Model	RMSE
CO	VISSIM 1	273.773389
	VISSIM 2	1002.256307
	NGSIM	**174.2595554**
NO_x	VISSIM 1	16.79416349
	VISSIM 2	25.99811962
	NGSIM	**14.01293465**
SO_2	VISSIM 1	
	VISSIM 2	
	NGSIM	0.462973685
Energy Consumption	VISSIM 1	89278817.58
	VISSIM 2	261109742.2
	NGSIM	**73008304.88**
Atmospheric CO_2	VISSIM 1	
	VISSIM 2	
	NGSIM	5249.687515
CO_2 Equivalent	VISSIM 1	6511.952166
	VISSIM 2	18878.4696
	NGSIM	**5249.687515**

Table 8. Adjusted R-squared Values for Two Models.

Emission / Model	VISSIM 1	NGSIM
CO	0.8444	**0.9047**
NO_x	0.8819	**0.9295**
SO_2	0.6122	**0.8548**
Energy Consumption	0.8737	**0.9378**
Atmospheric CO_2	0.8737	**0.9378**
CO_2 Equivalent	0.8737	**0.9378**

CHAPTER 4

EMISSION ESTIMATION BASED ON AVI DATA

With the advancement in ITS technologies, automatic vehicle identification (AVI) data, such Bluetooth and Wi-Fi data and third party vendor data such as those from Inrix and HERE, becomes an important data source for urban arterial streets. This data have been used to estimate mobility and reliability measures but no effort has been done to estimate emission based on the collected data. This chapter focuses on developing a methodology to estimate emissions based on AVI data and Inrix data and the emission estimation models obtained in the previous chapter.

METHODOLOGY

It is concluded from the previous chapter that the NGSIM data-based emission estimation models perform better than other models, developed in this study and in a previous study by USF. Therefore, the NGSIM-based models will be used in this analysis to estimate emissions based on the real-world data. As shown in Equations 12 to 17, the NGSIM data-based emission estimation models require three inputs: vehicle mile traveled (VMT), average speed, and number of stops. These parameters have to be calculated from the real-world data (AVI data or Inrix) before plugging in the emission estimation models.

The Inrix data provides trajectories of vehicles. Thus, the number of vehicles passing through the study intersection can be counted by examining the latitudes and longitudes of those trajectories. Similarly, vehicle counts traveling through the study intersection can be obtained from the Wi-Fi data by matching the same MAC address at two Wi-Fi reader locations upstream and downstream of the intersection. However, it should be pointed out that these vehicle counts are

only sampled data and they have to be expanded using an expansion factor to obtain the total VMT. In this study, instead of using the vehicle counts from these two data sources, traffic volume count data for all 12 movements available from a previous study were directly used to calculate the VMT for each movement. The AVI and Inrix data are used to estimate the average speed and number of stops.

To estimate the average speed of the vehicles passing through the intersection, the average speed for each individual vehicle was first calculated by dividing the distance it travels by its travel time. Then, these speeds were averaged by the number of vehicles used in the speed estimation for each turning movement. Note that the distance and travel time for each turning movement were determined differently when utilizing Inrix data and Wi-Fi data since the Wi-Fi data has no trajectory information available as is the case with Inrix data. For the Inrix data, the distance was specified as 500 feet upstream and 500 feet downstream from the intersection. Three buffer areas were created at the upstream and downstream locations and the study intersection, respectively, to capture the vehicle IDs in these buffer areas. The vehicles IDs within these buffer areas were matched and the time difference at the center of the starting and ending buffers is considered as a vehicle's travel time. For the AVI (Wi-Fi) Data, the buffer areas were located at the upstream, the downstream, and the study intersections also considering the reading radius of the Wi-Fi readers . The same MAC addresses passing through these areas were matched to get the travel time based on maximum strength.

To estimate the total number of stops at the study intersection, the AVI data and the signal timing data were used to estimate the average number of stops per vehicle, and this value was multiplied by the total number of volume counts collected from the traffic volume study to get the estimated number of stops at the intersection. The number of stops per vehicle was estimated

based on vehicle waiting time at the intersection and cycle length. If a vehicle's waiting time is zero, its number of stops is 0. If a vehicle's waiting time is more than zero but less than or equal to one cycle length, its number of stops is assumed to 1. If a vehicle's waiting time is more than one cycle length but less than or equal to two cycle length, its number of stops is assumed to be 2.

Vehicle's waiting times were estimated based on both the AVI or Inrix data and the signal timing data. If a vehicle arrives during the green time, its waiting time is assumed to be zero, otherwise, the time difference between its arrival time and the green time during which it exits the intersection is calculated as the waiting time.

ANALYSIS RESULTS

The intersection of SW 8th St. and SW 107th Ave in Miami-Dade County was selected as the study location in this study. Based on the data availability, the AM peak period (3 hours from 7:00 AM to 10:00 AM) in the weekdays of April, 2016 (totally 21 days) was chosen as the study period.

Comparison of Inrix and Wi-Fi Data

Before applying the real-world data for emission estimation, the data from the two sources, Inrix data and Wi-Fi data were compared at the 5-minute aggregation level in this study. As examples, Figures 19 to 26 shows the comparison results for the eastbound through movement, while Figures 27 to 34 presents the comparison results for westbound through movement. Additional figures are presented in Appendix. Note that the comparison can only be conducted when both Inrix and Wi-Fi data are reported for the same 5-minute interval. The results in these figures indicate that in general, the Wi-Fi data samples more vehicles than the Inrix data. The

vehicle speeds produced from the Inrix data is relatively higher than those estimated from the Wi-Fi data for most of the cases due to limited sample size.

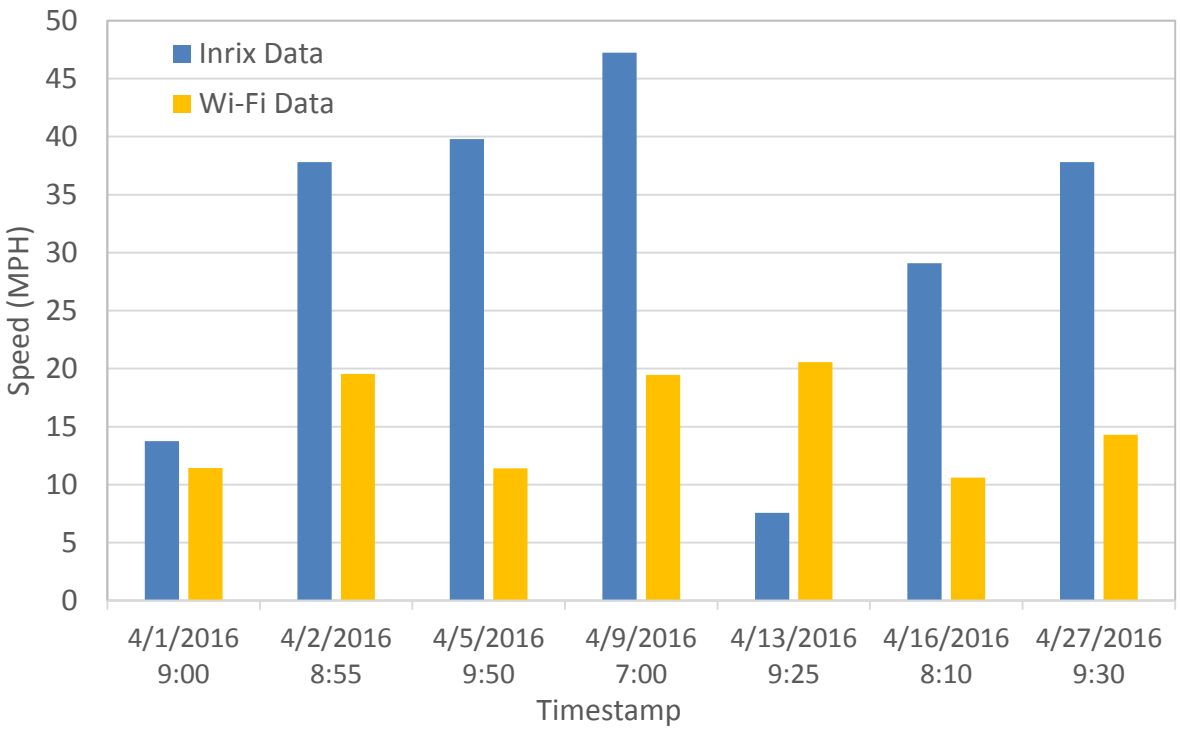

Figure 19. Comparison of speed for eastbound through movement during the AM peak period.

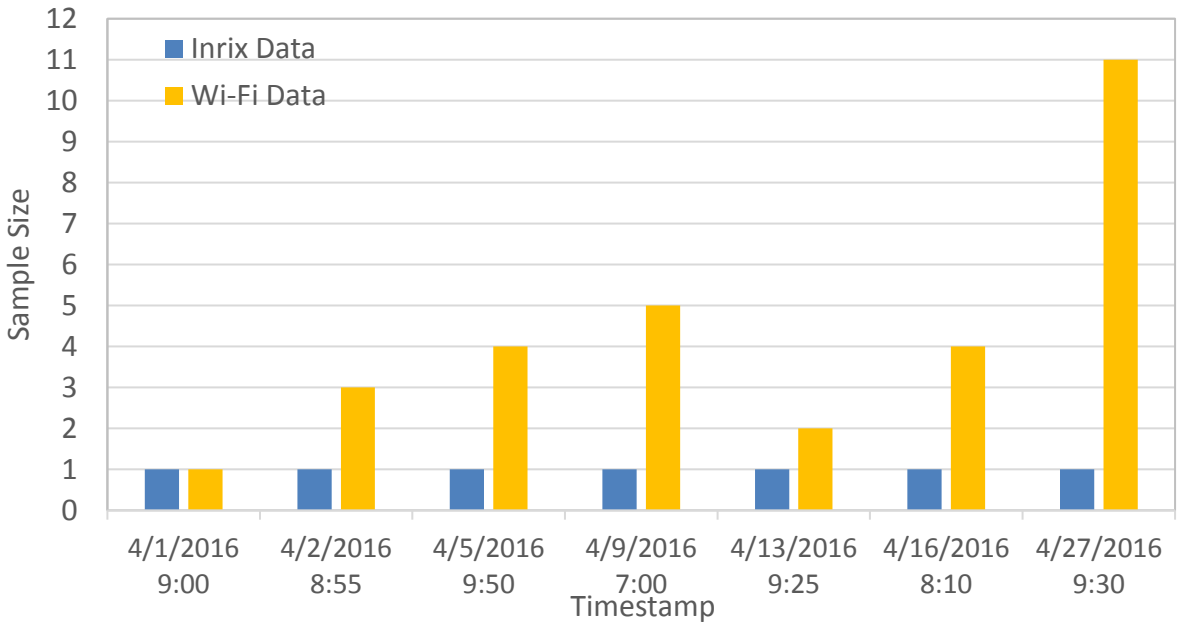

Figure 20. Comparison of sample size for eastbound through movement during the AM peak period.

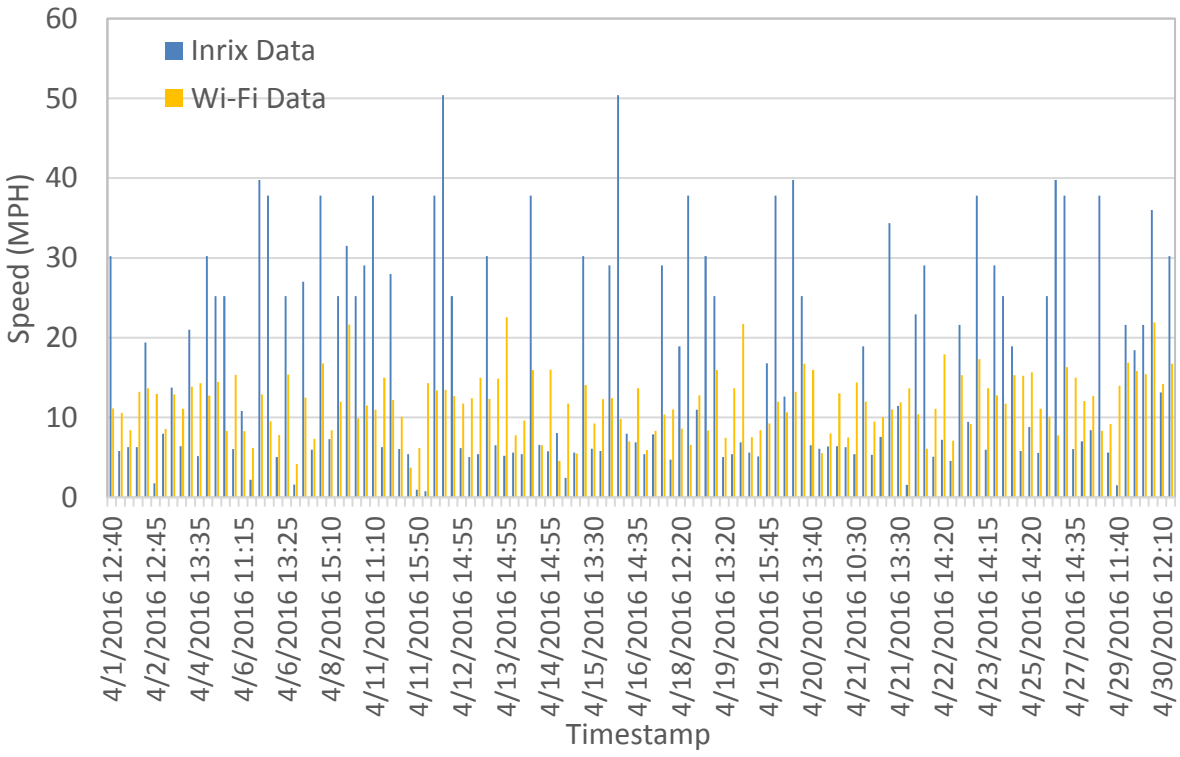

Figure 21. Comparison of speed for eastbound through movement during the midday.

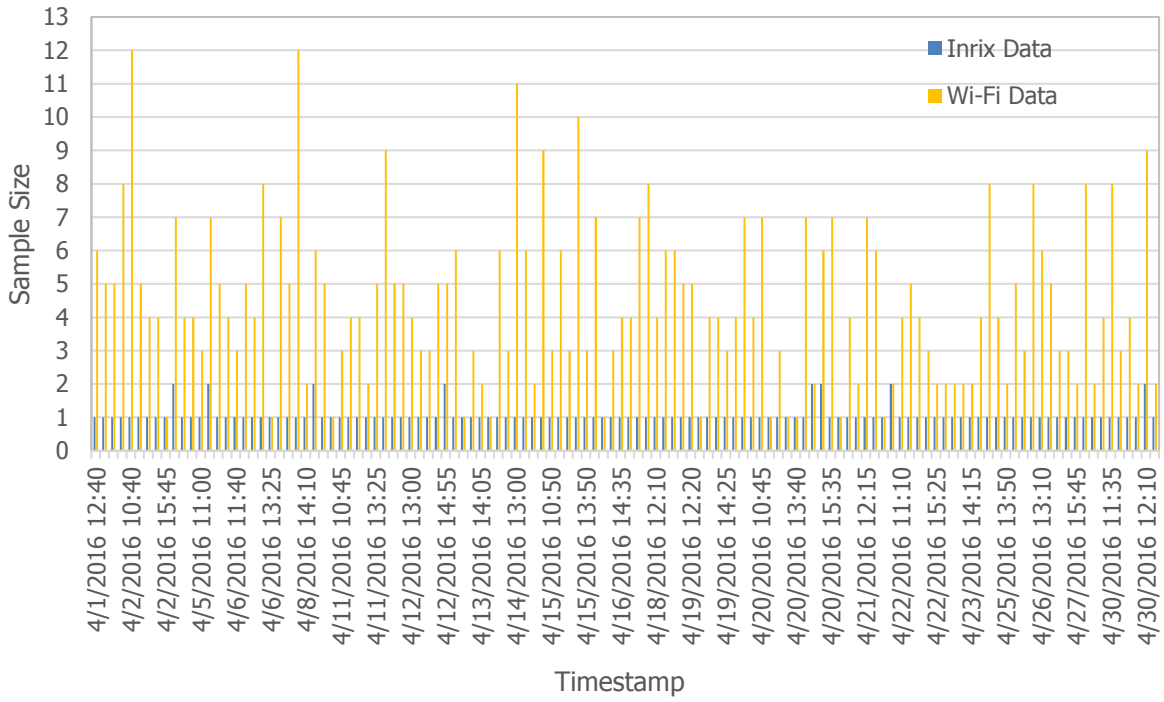

Figure 22. Comparison of sample size for eastbound through movement during the midday.

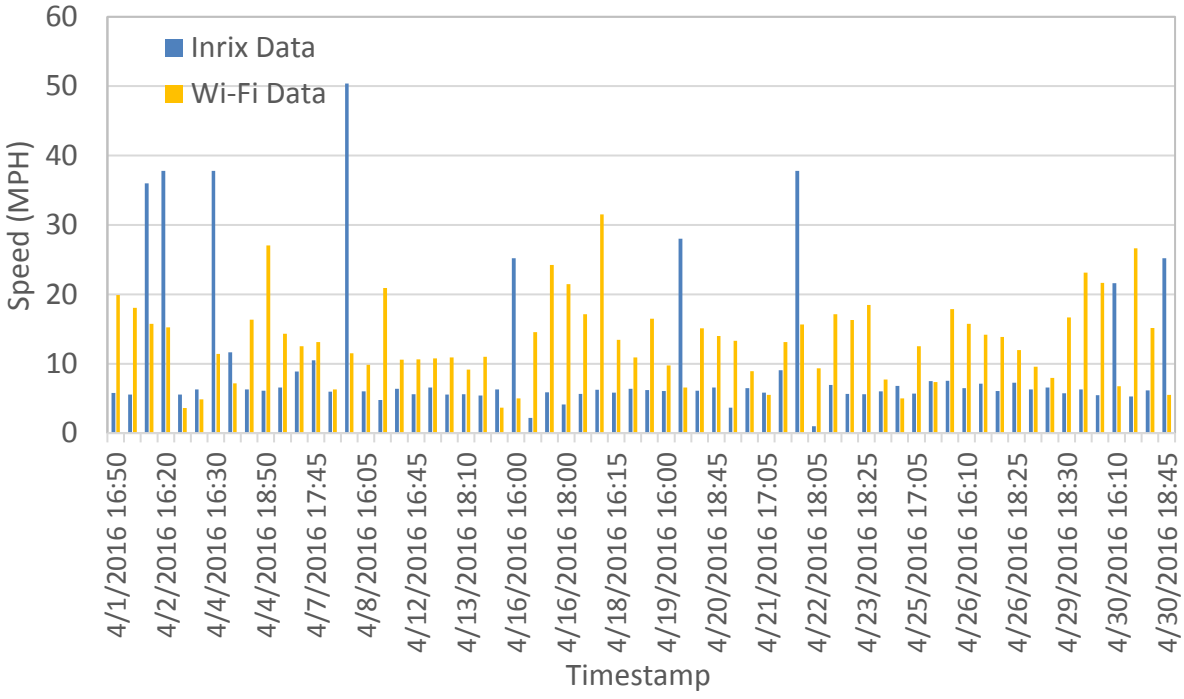

Figure 23. Comparison of speed for eastbound through movement during the PM peak period.

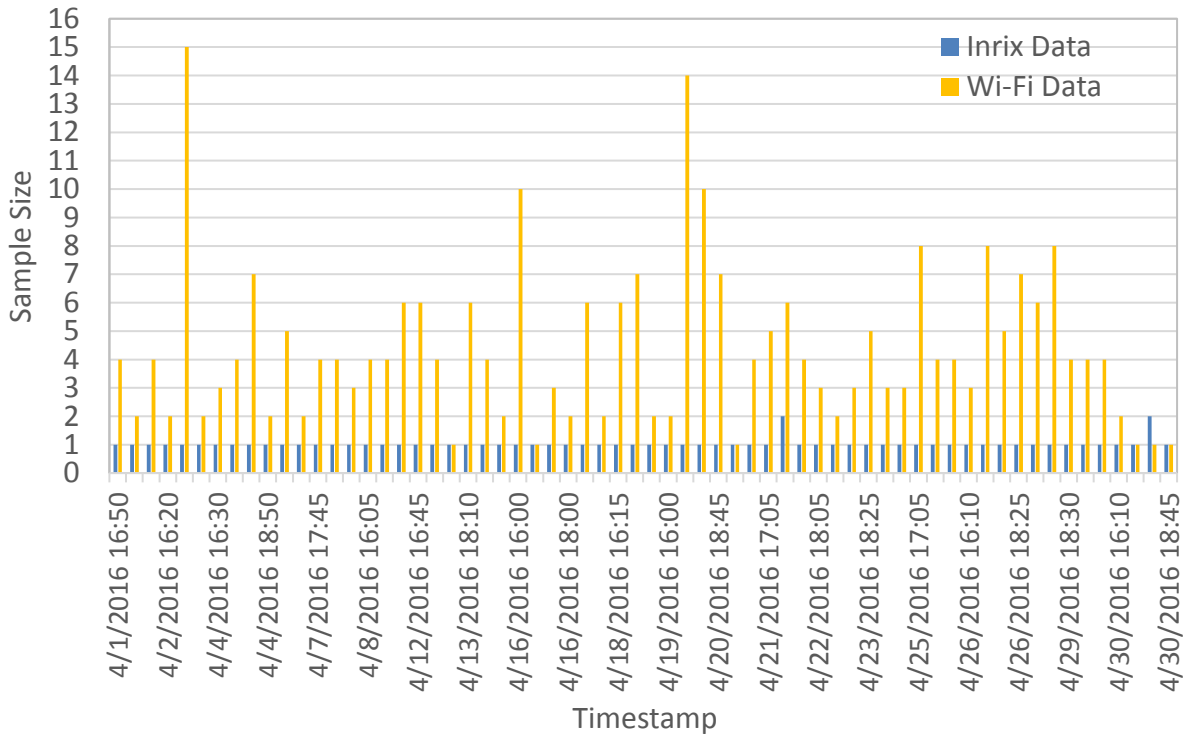

Figure 24. Comparison of sample size for eastbound through movement during the PM peak period.

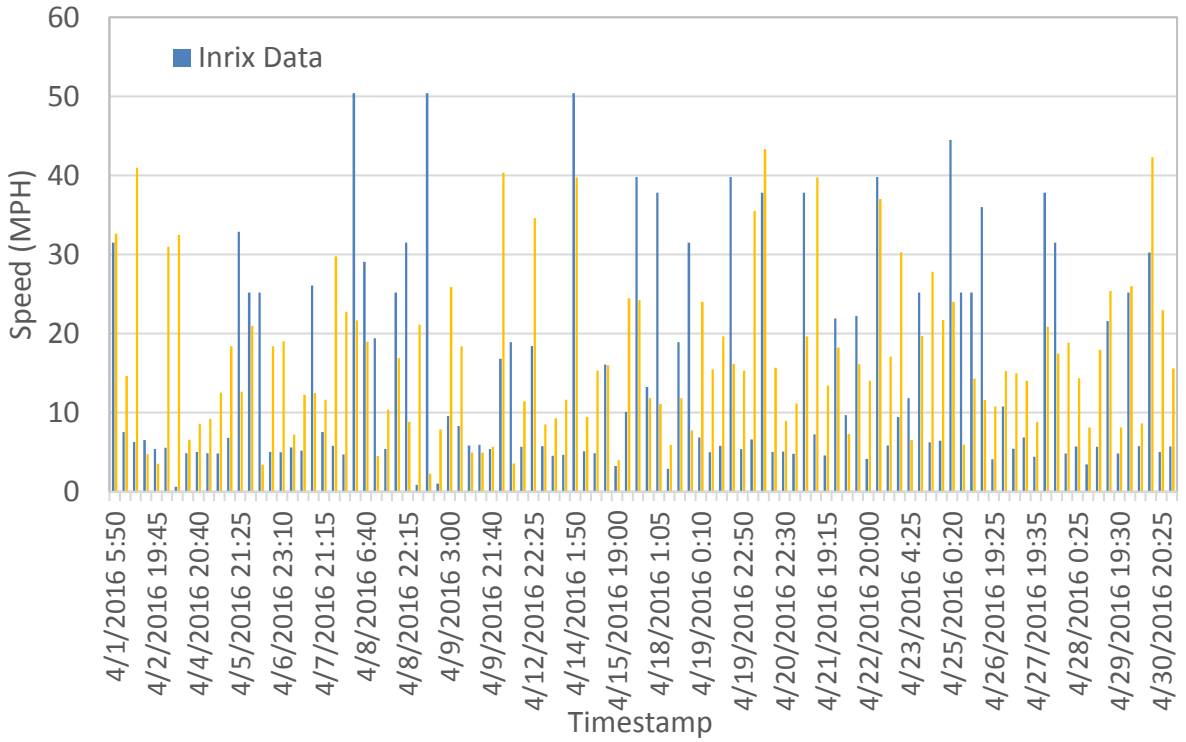

Figure 25. Comparison of speed for eastbound through movement during the night and early morning period.

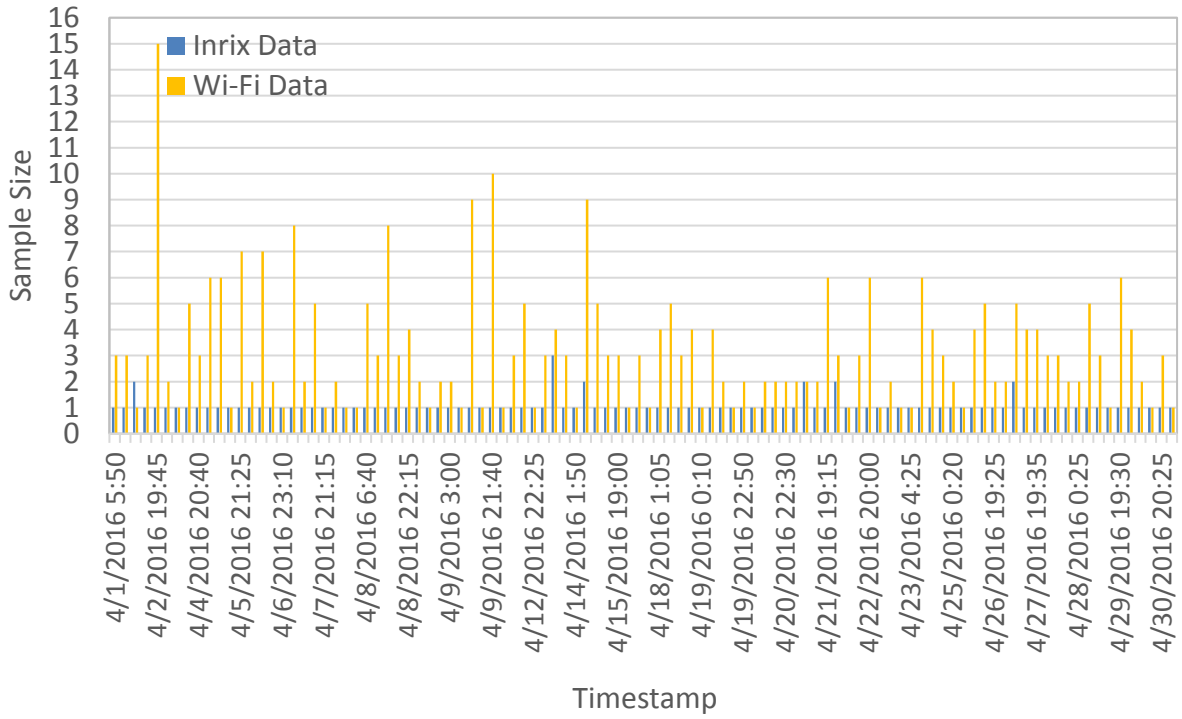

Figure 26. Comparison of sample size for eastbound through movement during the night and eraly morning period.

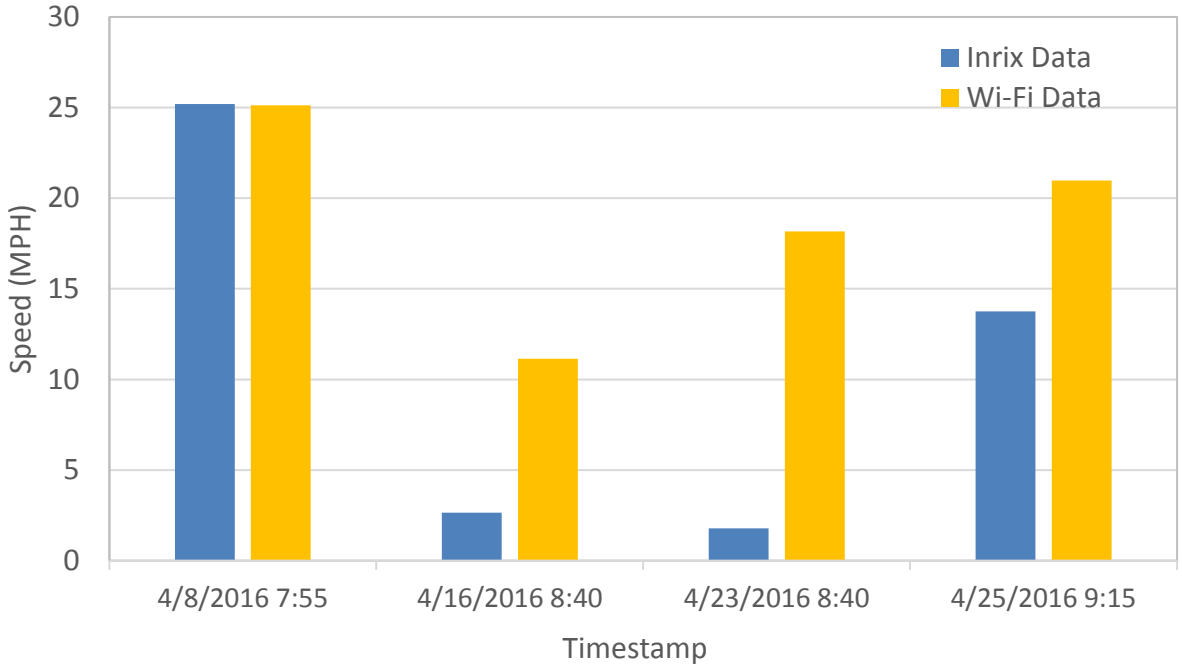

Figure 27. Comparison of speed for westbound through movement during the AM peak period.

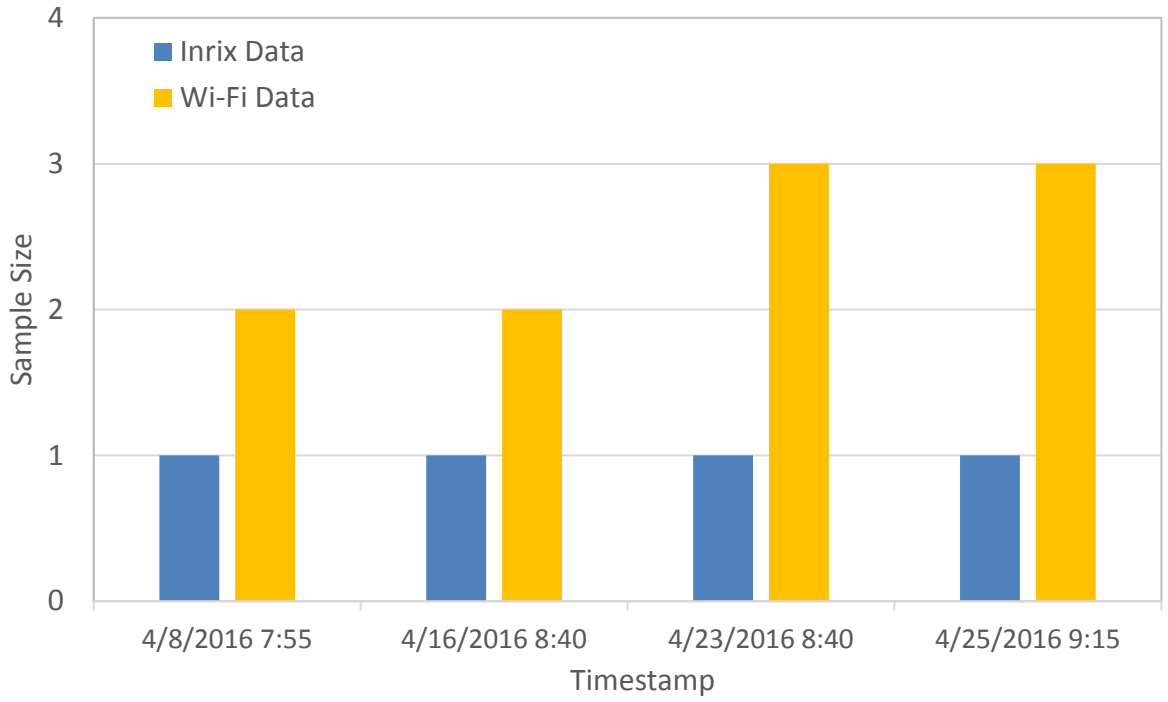

Figure 28. Comparison of sample size for westbound through movement during the AM peak period.

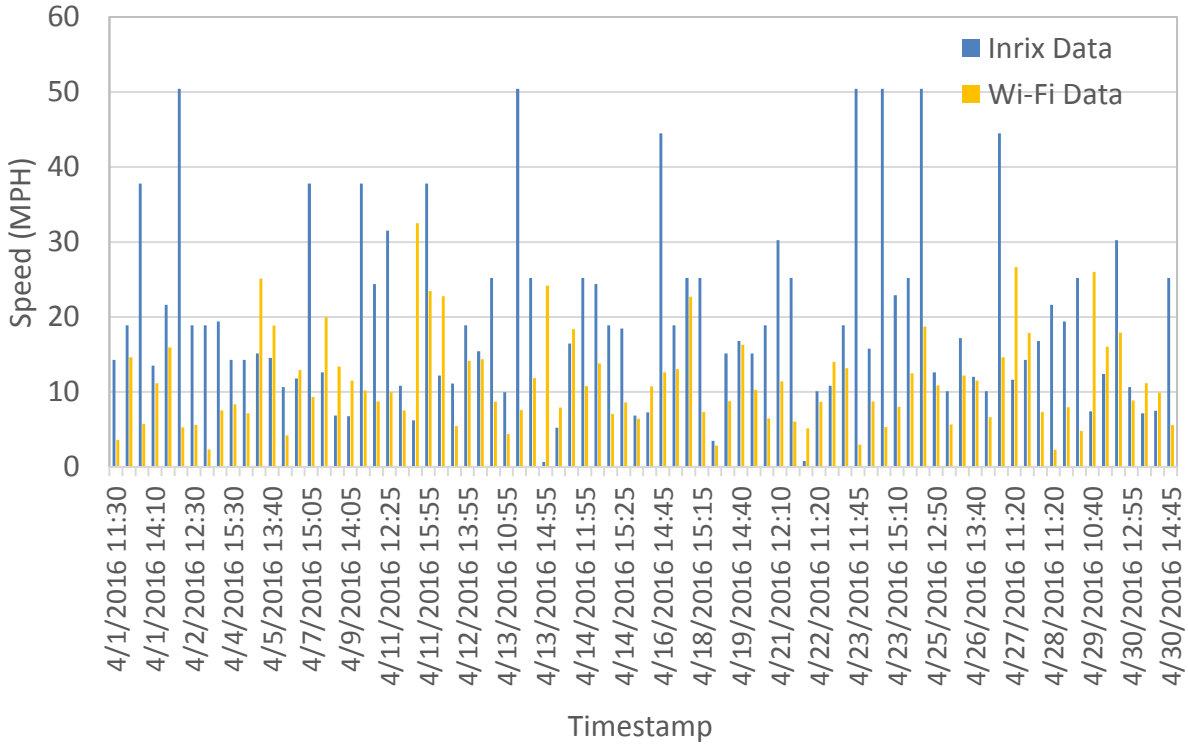

Figure 29. Comparison of speed for westbound through movement during the midday.

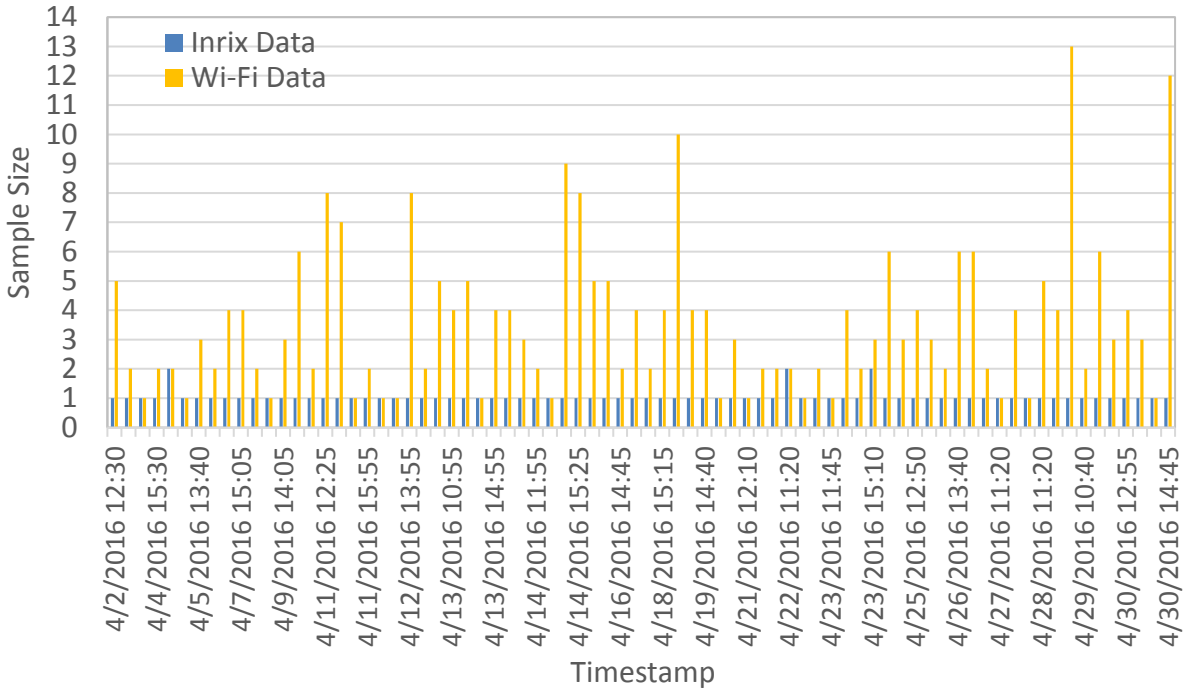

Figure 30. Comparison of sample size for westbound through movement during the midday.

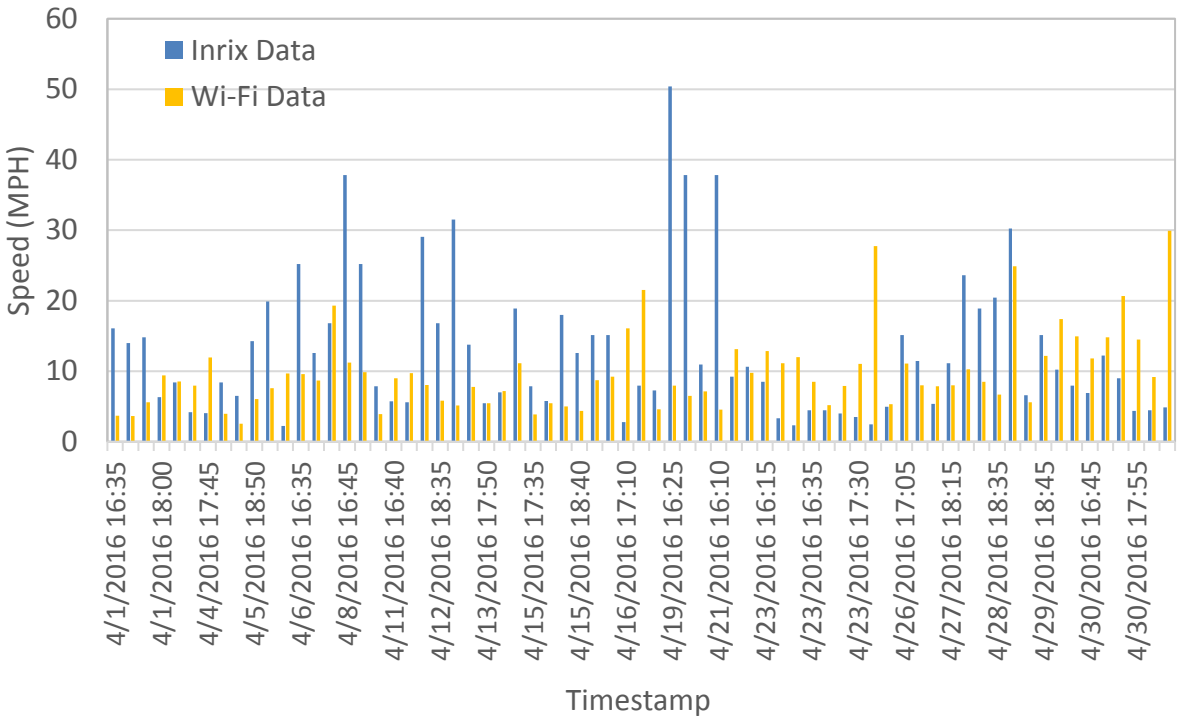

Figure 31. Comparison of speed for westbound through movement during the PM peak period.

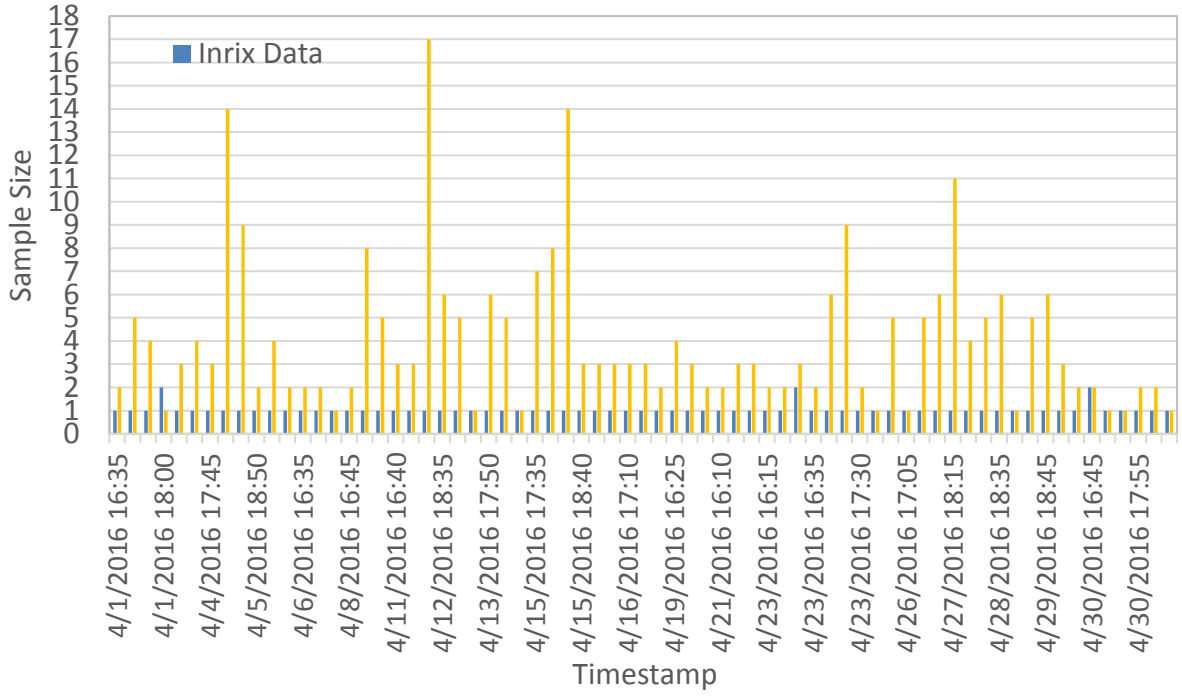

Figure 32. Comparison of sample size for westbound through movement during the PM peak period.

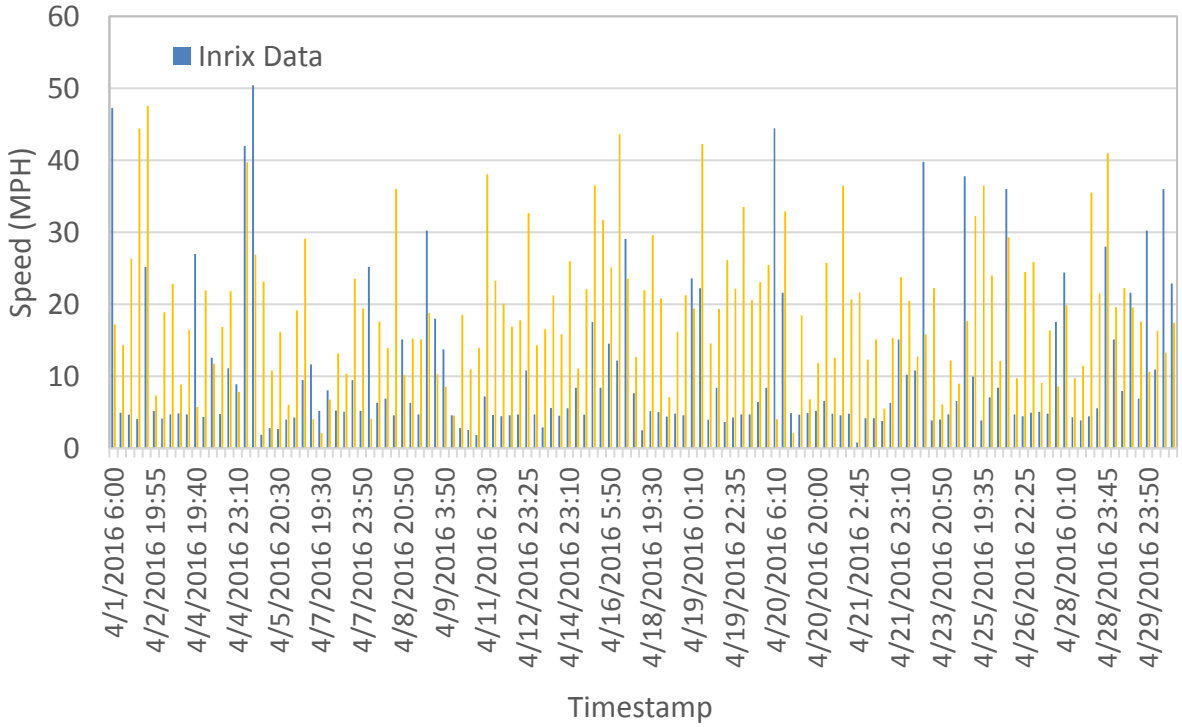

Figure 33. Comparison of speed for westbound through movement during the night and early morning period.

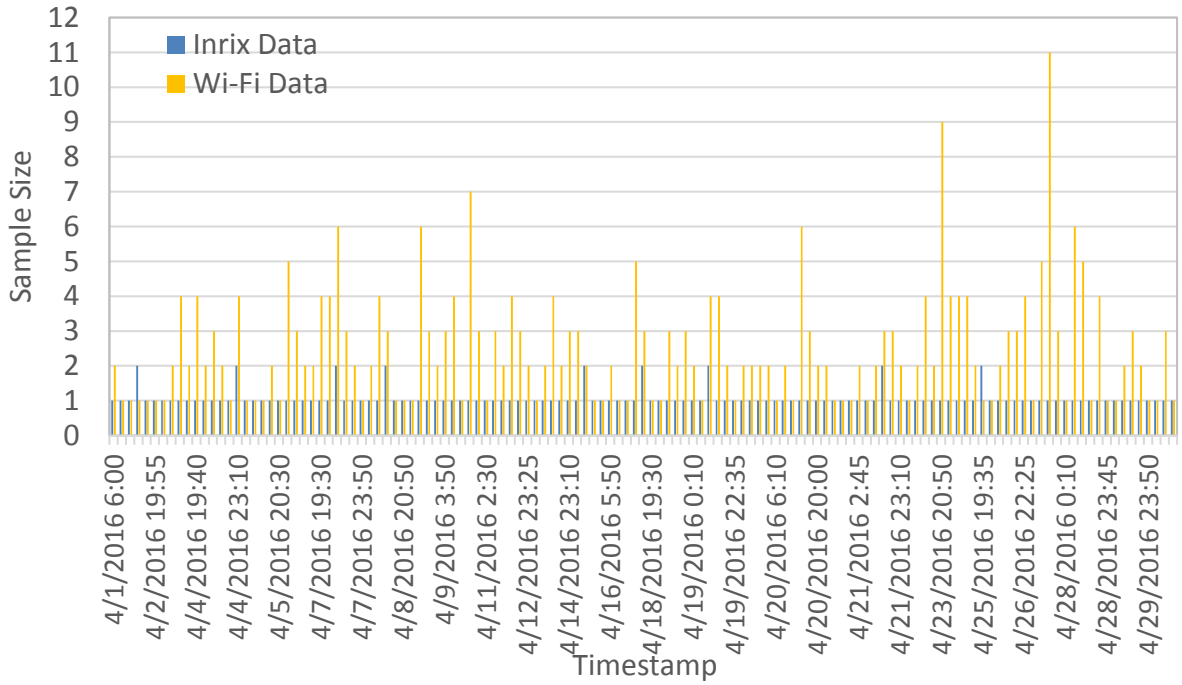

Figure 34. Comparison of sample size for westbound through movement during the night and early morning period.

Emission Estimation Results

The VMT, average speed, and number of stops were calculated for all the 12 movements at the study intersection based on the AVI data following the procedure, described above. These values were input to the NGSIM data-based emission estimation model developed in the previous chapter to calculate the emissions. Both the independent variables and the emission results based on Inrix data and Wi-Fi data are shown in Table 9. It can be seen that the two AVI data sets produce very similar emission estimation results.

Table 9. Emission Estimation Results using NGSIM Model based on AVI data

			Inrix Data	Acyclica Wi-Fi Data
Whole Intersection	**Variables**	**VMT (vehicle-miles)**	83,310	83,310
		Average Speed	15	10
		Volume	388,815	388,815
		Stops per Vehicle	0.53	0.44
		Number of Stops	204,639	169,584
	Emission	**CO (g)**	925,500	931,040
		NO_x (g)	105,622	106,364
		SO_2 (g)	367	367
		EC (joule)	634,548,319,552	643,316,416,996
		AtmCO_2 (g)	45,603,223	46,233,294
		CO_2Equi (g)	45,603,223	46,233,294
EBT	**Variables**	**VMT (vehicle-miles)**	21,601	21,601
		Average Speed	16	17
		Volume	388,815	388,815
		Stops per Vehicle	0.75	0.53
		Number of Stops	291,611	207,054
	Emission	**CO (g)**	262,627	253,383
		NO_x (g)	30,443	29,192
		SO_2 (g)	95	95
		EC (joule)	200,765,250,319	185,925,054,782
		AtmCO_2 (g)	14,428,156	13,361,750
		CO_2Equi (g)	14,428,156	13,361,750
WBT	**Variables**	**VMT (vehicle-miles)**	13,761	13,761
		Average Speed	18	19
		Volume	388,815	388,815
		Stops per Vehicle	0.50	0.46
		Number of Stops	194,408	178,542
	Emission	**CO (g)**	165,886	163,660
		NO_x (g)	19,198	18,897
		SO_2 (g)	61	61
		EC (joule)	125,554,575,860	121,989,693,908
		AtmCO_2 (g)	9,023,096	8,766,926
		CO_2Equi (g)	9,023,096	8,766,926
NBT	**Variables**	**VMT (vehicle-miles)**	13,512	13,512
		Average Speed	7	16
		Volume	388,815	388,815
		Stops per Vehicle	0.50	0.57
		Number of Stops	194,408	221,429
	Emission	**CO (g)**	187,321	167,965
		NO_x (g)	22,139	19,536
		SO_2 (g)	61	60
		EC (joule)	162,227,776,967	131,410,391,974

		AtmCO_2 (g)	11,658,396	9,443,877
		CO_2Equi (g)	11,658,396	9,443,877
SBT	**Variables**	**VMT (vehicle-miles)**	8,144	8,144
		Average Speed	15	16
		Volume	388,815	388,815
		Stops per Vehicle	0.75	0.49
		Number of Stops	291,611	189,652
	Emission	**CO (g)**	116,751	106,544
		NO_x (g)	13,869	12,488
		SO_2 (g)	36	36
		EC (joule)	104,032,282,094	87,635,759,346
		AtmCO_2 (g)	7,476,181	6,297,939
		CO_2Equi (g)	7,476,181	6,297,939

CHAPTER 7

CONCLUSIONS AND RECOMMENDATIONS

This study aims to develop models that estimate pollutant emissions based on macroscopic mobility measures, which can be estimated using macroscopic/mesoscopic analysis tools or can be measured or estimated using sensors in the real world. Such models can be used in signal optimization tools to allow the optimization of signal timings based on emission, combined with other measures. These models can also be used as part of sketch planning tools, macroscopic and mesoscopic simulation models, and real-world data analytical tools to allow for the assessment of environmental impacts of traffic controls.

The first effort of this study is to derive emission and energy consumption estimation models based on emission estimates from the MOVES operating mode distribution analysis procedure and performance measures from a microscopic simulation network. The MOVES operating mode distribution analysis procedure is believed to be the most accurate tool for emissions estimation when using vehicle trajectories from microscopic simulation model runs as input. Models with various combinations of independent variables were tested, and the study selected two models as the final models. The first model is based on the combination of vehicle miles traveled (VMT) and the total vehicle delays. The second model is based on a combination of VMT, vehicle delays, stop delays, and number of stops.

The two models were tested using a simulated real-world arterial in microscopic simulation. Both of these models showed acceptable performance for most of the investigated cases. However, in this test, it is recognized that both the model development and evaluation were based on microscopic simulation. Questions have been raised about the validity of the vehicle trajectories

from microscopic simulation models, particularly as they relate to vehicle acceleration and deceleration. Thus, vehicle trajectories from the Next Generation Simulation (NGSIM) program databases were used in a second test for model validation. It was found that in this test that the developed model with VMT and total vehicle delays showed reasonable estimations, and the percentage errors were within acceptable ranges. However, the second model, which is based on VMT, total vehicle delays, total stop delays, and number of stops, did not perform well. This could be because that model development required accurate vehicle trajectories, including accurate acceleration and deceleration estimates. The quality of the trajectories in microscopic simulation is expected to have affected the accuracy of the second model. Thus, it is recommended to use the first model based on VMT and vehicle delays to estimate estimation, if one of the two simulation-based models is used. Future work is needed with regard to the accuracy of vehicle trajectories from microscopic simulation models, as well as how can they be better calibrated and validated, and how they can impact the performance of models of the type developed in this study.

An additional effort was made to utilize the real-world trajectory data (NGSIM) data to develop emission and energy consumption estimation models utilizing a similar procedure as that used in the development of the simulation-based models, mentioned above. The independent variables included in the final estimation models are the VMT, average speed, and number of stops. The NGSIM data-based estimation models were compared to the simulation-based estimation models and the emission estimation models developed by USF in a previous study by examining the emission estimation for real-world roadway segments included in the NGSIM study. The comparison results indicate that the NGSIM data-based models perform better than simulation-based models.

As an example of the application of the developed emission models, this study developed a method to extract the required macroscopic input variables for the developed NGSIM data-based models (that is, VMT, average speed, and number of stops) from Wi-Fi and Inix data and used them in emission estimation. Instead of estimating the traffic count for each movement at the study intersection by multiplying the sampled vehicle counts from AVI data with an expansion factor, the turning movement counts available from a previous study were used to estimate the VMT for each movement. The average speed was obtained based on individual vehicle travel speed estimated from Inrix trajectory data and Wi-Fi matched vehicle data. The number of stops was esimated from both Inrix and Wi-Fi data by comparing the vehicle arriving time at the study intersection with signal timing data. The developed method was applied to the intersection located at SW 8th St. and SW 107th Ave in Miami, FL and the emission estimation results show that both Inrix and Wi-Fi data produce similar estimates of emissions. The case study demonstrates the proposed new approach for use by transportation agencies to assess environmental impacts of traffic control based on real-world data.

REFERENCES

Ahn, Kyoungho. Microscopic Fuel Consumption and Emission Modeling. Thesis, Blacksburg, Virginia: Virginia Polytechnic Institute and State University, 1998.

Cambridge Systematics, Summary Report: NGSIM Peachtree Street (Atlanta) Data Analysis (4:00 PM to 4:15 PM). FHWA, U.S. Department of Transportation, 2007.

Chamberlin, R., B. Holmén, E. Talbot, and K. Sentoff. "Comparative Analysis of the EPA Operating Mode Generator with Real World Operating Mode Data." Presented at 91st Annual Meeting of the Transportation Research Board, Washington D.C., 2012.

De Coensel, B., A. Cana, B. Degraeuwe, I. De Vlieger, D. Botteldooren. Effects of Traffic Signal Coordination on Noise and Air Pollutant Emissions. Environmental Modelling & Software. Vol. 35, pp74-83. 2012.

De Coensel, B., and D. Botteldooren. "Traffic Signal Coordination: A Measure to Reduce the Environmental Impact of Urban Road Traffic?" The 40th International Congress and Exposition on Noise Control Engineering. Japan, 2011.

Desarnaulds, V., G. Monay, and A. Carvalho. "Noise Reduction by Urban Traffic Management." the International Congresses on Acoustics. Kyoto, Japan, 2004.

Ellenberg, Marc, and Jean-Francois Bedeaux. "Calming Waves for Safety: A Time to Rethink Green Waves?" Traffic Technology International, 1999.

EPA. MOVES2010 Highway Vehicle Population and Activity Data. EPA-420-R-10-026, Environmental Protection Agency, 2010.

Frey, C., N. Rouphail, A. Unal, and J. Colyar. Emissions Reduction Through Better Traffic Management: An Empirical Evaluation Based upon On-Road Measurements. Final Report, Washington D.C.: Federal Highway Administration, 2001.

Frey, H. C., A. Unal, J. Chen, S. Li, and C. Xuan. Methodology for Developing Modal Emission Rates for EPA's Multi-Scale Motor Vehicle and Equipment Emission System. EPA-420-R-02-027, Environmental Protection Agency, 2002.

Ghafghazi, G., and M. Hatzopoulou. “Simulating the Environmental Effects of Isolated and Area-Wide Traffic Calming Schemes Using Traffic Simulation and Microscopic Emission Modeling.” Transportation, Vol. 41, No. 3, 2014, pp. 633-649.

Grumert, E., X. Ma, and A. Tapani. "Effects of A Cooperative Variable Speed Limit System on Traffic Performance and Exhaust Emissions." The 92nd Annual Meeting of the Transportation Research Board. Washington D.C., 2013.

Guo, R. An Investigation of the Relationship between Mobility and Environmental Externalities at Signalized Intersections. Presented at 26th Annual Conference of the International Chinese Transportation Professionals Association, Tampa, FL, 2013.

Guo, R. and Y. Zhang. An Investigation of the relationship between mobility and environmental externalities at signalized intersection. Presented at the ICTPA 2013, Tampa, FL, 2013.

Guo, R., and Y. Zhang. “Exploration of Correlation between Environmental Factors and Mobility at Signalized Intersections.” Transportation Research Part D: Transport and Environment, Vol. 32, 2014, pp. 24-34.

Hadi, M., D. Ni, T. Rioux, and P. Vortisch. Microscopic Simulation Model Support of Emission Estimation. In SimSub Annual Report, 2011, pp. 32-36.

Hallmark, S., I. Fomunung, R. Guensler, and W. Bachman. "Assessing Impacts of Improved Signal Timing as a Transportation Control Measure Using an Activity-Specific Modeling Approach." Transportation Research Record: Journal of the Transportation Research Board 1738, no. 1 (2000): 49-55.

Highway Capacity Manual. Transportation Research Board of the National Academies, 2010.

Kim, E., and E. Choi. "Estimates of Critical Values of Aggressive Acceleration from a Viewpoint of Fuel Consumption and Emission." The 92nd Annual Meeting of the Transportation Research Board. Washington D.C., 2013.

Koupal, J., L. Landman, E. Nam, J. Warila, C. Scarbro, E. Glover, and R. Giannelli. MOVES2004 Energy and Emission Inputs Draft Report. EPA-420-P-05-003, Environmental Protection Agency, 2005.

Li X., G. Li, S. Pang, X. Yang, J. Tian. "Signal Timing of Intersections Using Integrated Optimization of Traffic Quality, Emissions and Fuel Consumption: a Note." Transportation Research Part D, Vol.9, pp. 401–407, 2004

Liao, T. "A Fuel-Based Signal Optimization Model." Transportation Research Part D: Transport and Environment 23 (2013): 1-8.

Liao, T., and R. Machemehl. Energy Conservation through Enhanced Traffic Signal Responsiveness. Report Produced For the Southwest Region University Transportation Center, Austin, Texas, 1995.

Liao, T., and R. Machemehl. Optimal Traffic Signal Strategy for Fuel Consumption and Emissions Control at Signalized Intersections. Presented at 24th European Transport Forum, Brunel University, England, 1996.

Lin, J., Y. Chiu, S. Vallamsundar, and S. Bai. "Integration of MOVES and Dynamic Traffic Assignment Models for Fine-Grained Transportation and Air Quality Analyses." Presented at 2011 IEEE Forum on Integrated and Sustainable Transportation Systems, Vienna, Austria, 2011.

Meyer, M., C. Burbank, L. Zeimer, C. Porter, J. Potter, and J. Wilson. Practitioner's Guide to Incorporating Greenhouse Gas Emissions into the Collaborative Decision-Making Process. SHRP 2 Report S2-C09-RW-2, Transportation Research Board, Washington D.C., 2013.

Midenet, S., F. Boillot, and J. C. Pierrelée. Signalized Intersection with Real-Time Adaptive Control: On-Field Assessment of CO2 And Pollutant Emission Reduction. Transportation Research Part D: Transport and Environment, Vol. 9, No. 1, 2004, pp. 29-47.

Mitra, S. and P. Pravallika. An Approach to Tackle Urban Congestion and Vehicle Emission by Manimpuating Transport Operations and Vehicle Mix. Springer-Verlab Berlin Heidelberg, 2013.

Moore, S.E., and P.R. Lowrie. Further on the effect of coordinated traffic signal systems on traffic accidents. Proceedings of the 8th AARB Conference 8(5), Session 26, 10-15, 1976.

Motor Vehicle Emission Simulator (MOVES) User Guide for MOVES2010b. Environmental Protection Agency, 2012.

Pandian, S., S. Gokhale, and A.K. Ghoshal. Evaluating effects of traffic and vehicle characteristics on vehicular emissions near traffic intersections. Transportation Research Part D, Vol. 14, pp. 180–196, 2009.

Park, B., I. Yun, and K. Ahn. "Stochastic Optimization for Sustainable Traffic Signal Control." International Journal of Sustainable Transportation 3, no. 4 (2009): 263-284

Rakha, H., A. Medina, H. Sin, F. Dion, M. Van Aerde, and J. Jeng. "Traffic Signal Coordination across Jurisdictional Boundaries." Transportation Research Record: Journal of the Transportation Research Board 1727, no. 1 (2000): 42-51.

Rakha, H., M. V. Aerde, K. Ahn, and A. Trani. "Requirements for Evaluating Traffic Signal Control Impacts on Energy and Emissions Based on Instantaneous Speed and Acceleration Measurements." Transportation Research Record: Journal of the Transportation Research Board 1738, no. 1 (2000): 56-67.

Sabra, Z., D. Gettman, D. Henry, and V. Nallamothu. Balancing Safety and Capacity in an Adaptive Signal Control System—Phase 1. Final report for FHWA. Washington, D.C., 2010

Skabardonis, A. "ITS Benefits: The Case of Traffic Signal Control Systems." Presented at the Transportation Research Board 80th Annual Meeting, Washington, D.C., 2011.

Skabardonis, A., N. Geroliminis, E. Christofa. Vehicle Emissions Estimations under Oversaturated Conditions along Signalized Arterials. Presented at the 91st Transportation Research Board Annual Meeting, Washington, D.C., 2012.

Smaglik, E., D. Bullock, D. Gettman, C. Day, and H. Premachandra. "Comparison of Alternative Real-Time Performance Measures for Measuring Signal Phase Utilization and Identifying Oversaturation." Transportation Research Record: Journal of the Transportation Research Board 2259 (2011): 123-131.

Song, G., L. Yu, and L. Xu. Comparative Analysis of Car-Following Models for Emission Estimation. In Transportation Research Record: Journal of the Transportation Research Board, No. 2341, Transportation Research Board of the National Academies, Washington, D.C., 2013, pp. 12-22.

Stevanovic, A., J. Stevanovic, D. Jolovic, and V. Nallamothu. Retiming Traffic Signals to Minimize Surrogate Safety Measures on Signalized Road Networks. The 91st Transportation Research Board Annual Meeting, Washington, D.C., 2012.

Stevanovic, A., J. Stevanovic, K. Zhang, and S. Batterman. "Optimizing Traffic Control to Reduce Fuel Consumption and Vehicular Emissions." Transportation Research Record: Journal of the Transportation Research Board 2128, no. 1 (2009): 105-113.

TranSystems, and E.H. Pechan & Associates, Inc. MOVES Operating Mode Distribution Generator Documentation Report. EPA-420-B-12-037, Environmental Protection Agency, 2012.

Unal, Alper, Naugi Rouphail, and Christopher Frey. "Effect of Arterial Signalization and Level of Service on Measured Vehicle Emissions." Transportation Research Record: Journal of the Transportation Research Board 1842, no. 1 (2003): 47-56.

Yang, D. and Y. Ju. Multi-objective Optimization Method of Traffic Signal Based on CTM. Journal of Traffic and Transportation Engineering, Vol. 11, No. 3, pp. 105-110, 2011.

Zhang, L., Y. Yin, S. Chen. Robust Signal Timing Optimization with Environmental Concerns. Transportation Research Part C, Vol. 29, pp. 55–71, 2013.

Zhao, Y., and A. Sadek. Evaluating the Accuracy of Approaches to Integrating Microscopic Traffic Simulators with Emissions Models for Project-Level Emissions Analysis. Presented at 92nd Annual Meeting of the Transportation Research Board, Washington D.C., 2013.

Zimmerman, K.H. and J.A. Bonneson. In-Service Evaluation of a Detection-Control System for High-Speed Signalized Intersections, Implementation Report No. 5-4022-01-1, Texas Transportation Institute, College Station, TX, 2005

APPENDIX

COMPARISON OF INRIX AND WI-FI DATA

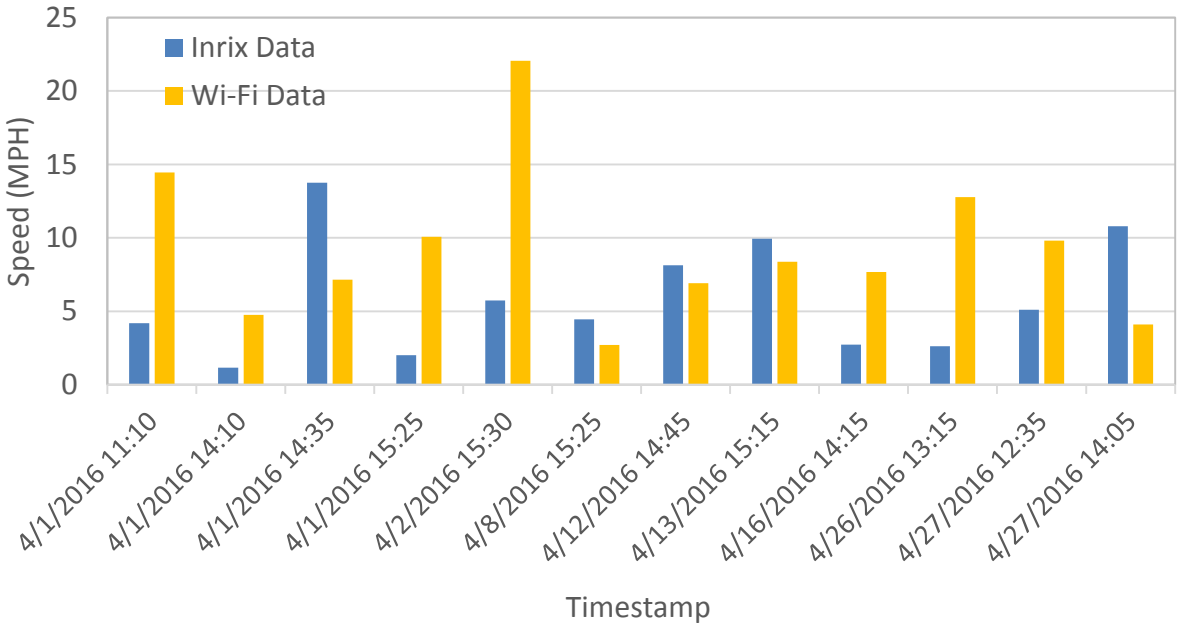

Figure A-1. Comparison of speed for eastbound left turn movement during the midday.

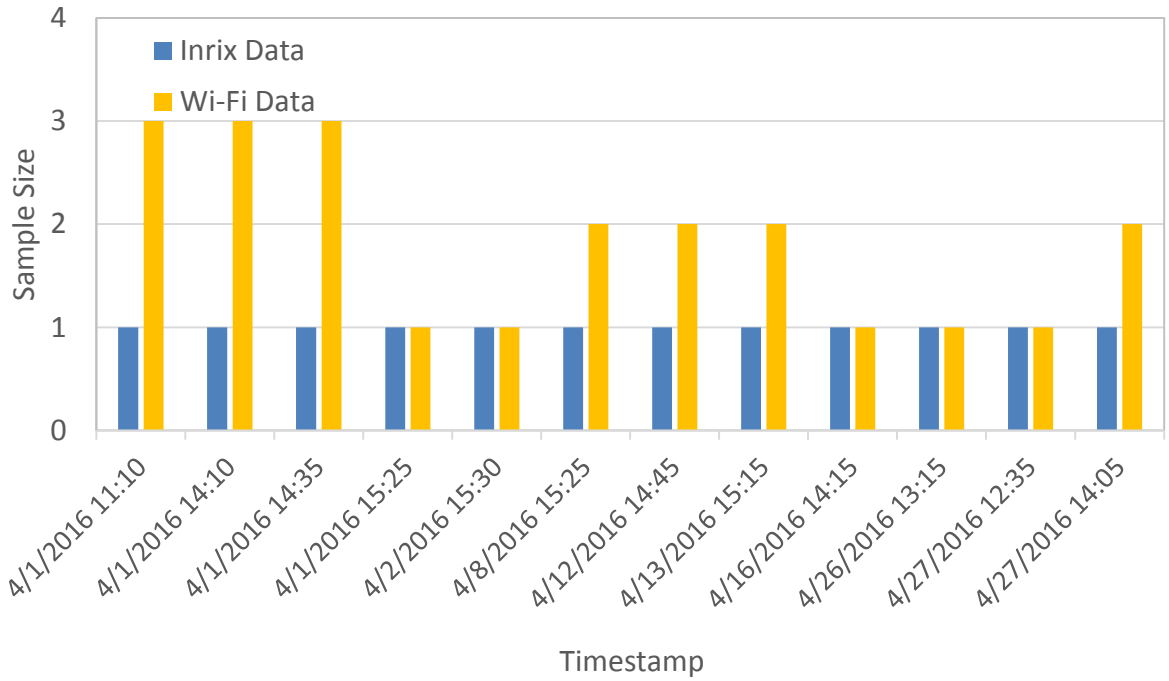

Figure A-2. Comparison of sample size for eastbound left turn movement during the midday.

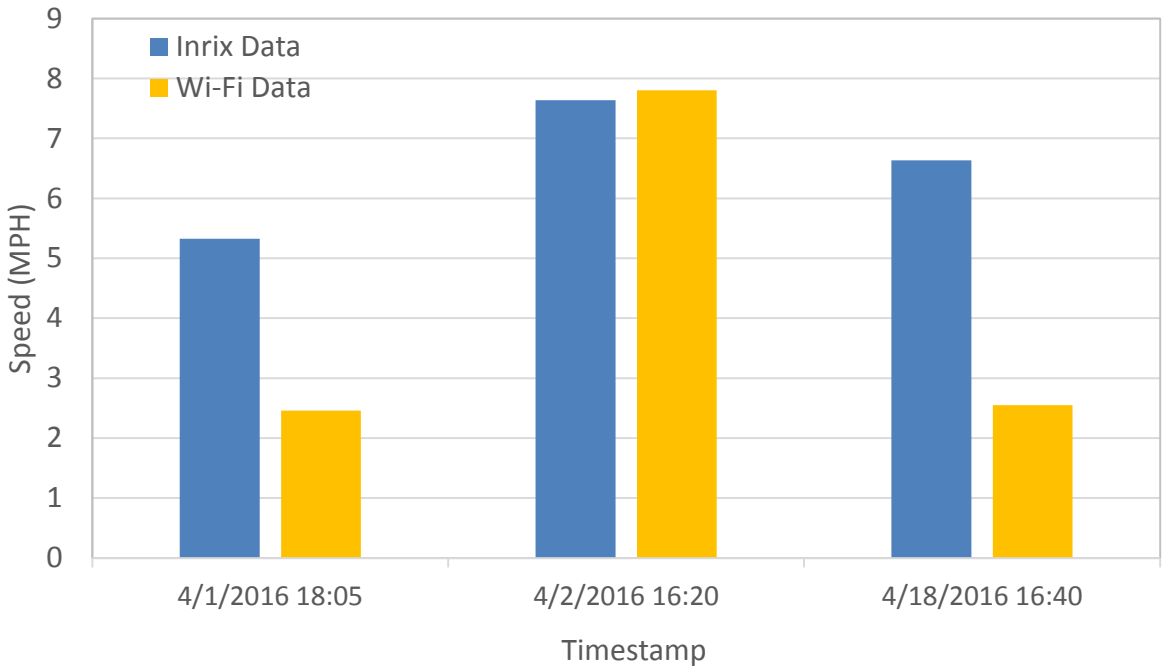

Figure A-3. Comparison of speed for eastbound left turn movement during the PM peak period.

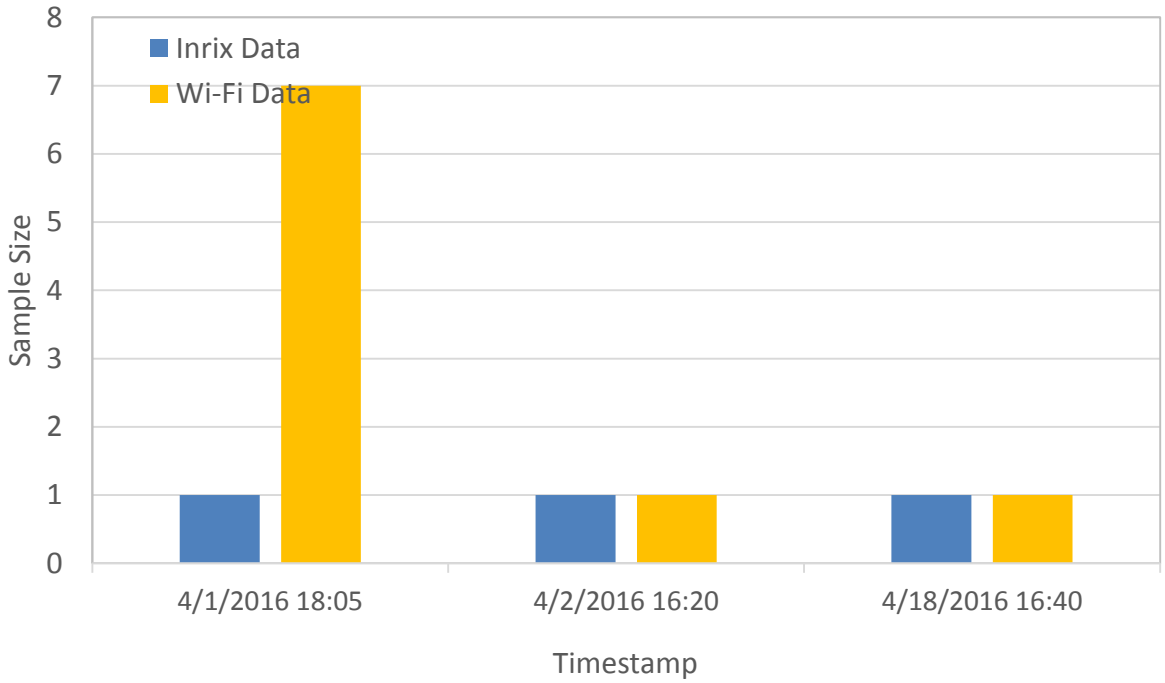

Figure A-4. Comparison of sample size for eastbound left turn movement during the PM peak period.

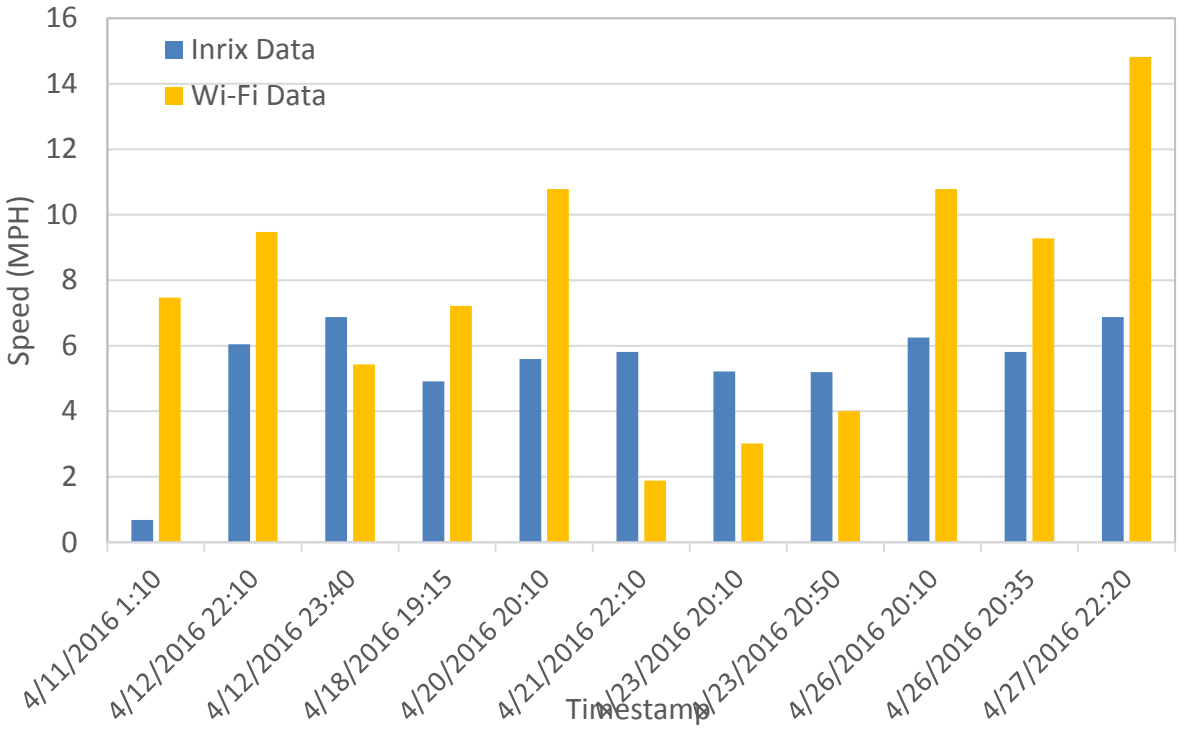

Figure A-5. Comparison of speed for eastbound left turn movement during the night and early morning period.

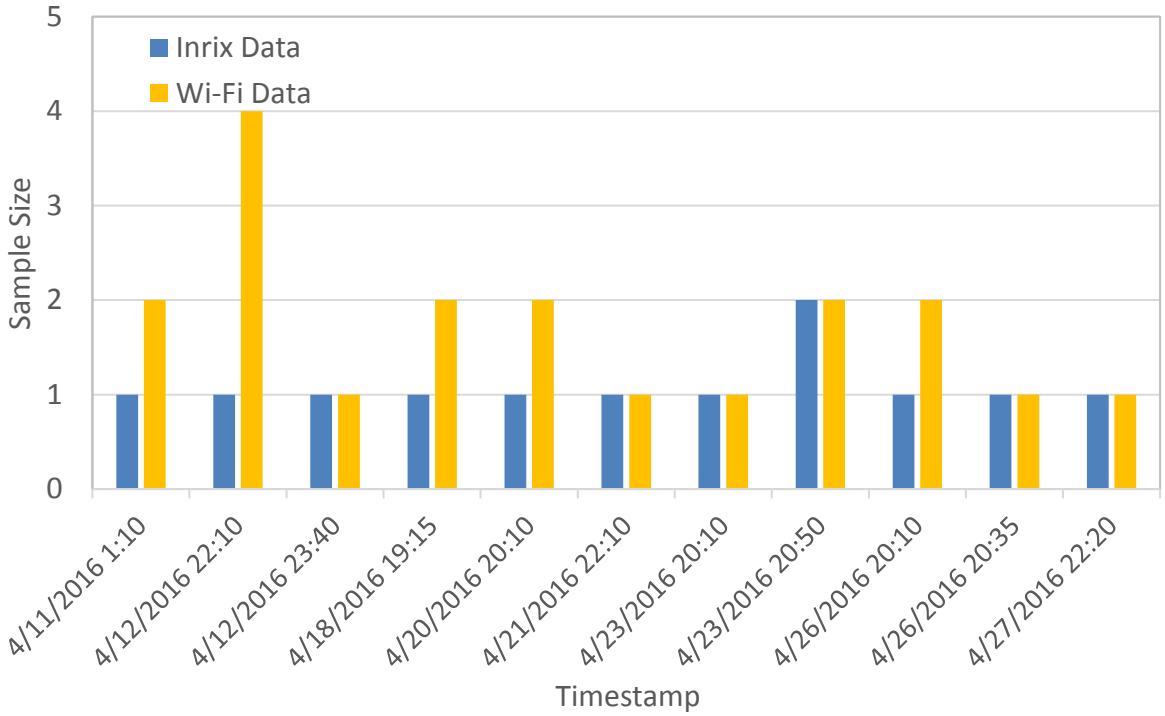

Figure A-6. Comparison of sample size for eastbound left turn movement during the night and early morning period.

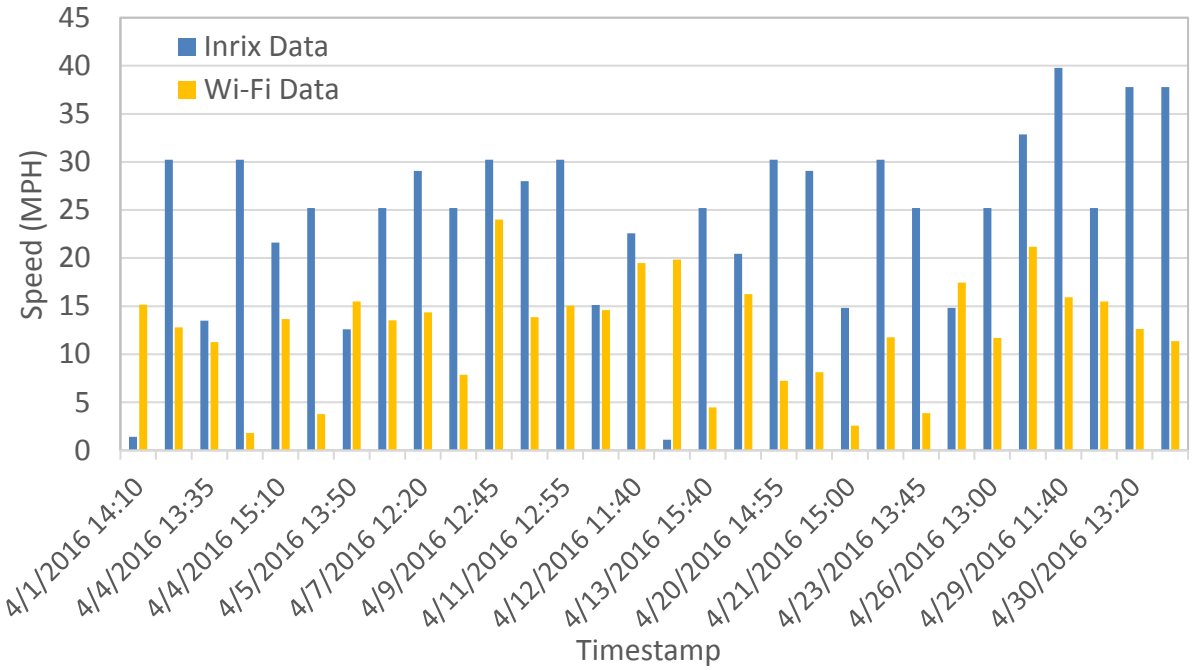

Figure A-7. Comparison of speed for eastbound right turn movement during the midday.

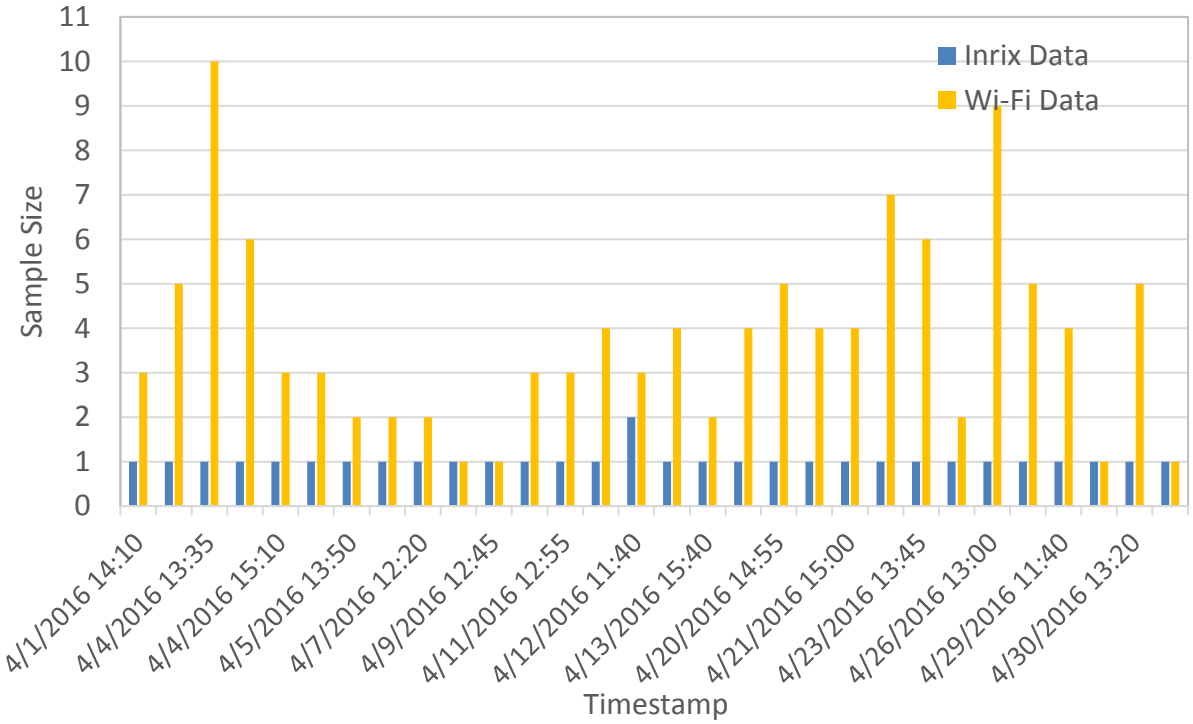

Figure A-8. Comparison of sample size for eastbound right turn movement during the midday.

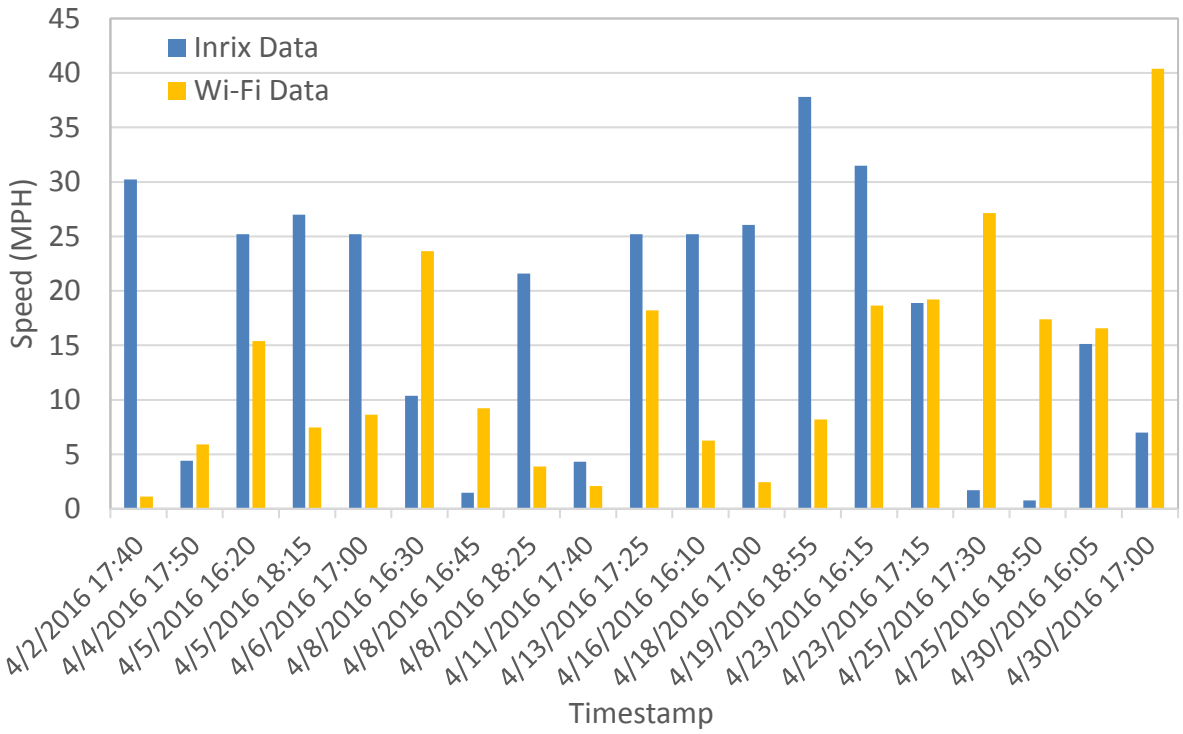

Figure A-9. Comparison of speed for eastbound right turn movement during the PM peak period.

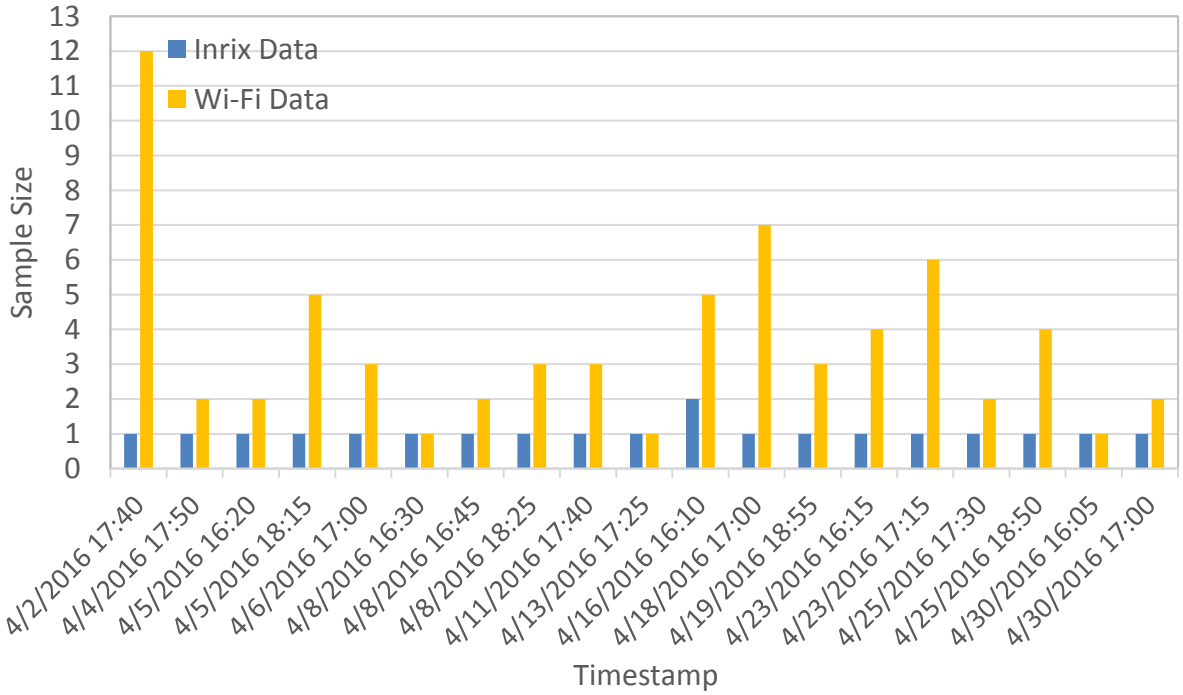

Figure A-10. Comparison of sample size for eastbound right turn movement during the PM peak period.

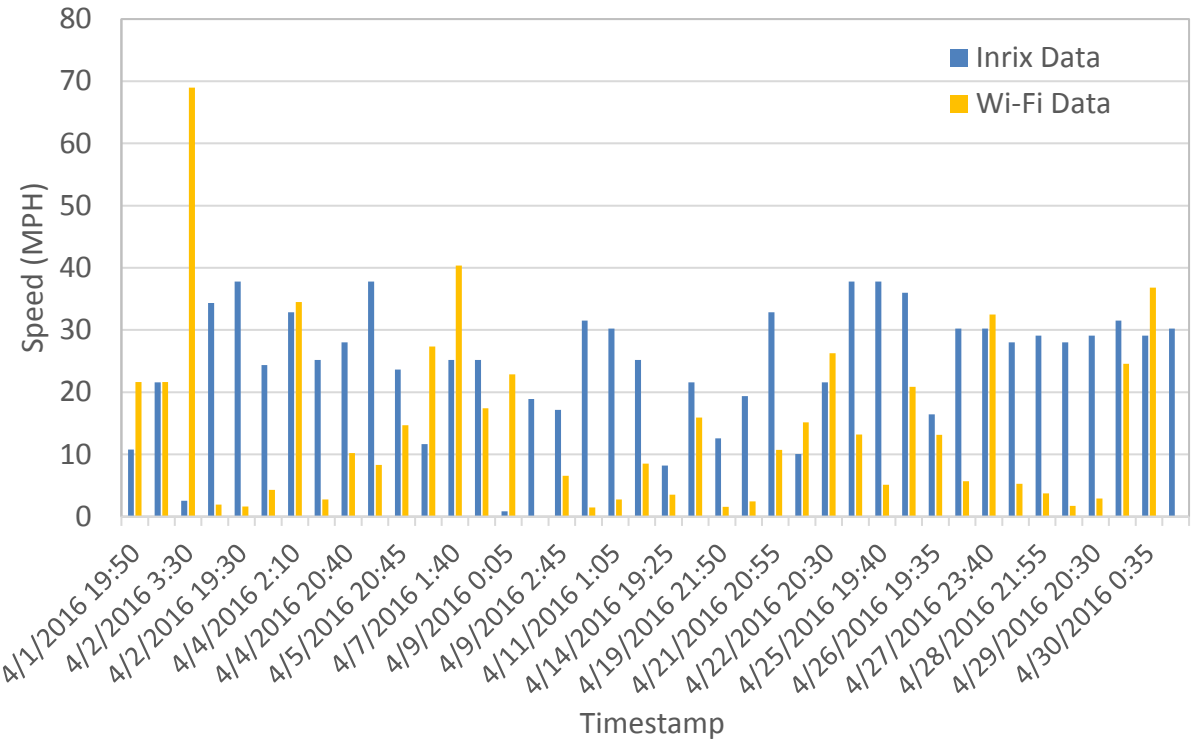

Figure A-11. Comparison of speed for eastbound right turn movement during the night and early morning period.

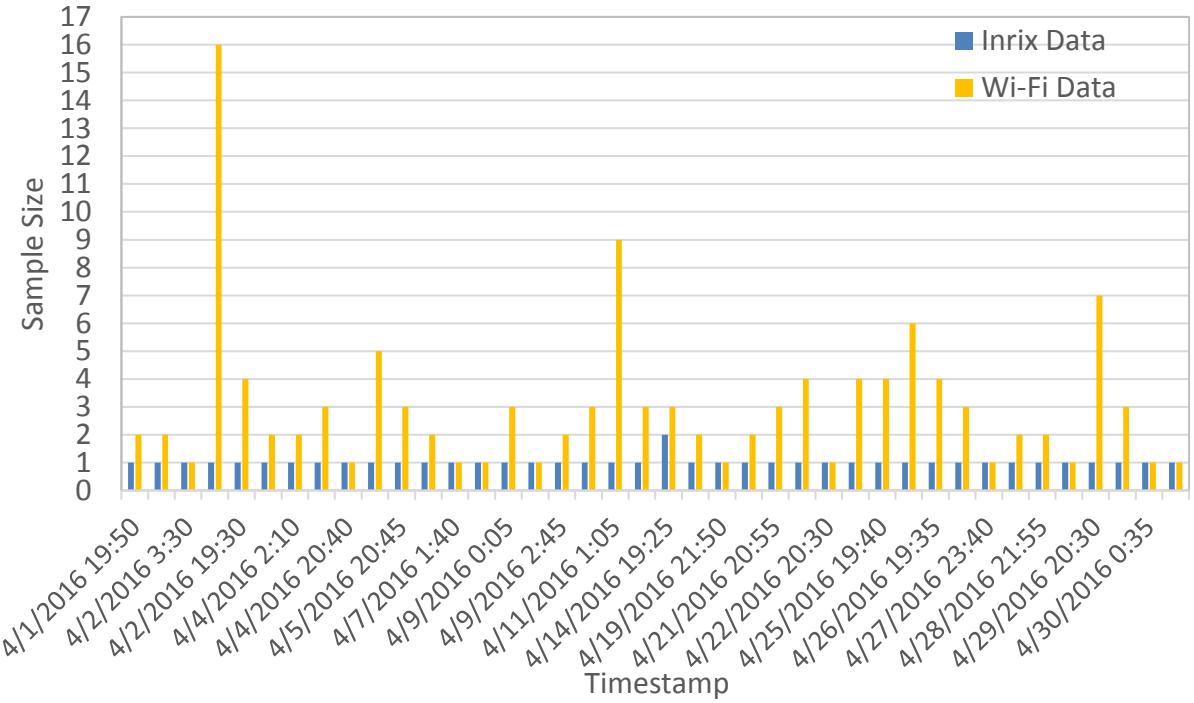

Figure A-12. Comparison of sample size for eastbound right turn movement during the night and early morning period.

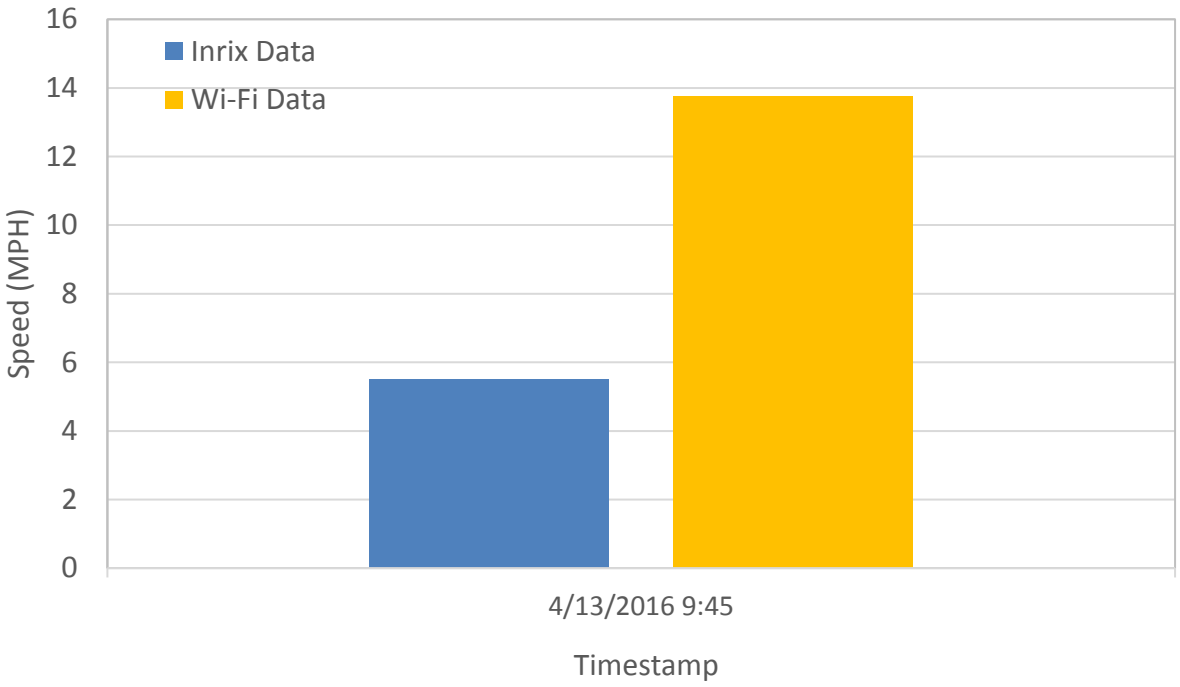

Figure A-13. Comparison of speed for westbound left turn movement during the AM peak period.

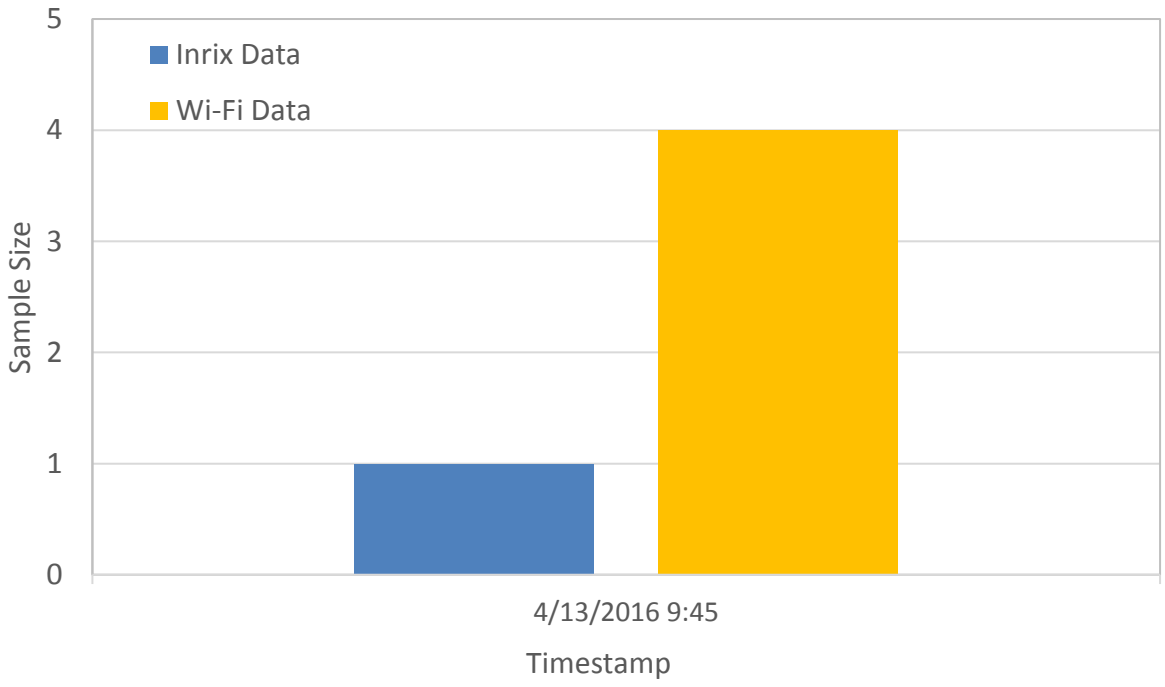

Figure A-14. Comparison of sample size for westbound left turn movement during the AM peak period.

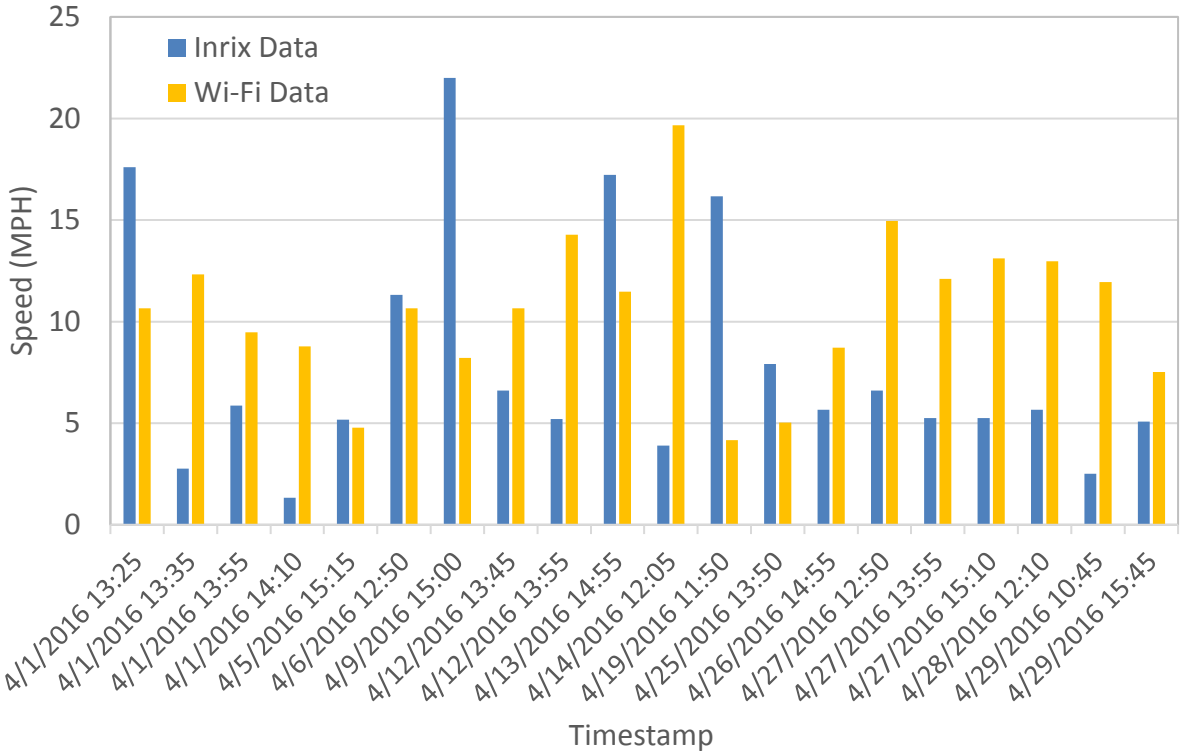

Figure A-15. Comparison of speed for westbound left turn movement during the midday.

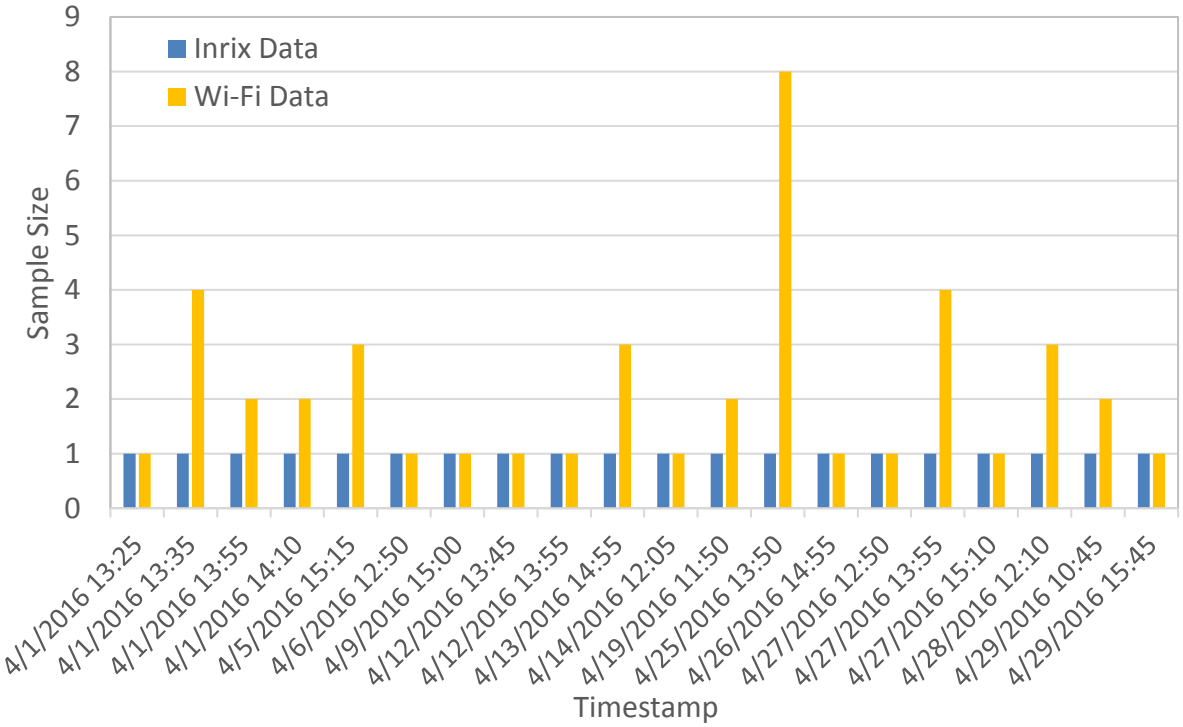

Figure A-16. Comparison of sample size for westbound left turn movement during the midday.

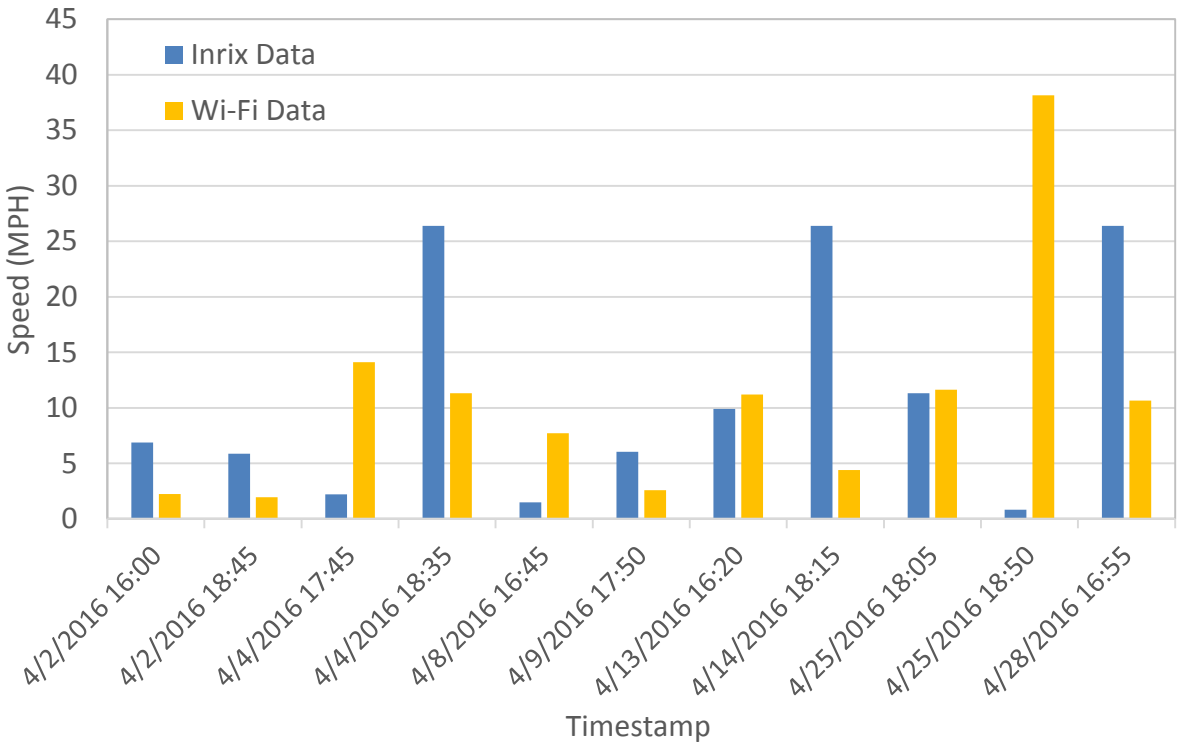

Figure A-17. Comparison of speed for westbound left turn movement during the PM peak period.

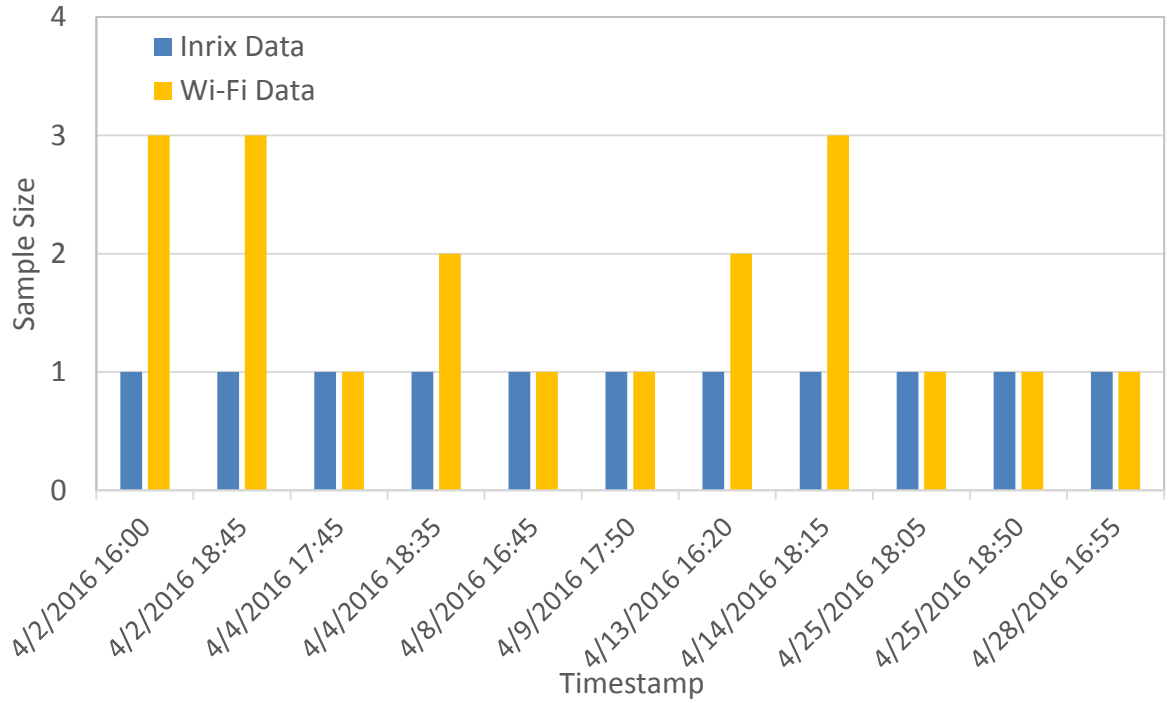

Figure A-18. Comparison of sample size for westbound left turn movement during the PM peak period.

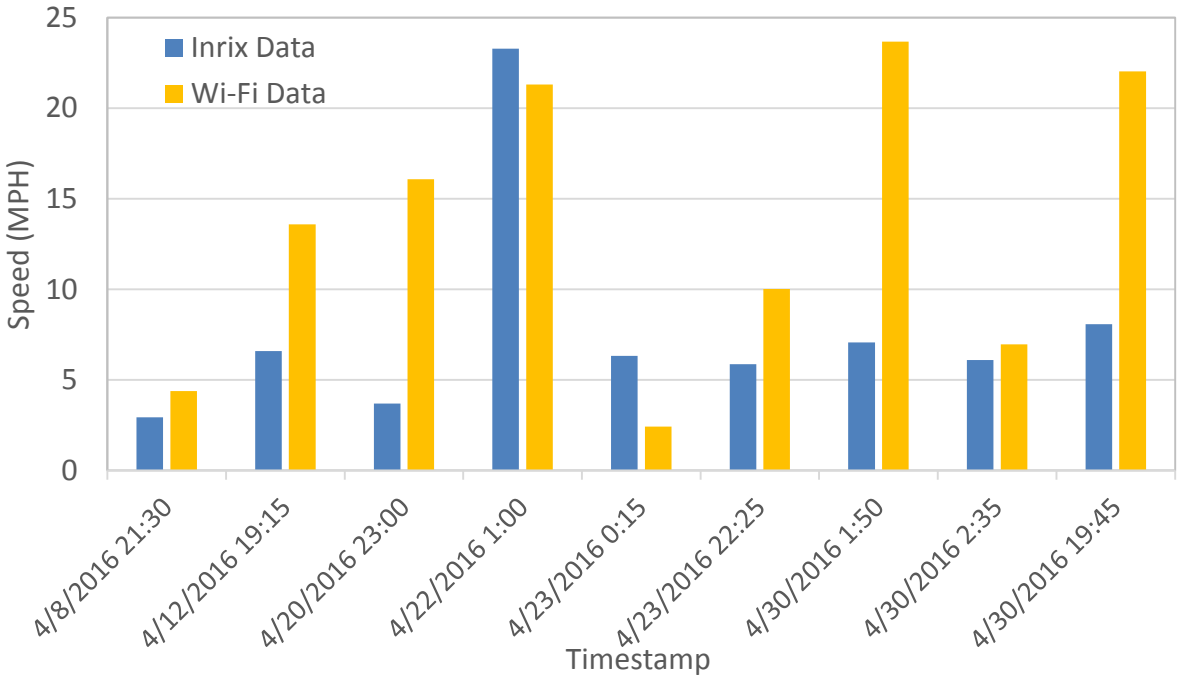

Figure A-19. Comparison of speed for westbound left turn movement during the night and early morning period.

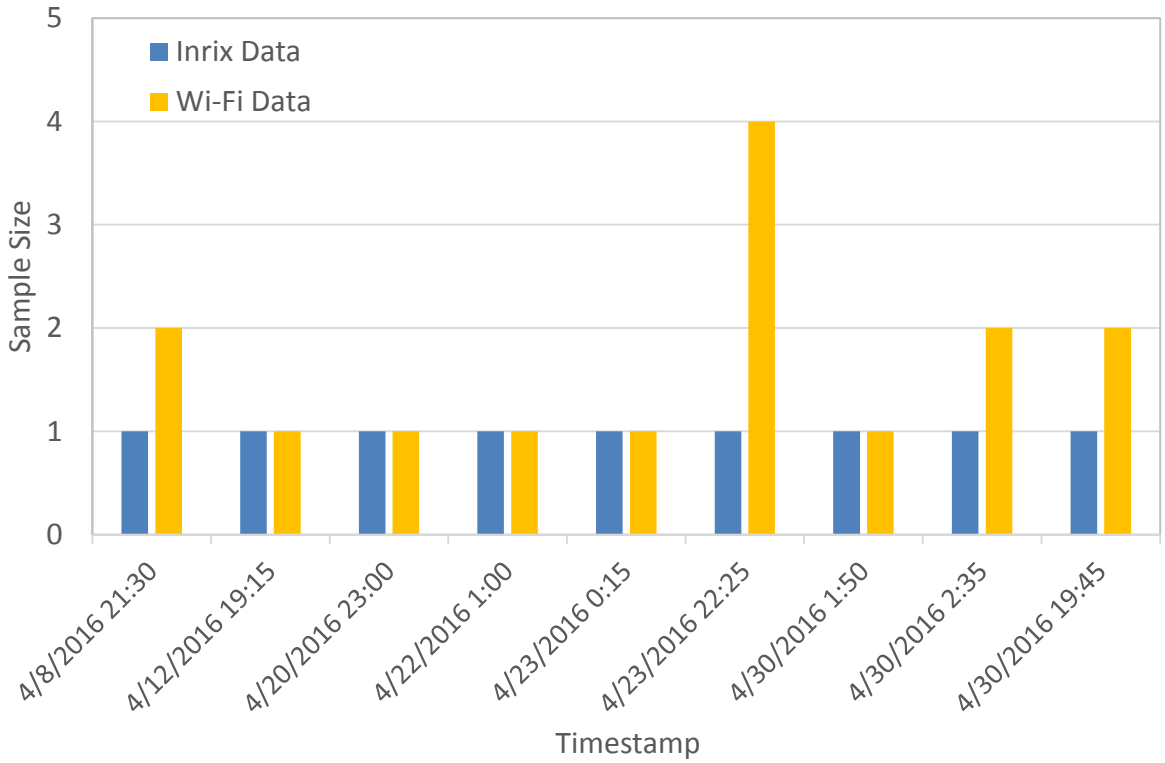

Figure A-20. Comparison of sample size for westbound left turn movement during the night and early morning period.

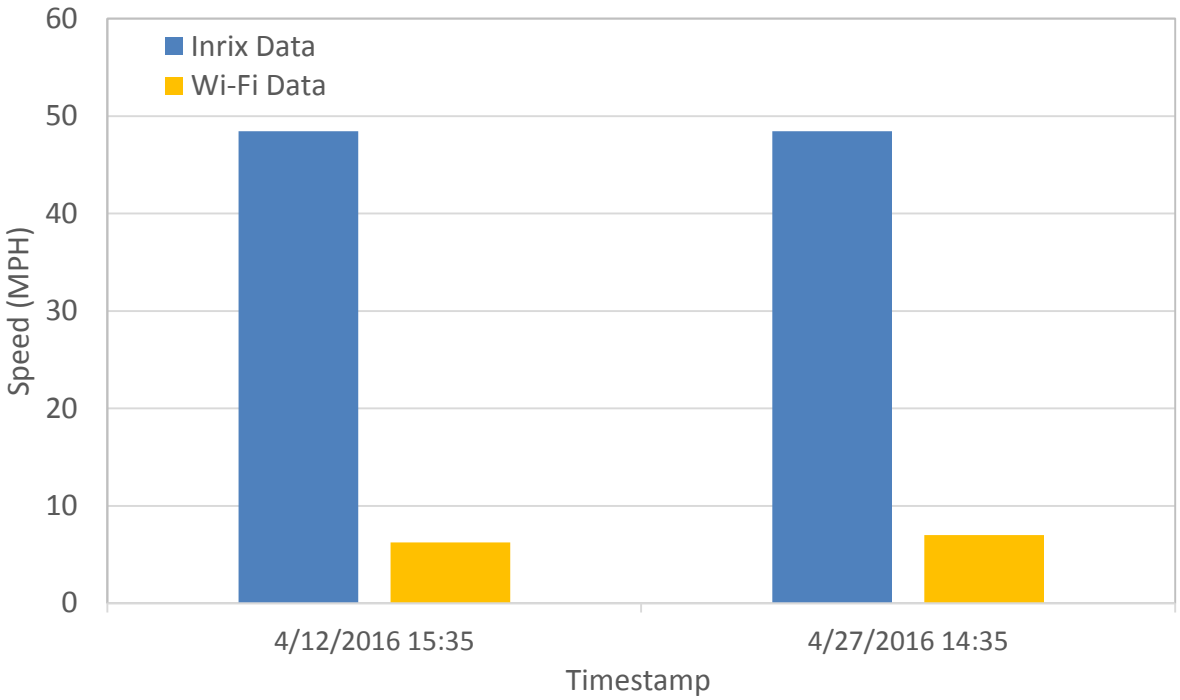

Figure A-21. Comparison of speed for westbound right turn movement during the midday.

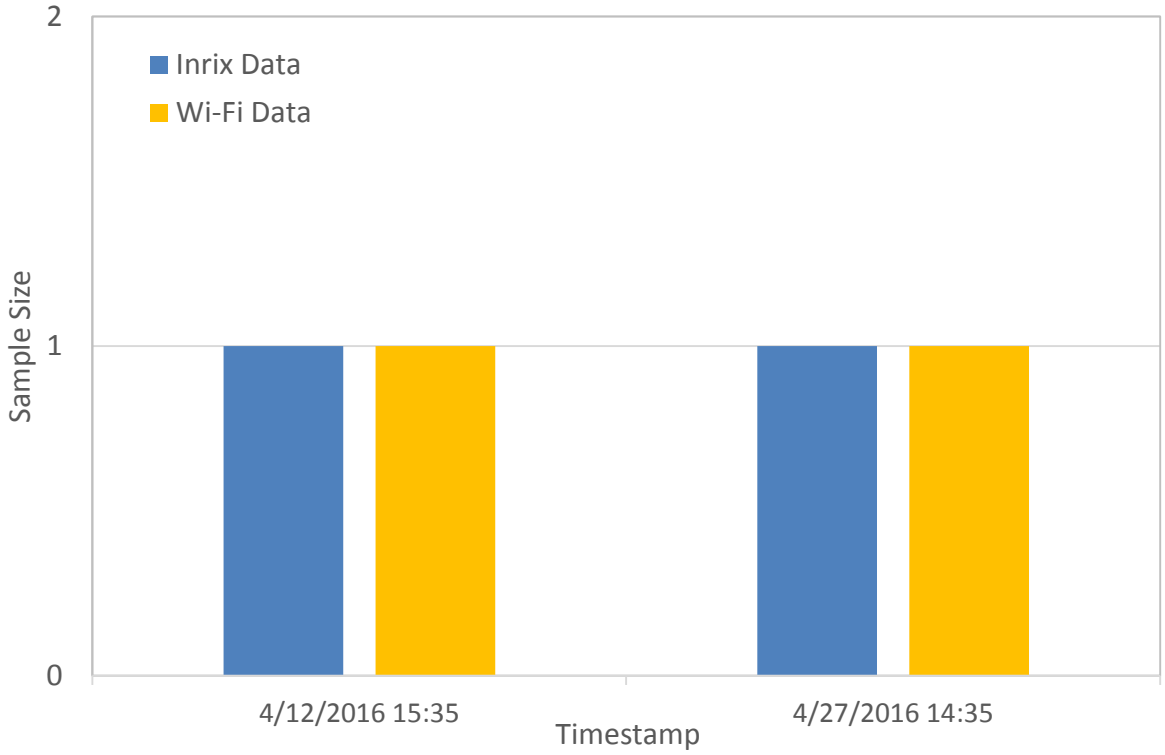

Figure A-22. Comparison of sample size for westbound right turn movement during the midday.

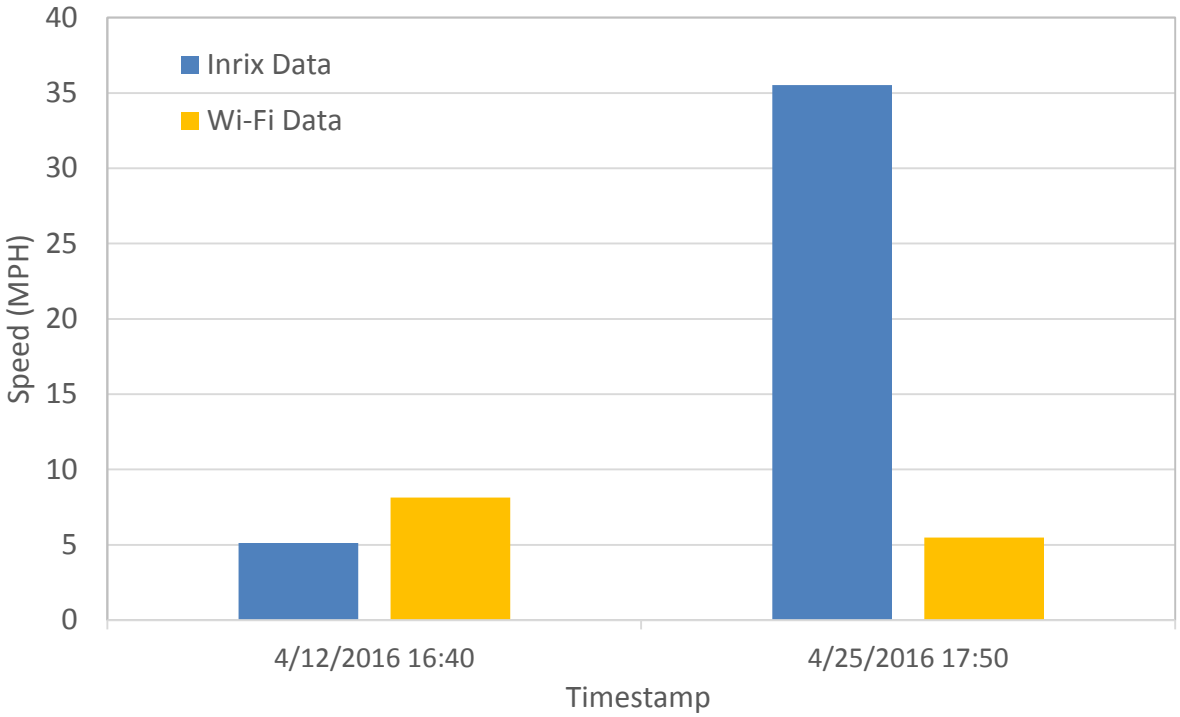

Figure A-23. Comparison of speed for westbound right turn movement during the PM peak period.

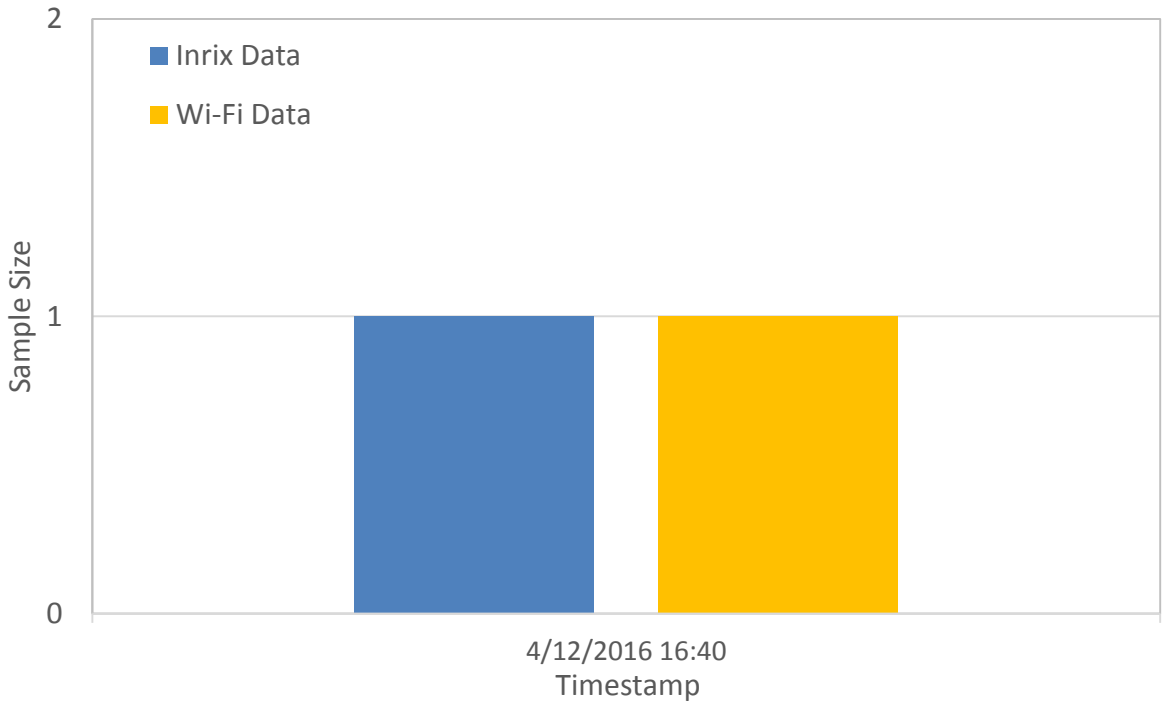

Figure A-24. Comparison of sample size for westbound right turn movement during the PM peak period.

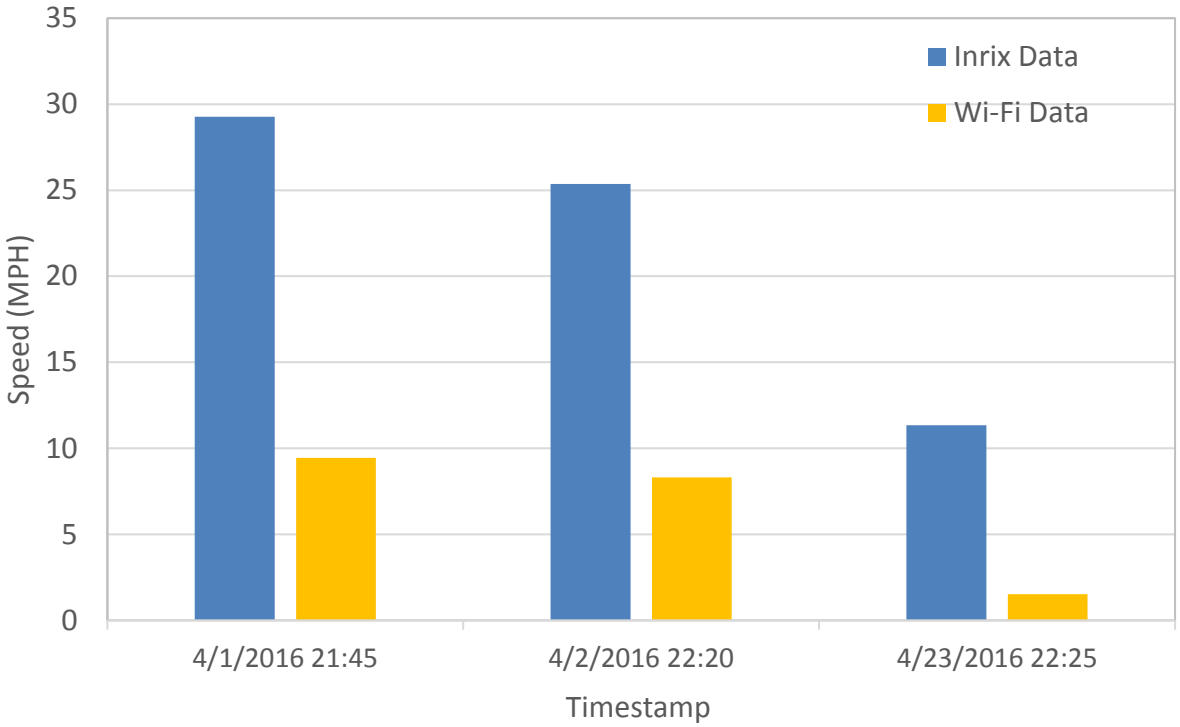

Figure A-25. Comparison of speed for westbound right turn movement during the night and early morning period.

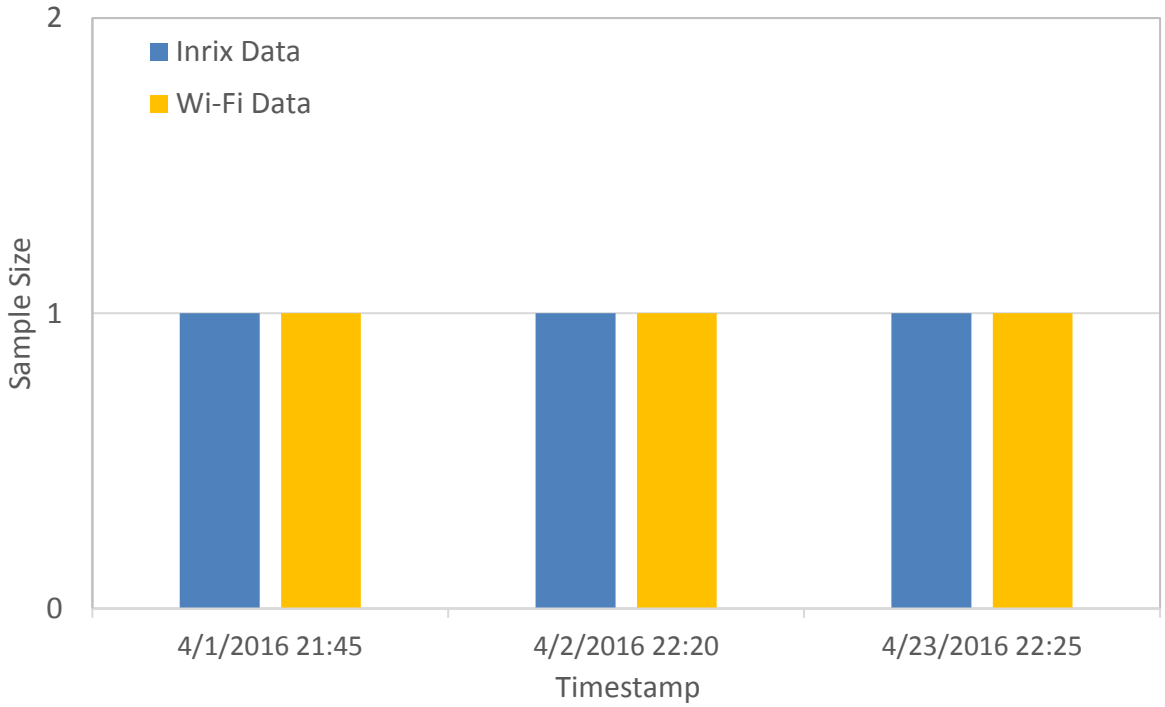

Figure A-26. Comparison of sample size for westbound right turn movement during the night and early morning period.

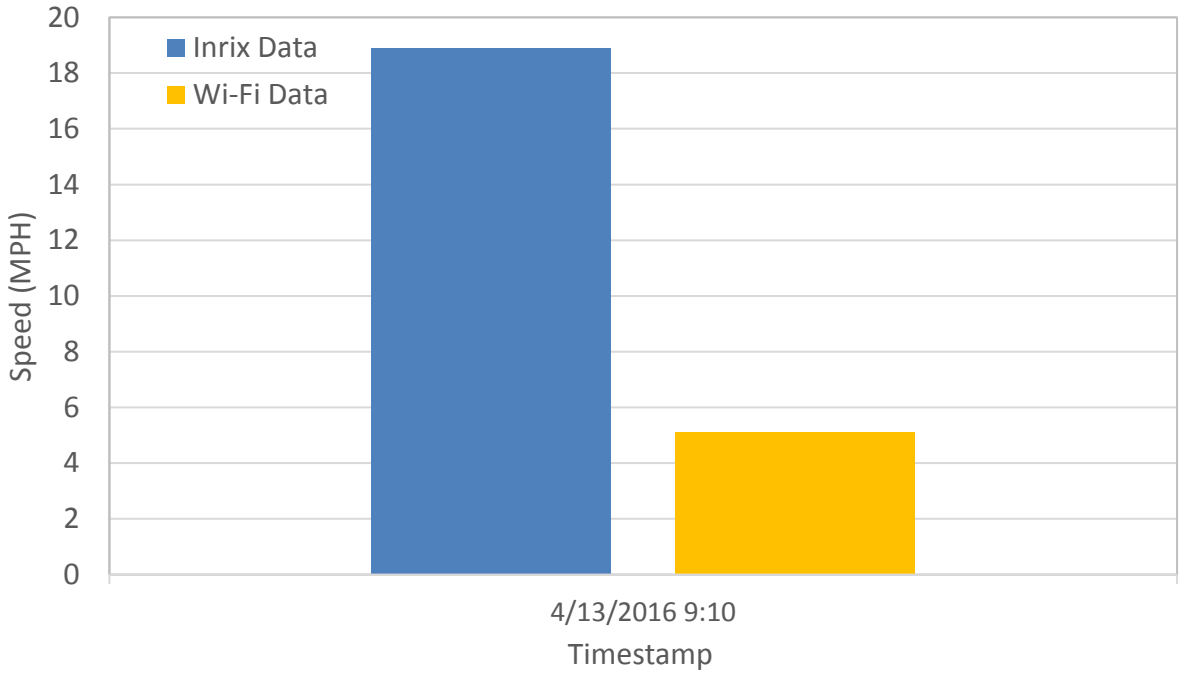

Figure A-27. Comparison of speed for northbound left turn movement during the AM peak period.

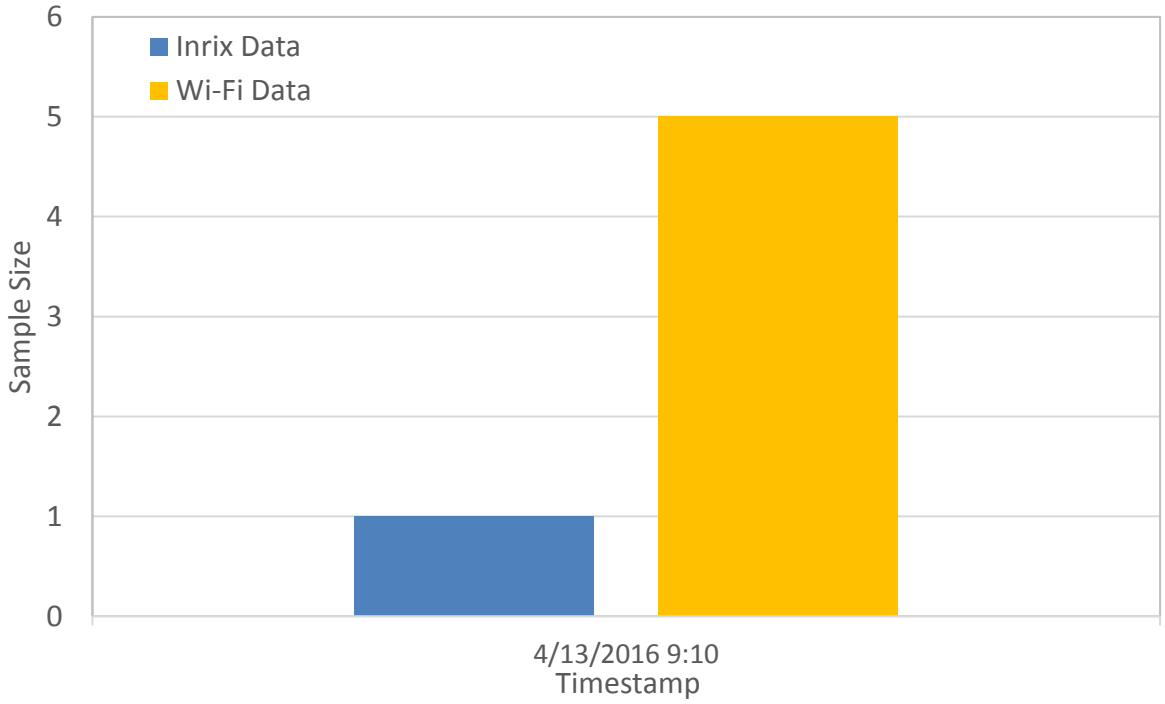

Figure A-28. Comparison of sample size for northbound left turn movement during the AM peak period.

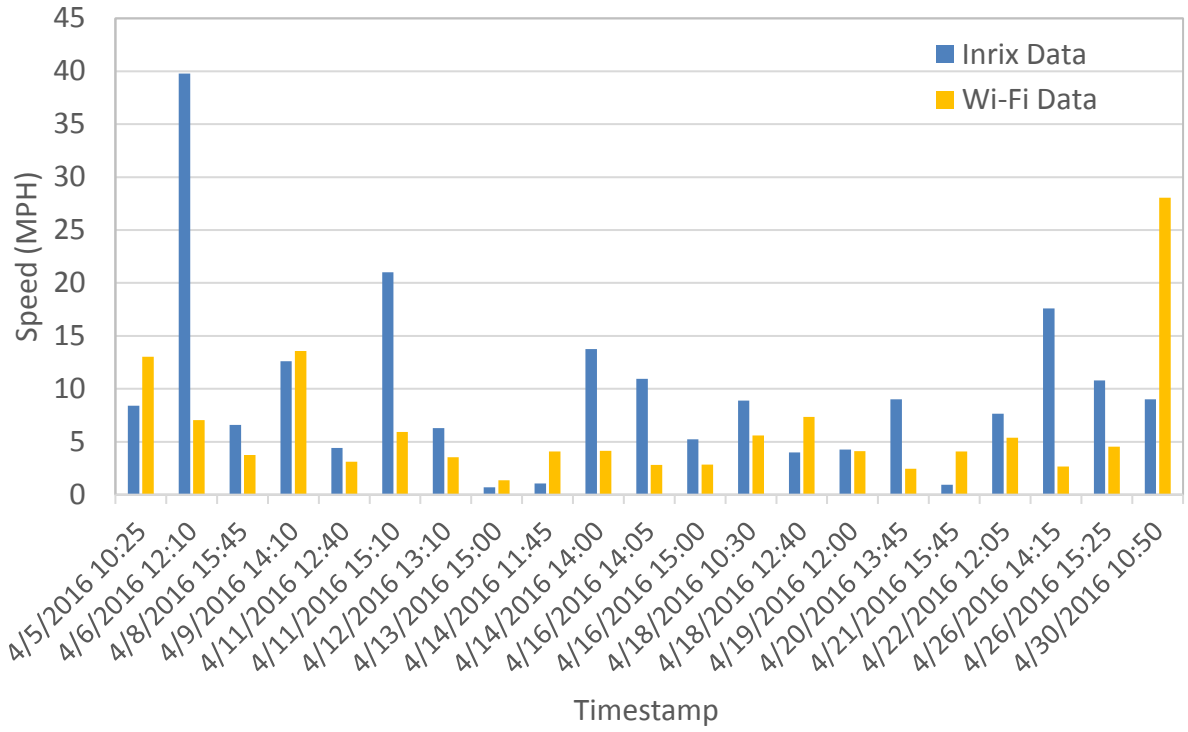

Figure A-29. Comparison of speed for northbound left turn movement during the midday.

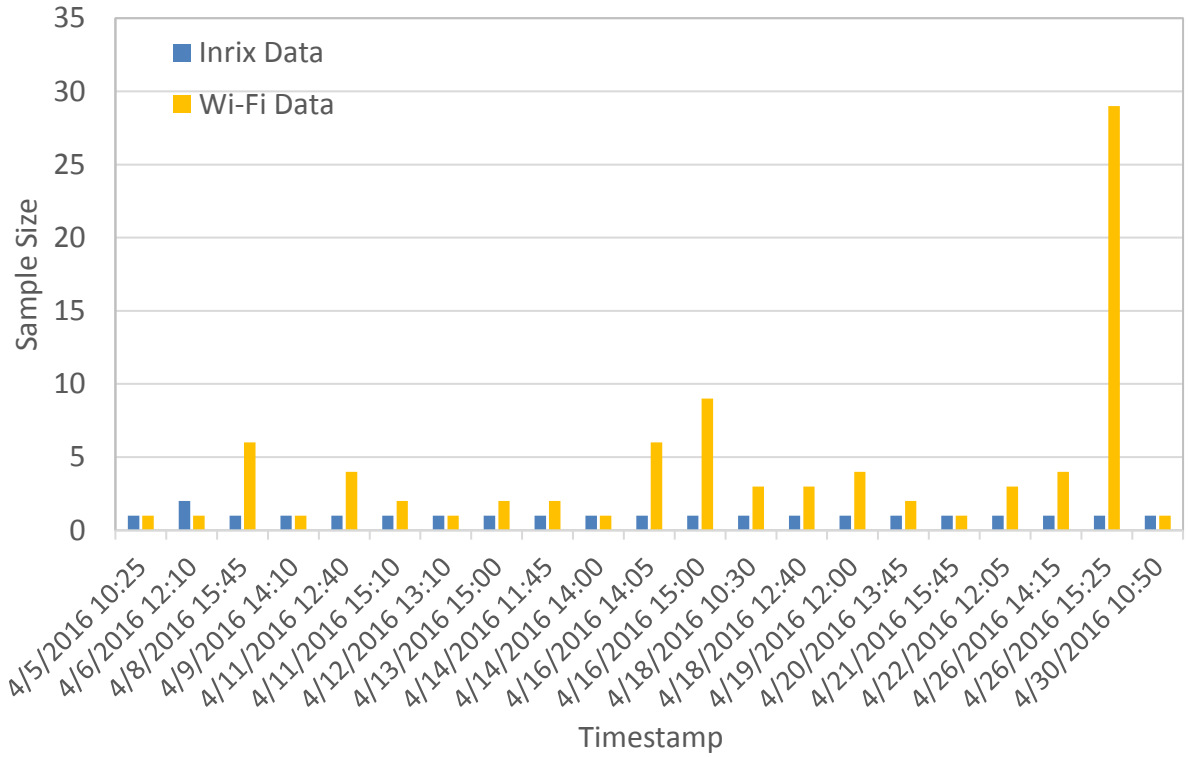

Figure A-30. Comparison of sample size for northbound left turn movement during the midday.

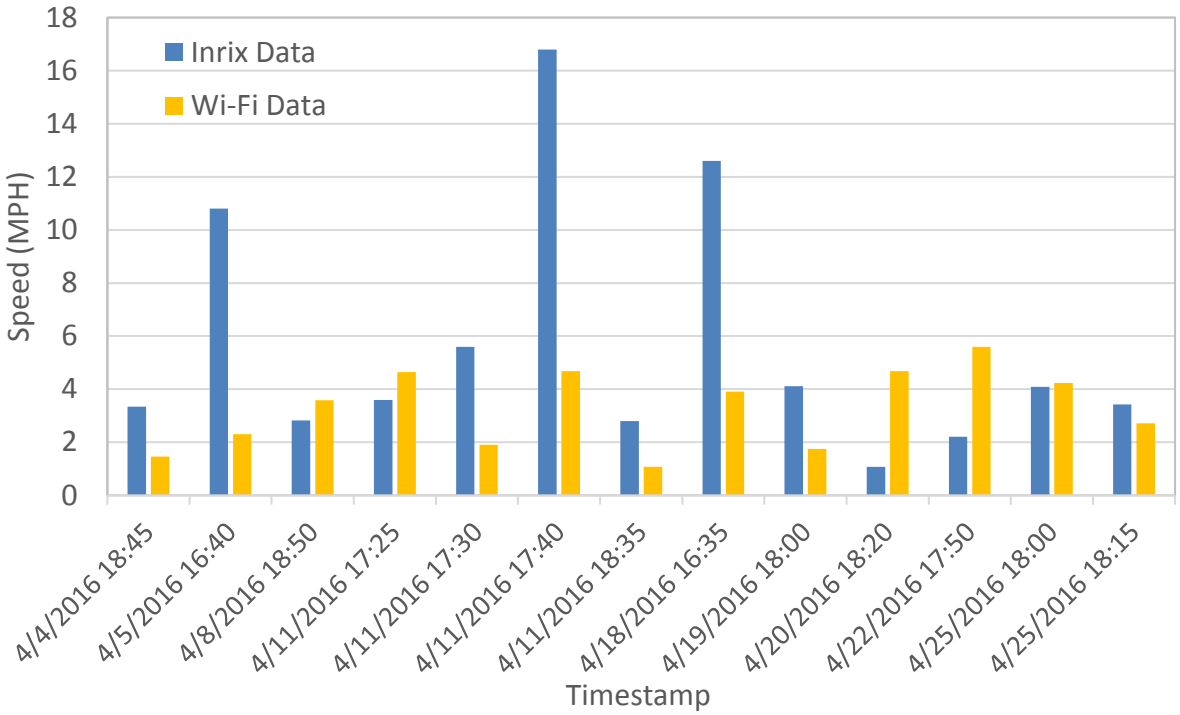

Figure A-31. Comparison of speed for northbound left turn movement during the PM peak period.

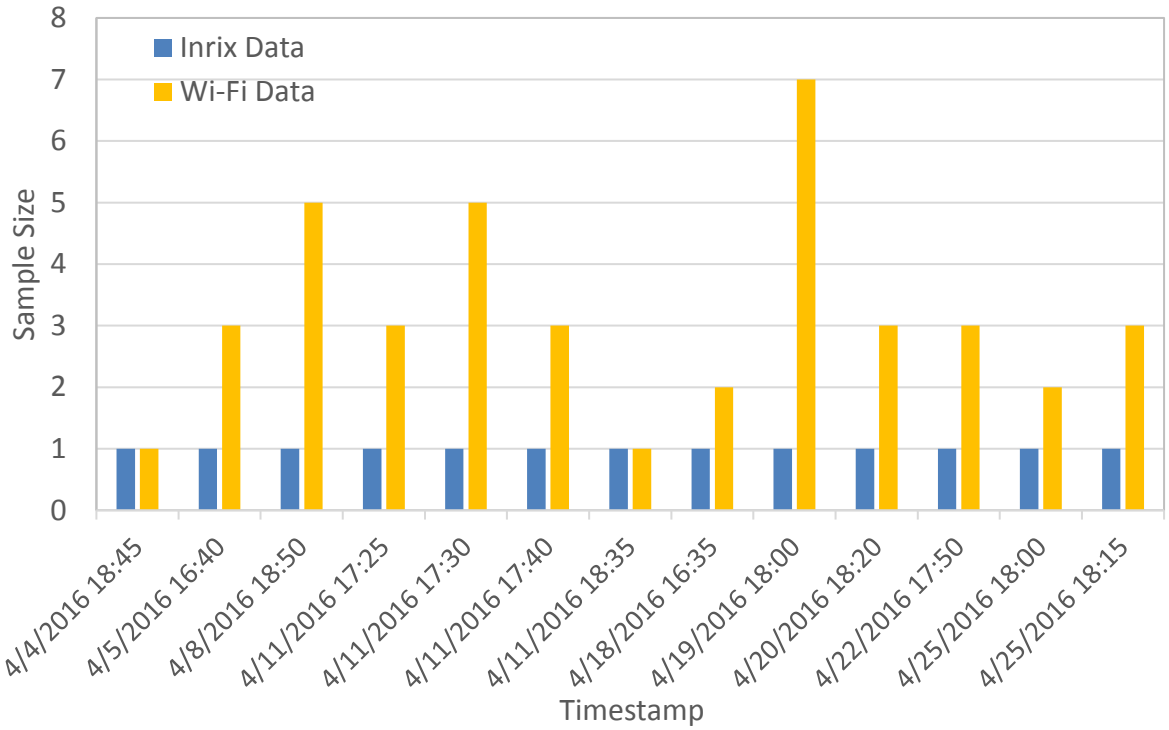

Figure A-32. Comparison of sample size for northbound left turn movement during the PM peak period.

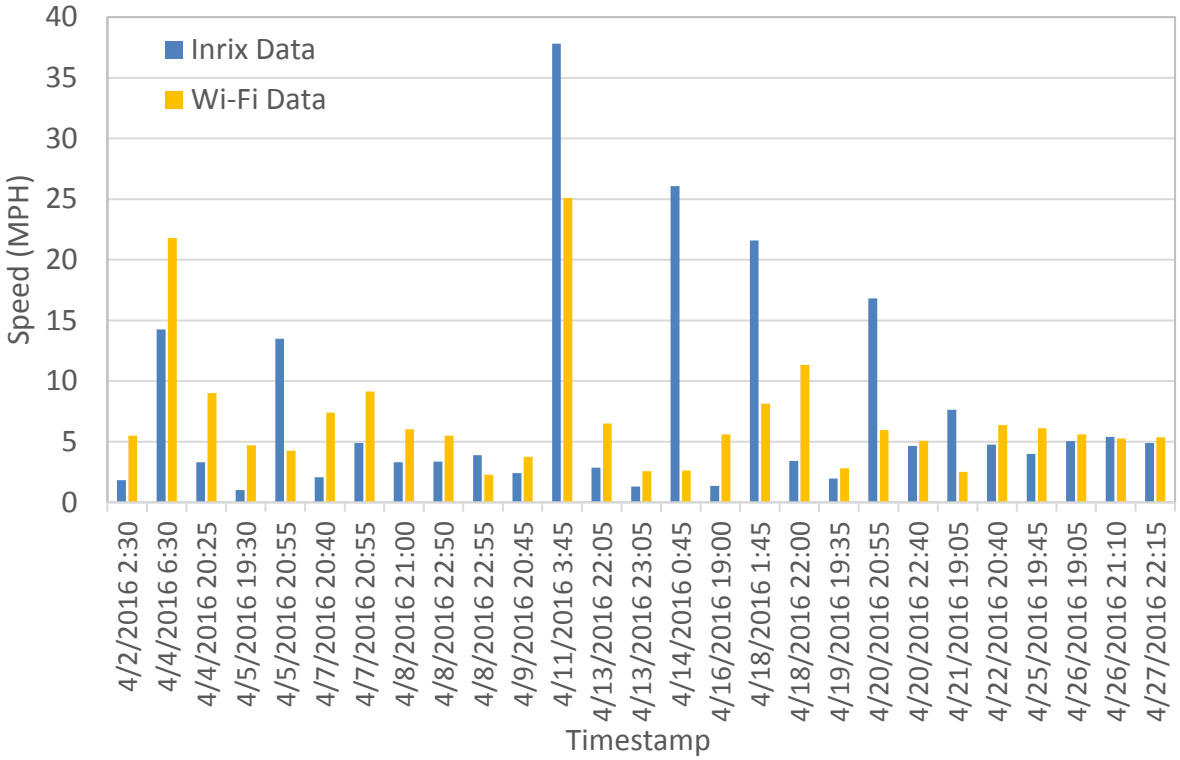

Figure A-33. Comparison of speed for northbound left turn movement during the night and early morning period.

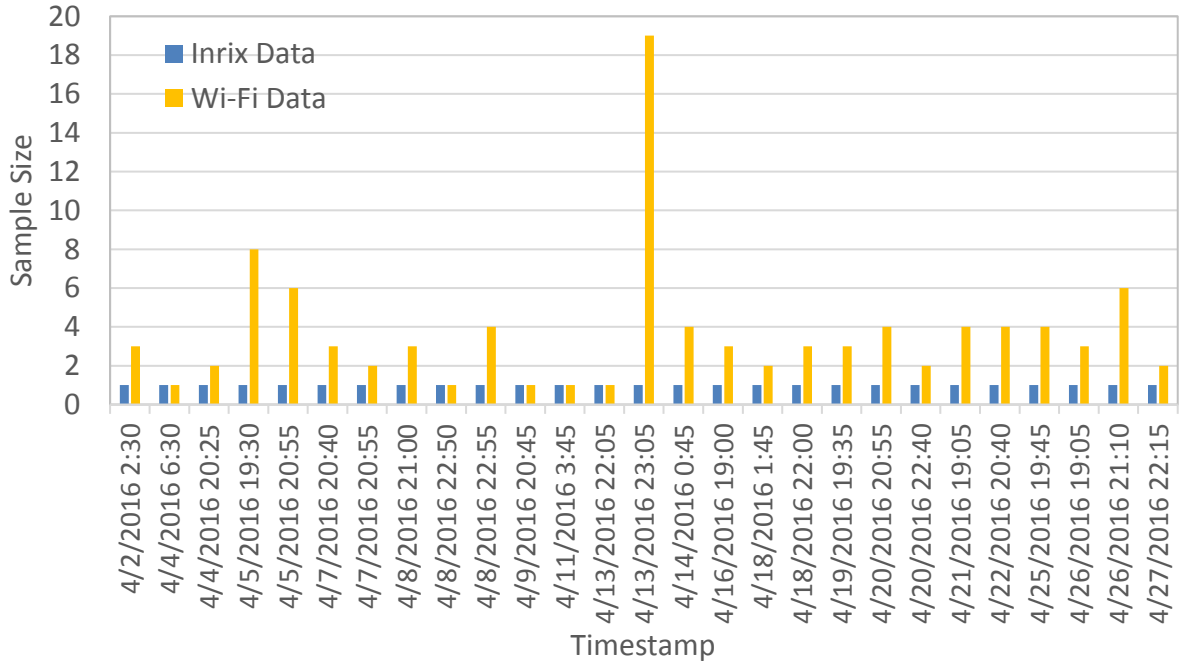

Figure A-34. Comparison of sample size for northbound left turn movement during the night and early morning period.

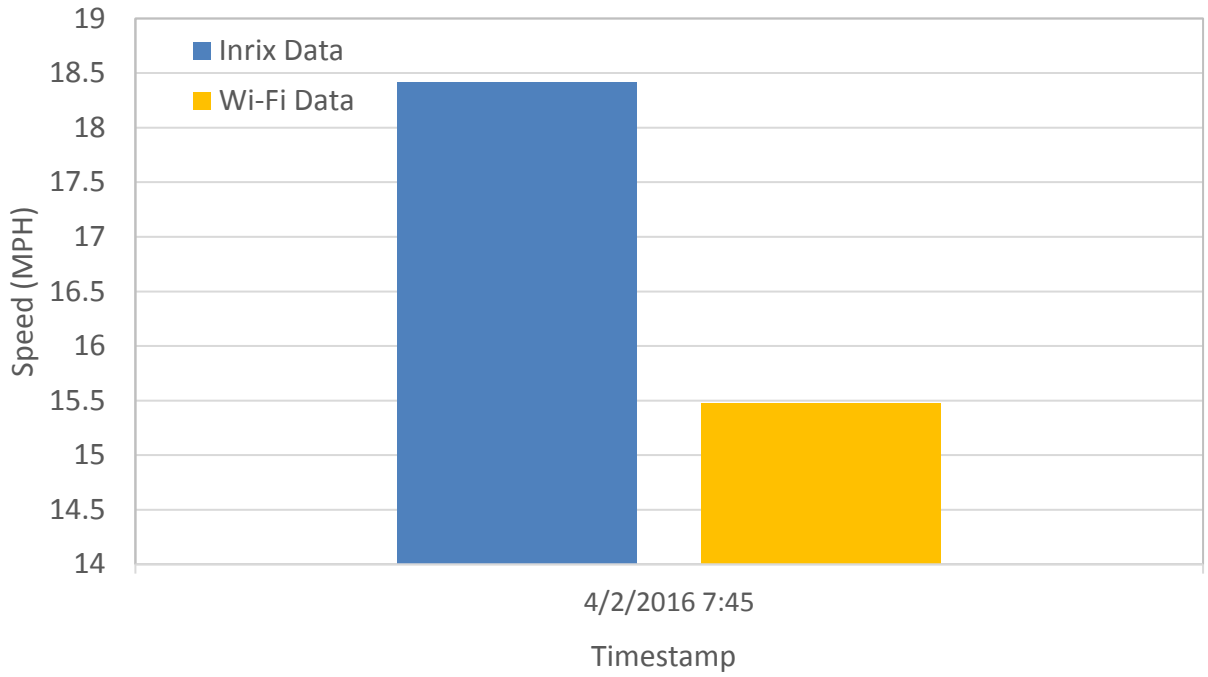

Figure A-35. Comparison of speed for northbound through movement during the AM peak period.

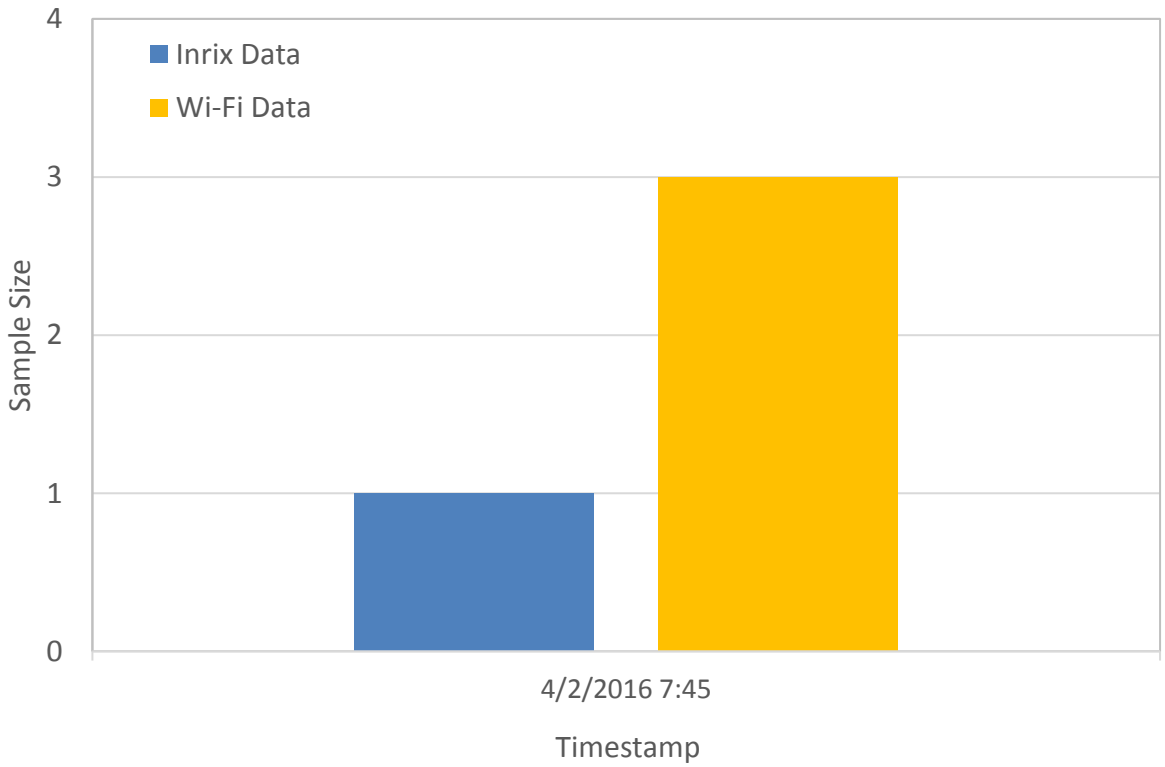

Figure A-36. Comparison of sample size for northbound through movement during the AM peak period.

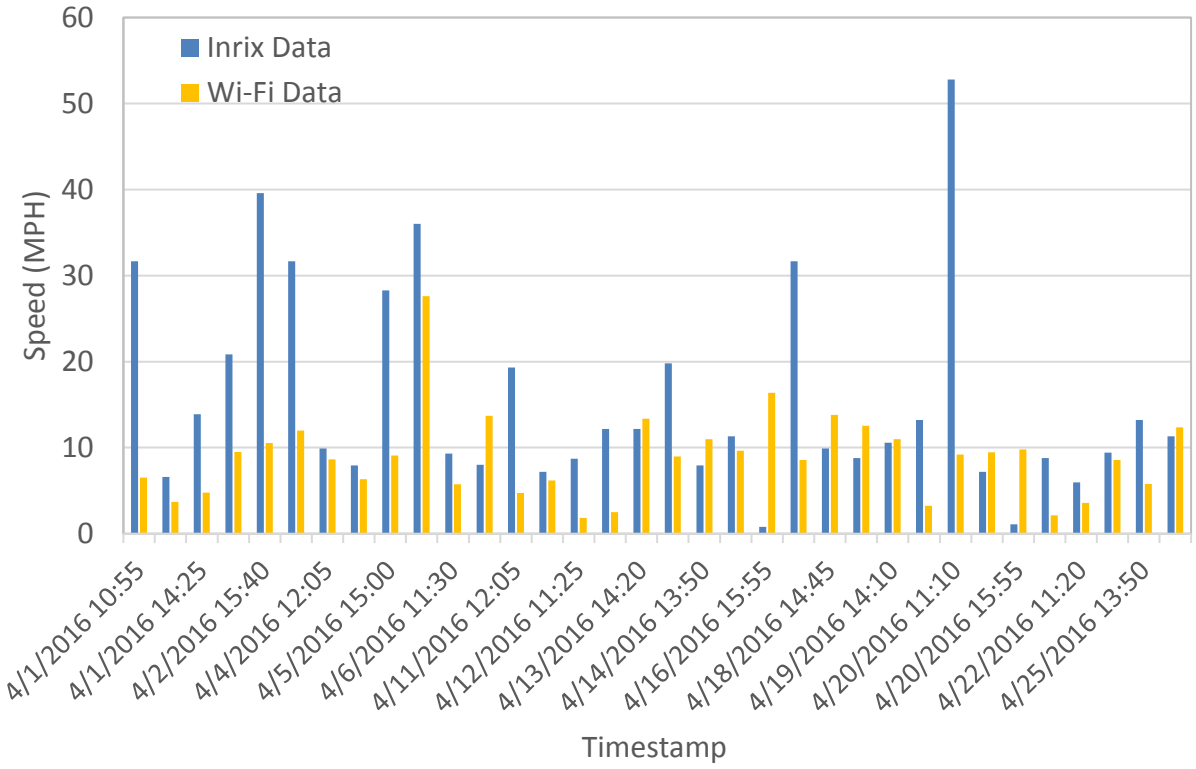

Figure A-37. Comparison of speed for northbound through movement during the midday.

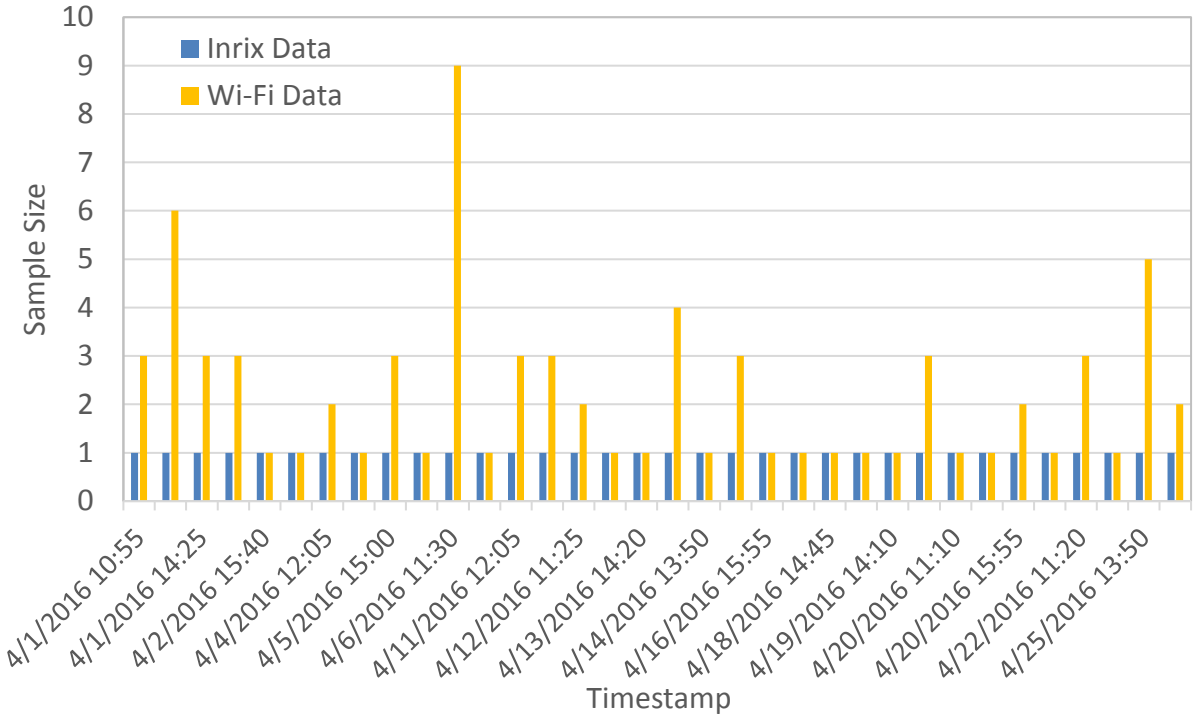

Figure A-38. Comparison of sample size for northbound through movement during the midday.

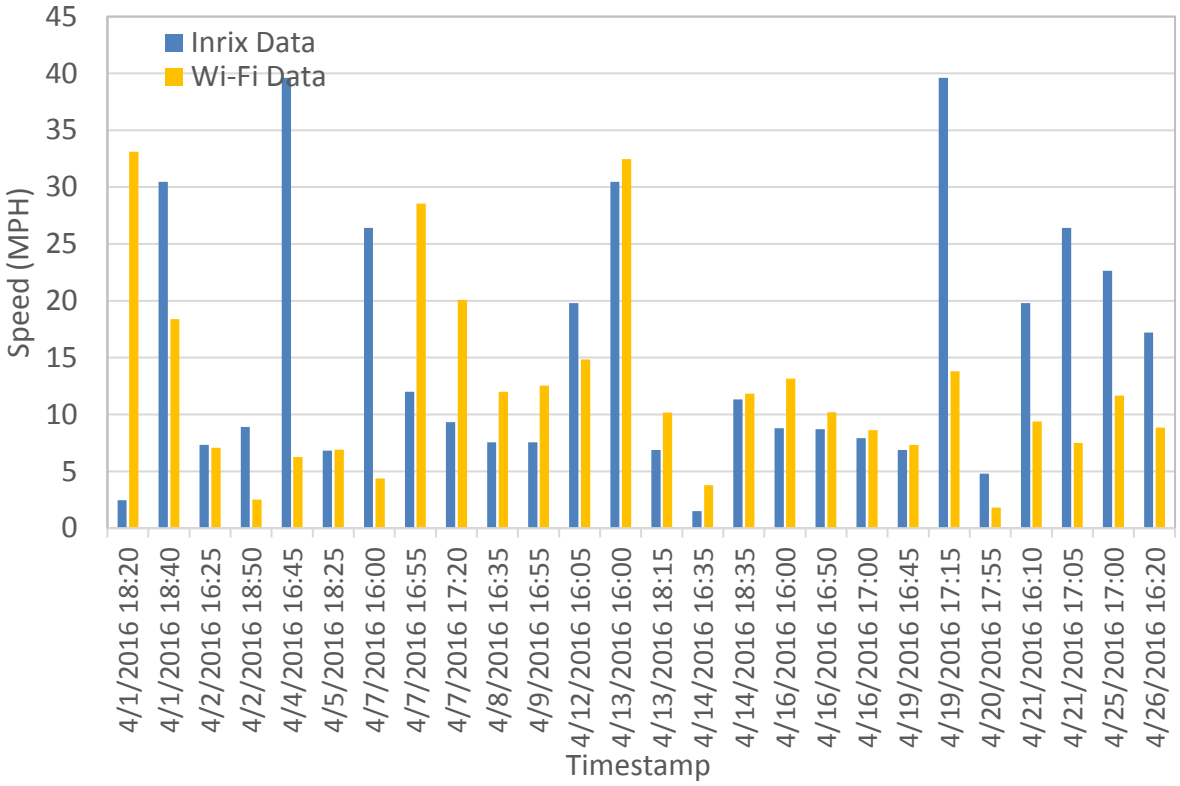

Figure A-39. Comparison of speed for northbound through movement during the PM peak period.

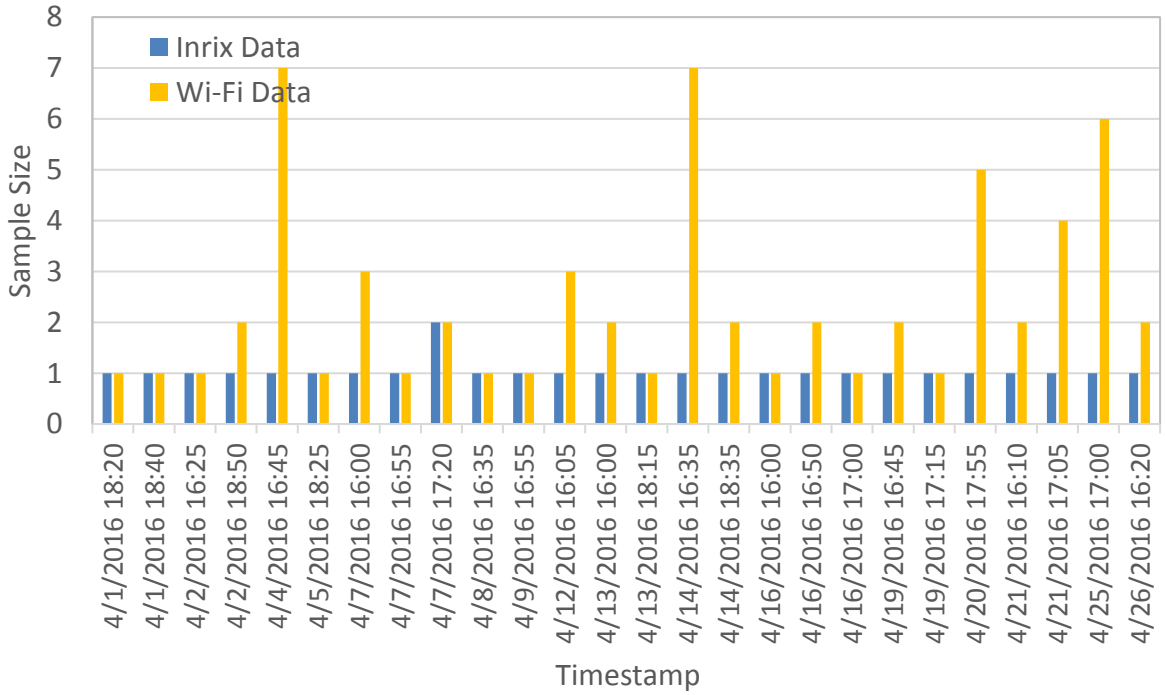

Figure A-40. Comparison of sample size for northbound through movement during the PM peak period.

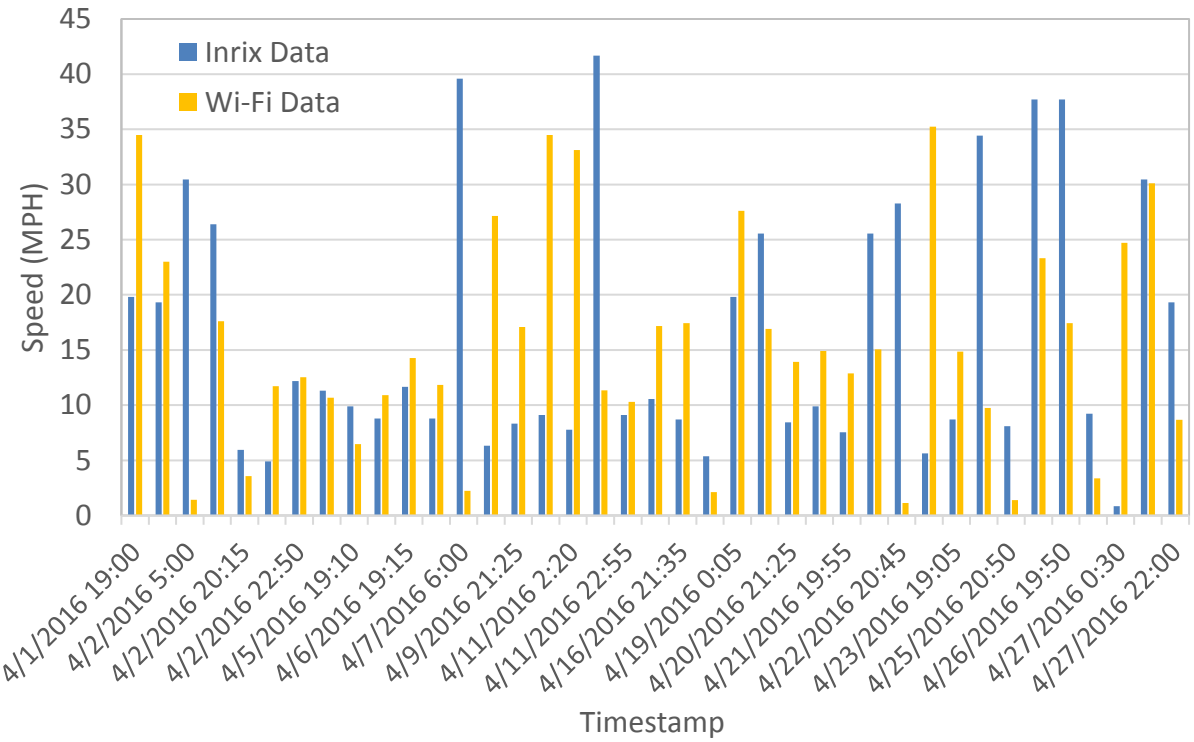

Figure A-41. Comparison of speed for northbound through movement during the night and early morning period.

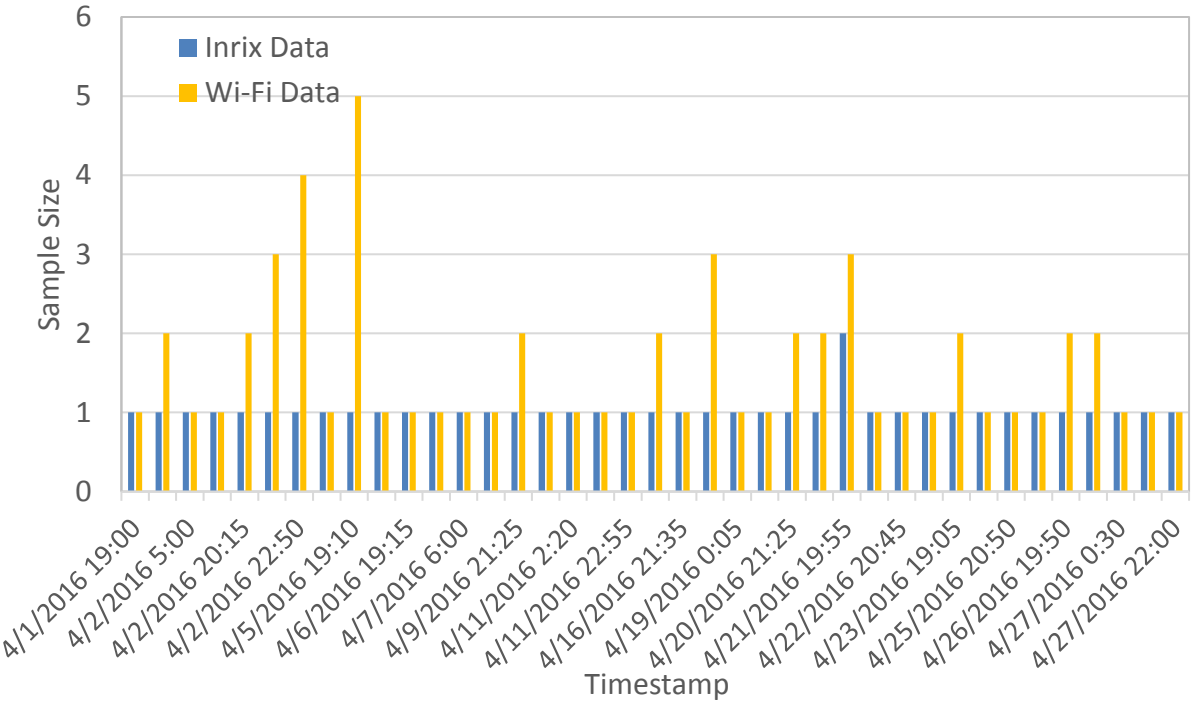

Figure A-42. Comparison of sample size for northbound through movement during the night and early morning period.

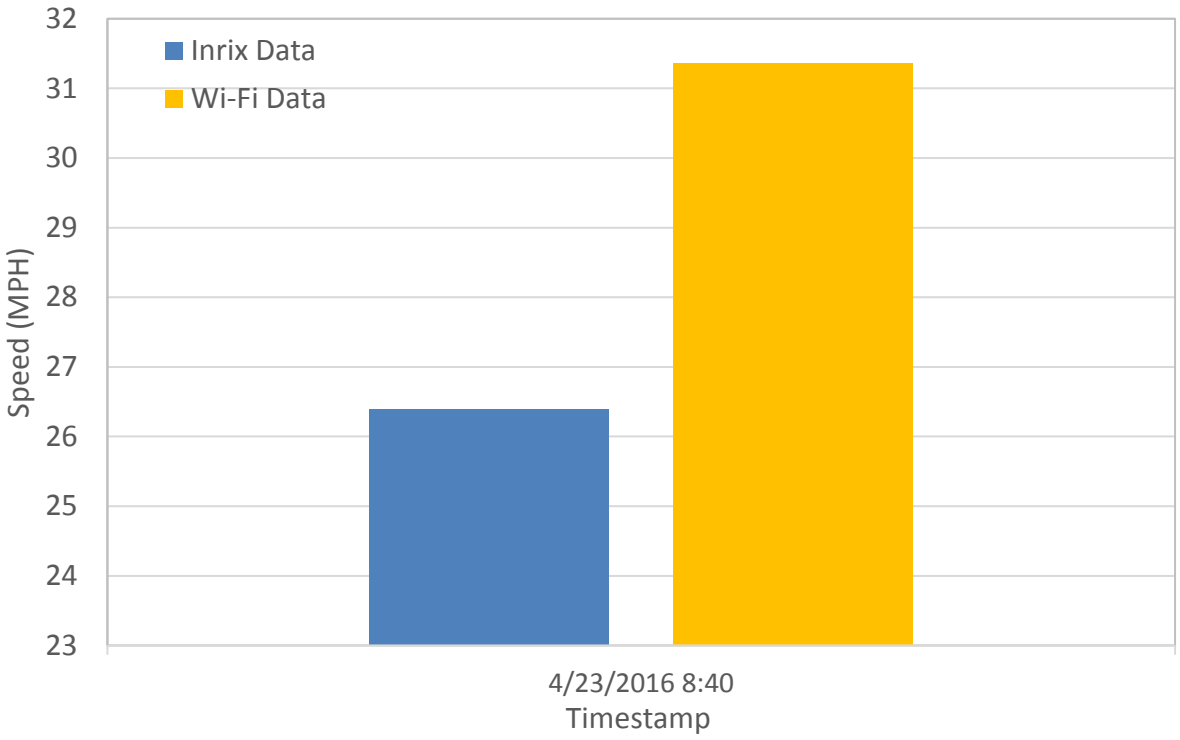

Figure A-43. Comparison of speed for northbound right turn movement during the AM peak period.

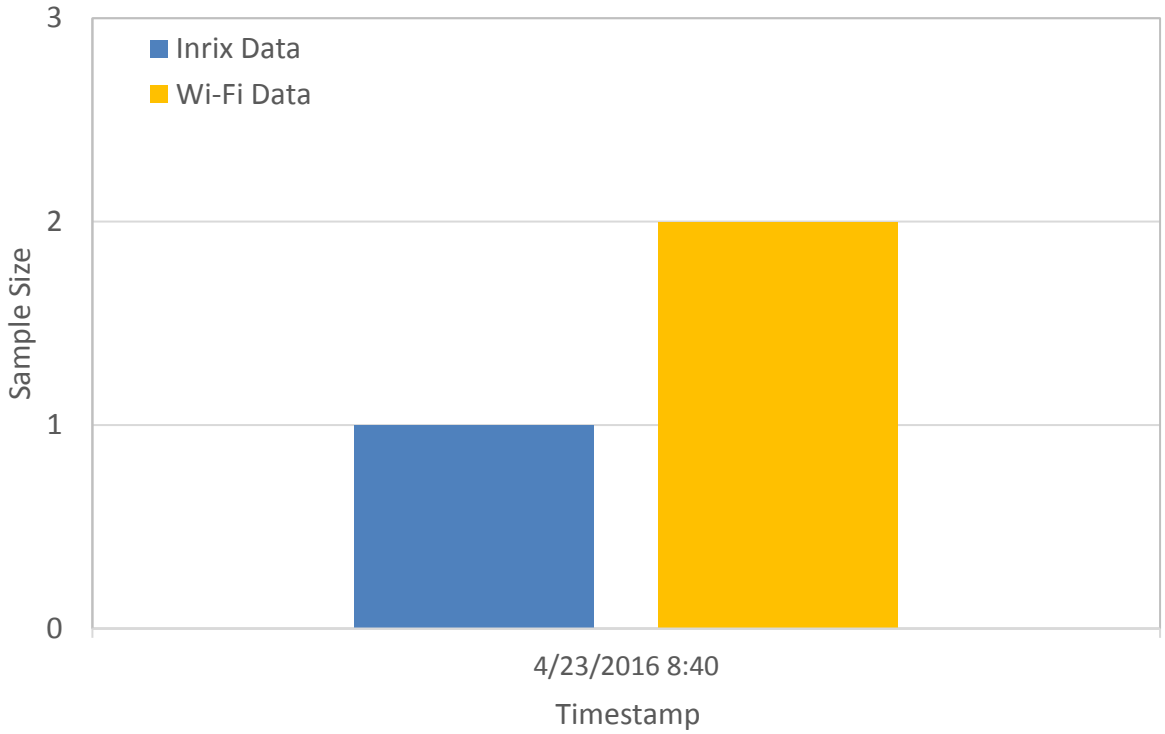

Figure A-44. Comparison of sample size for northbound right turn movement during the AM peak period.

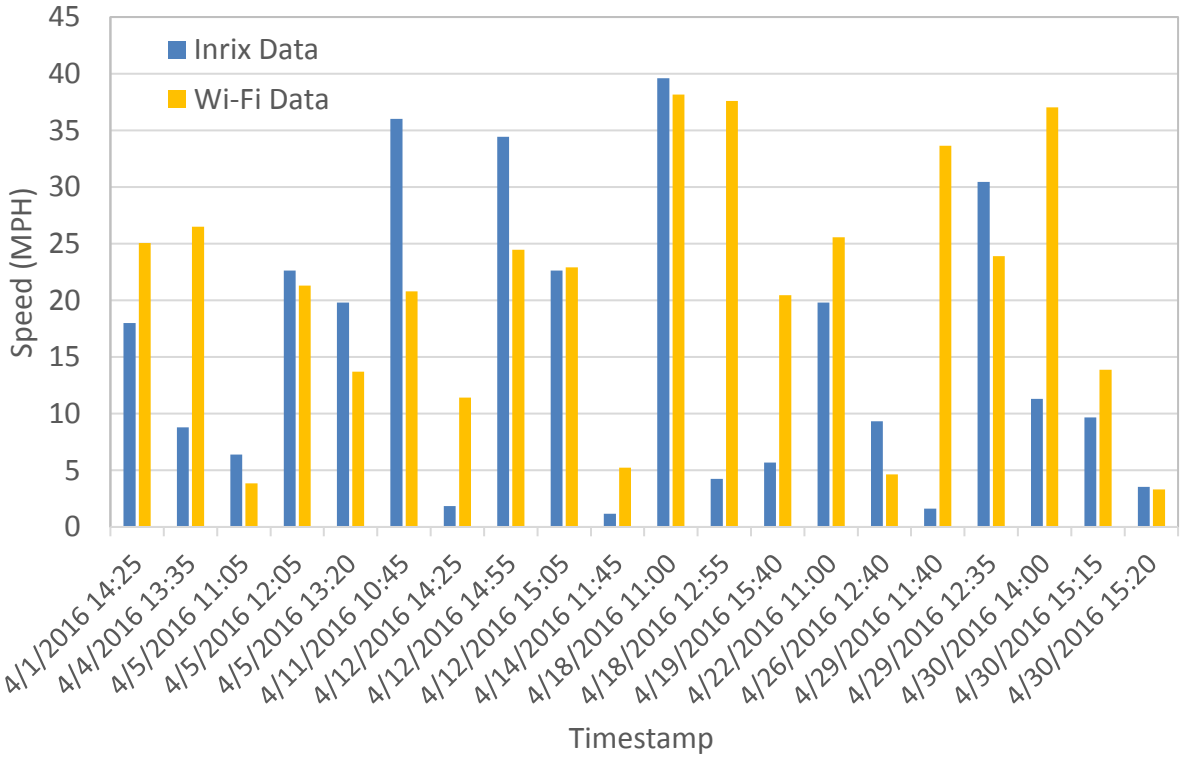

Figure A-45. Comparison of speed for northbound right turn movement during the midday.

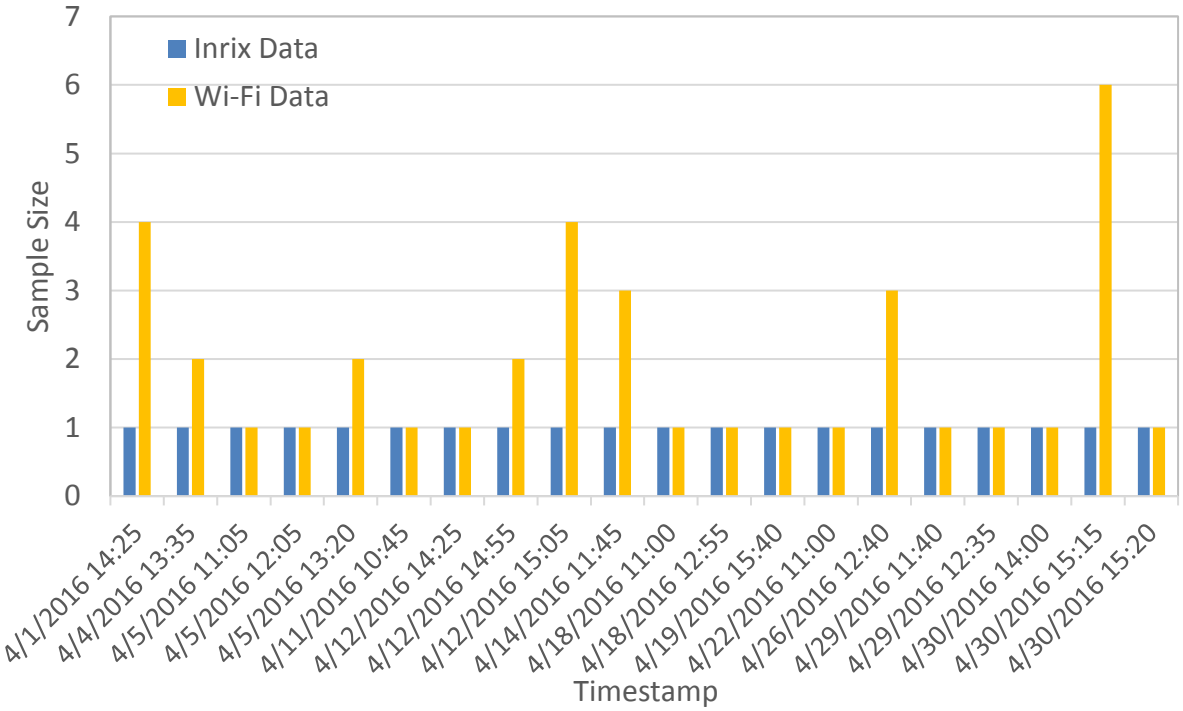

Figure A-46. Comparison of sample size for northbound right turn movement during the midday.

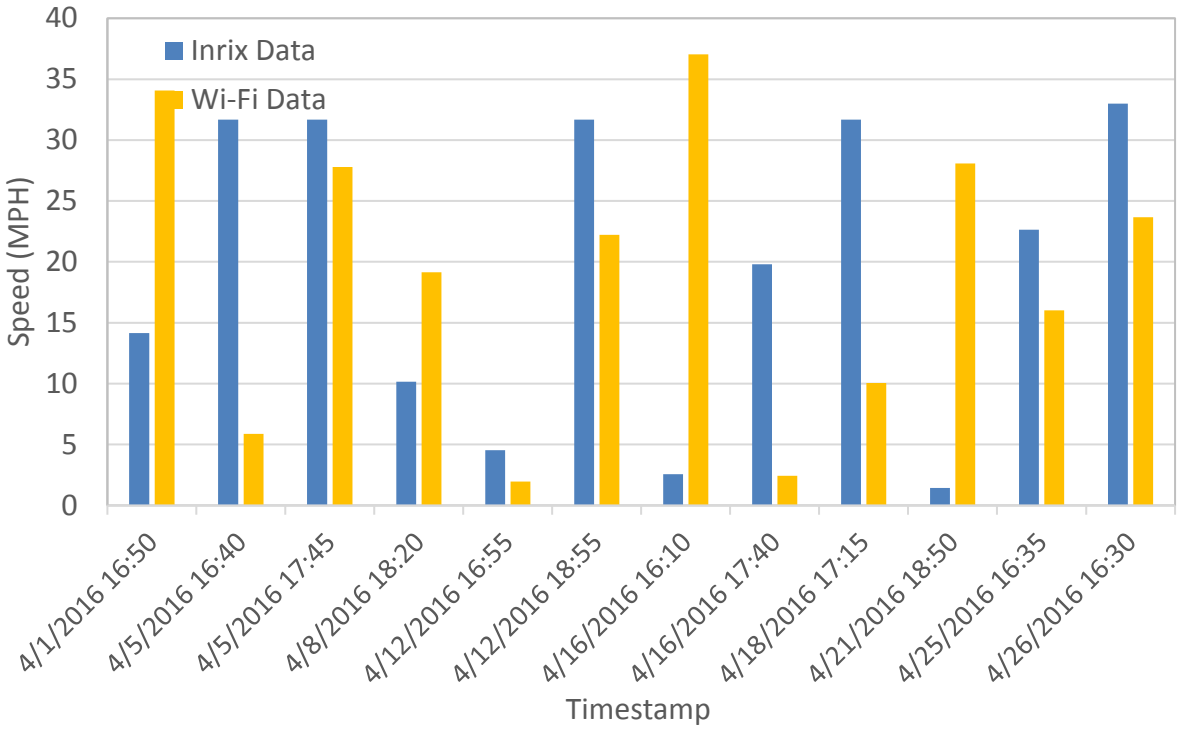

Figure A-47. Comparison of speed for northbound right turn movement during the PM peak period.

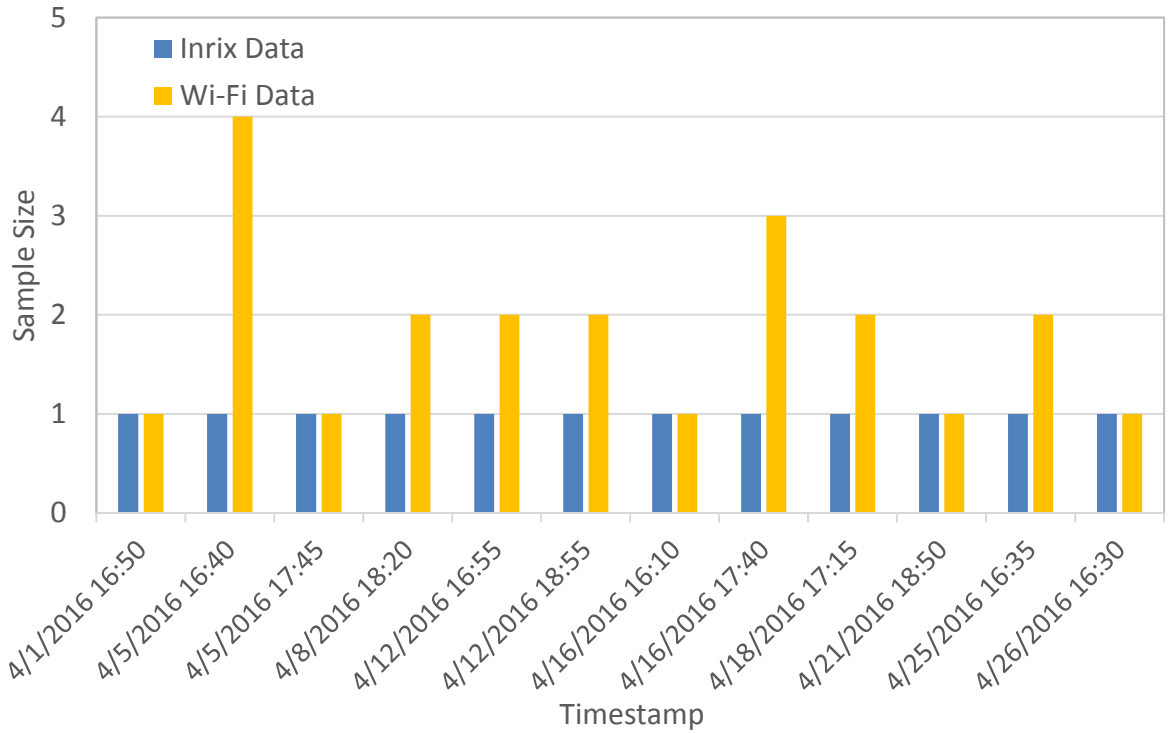

Figure A-48. Comparison of sample size for northbound right turn movement during the PM peak period.

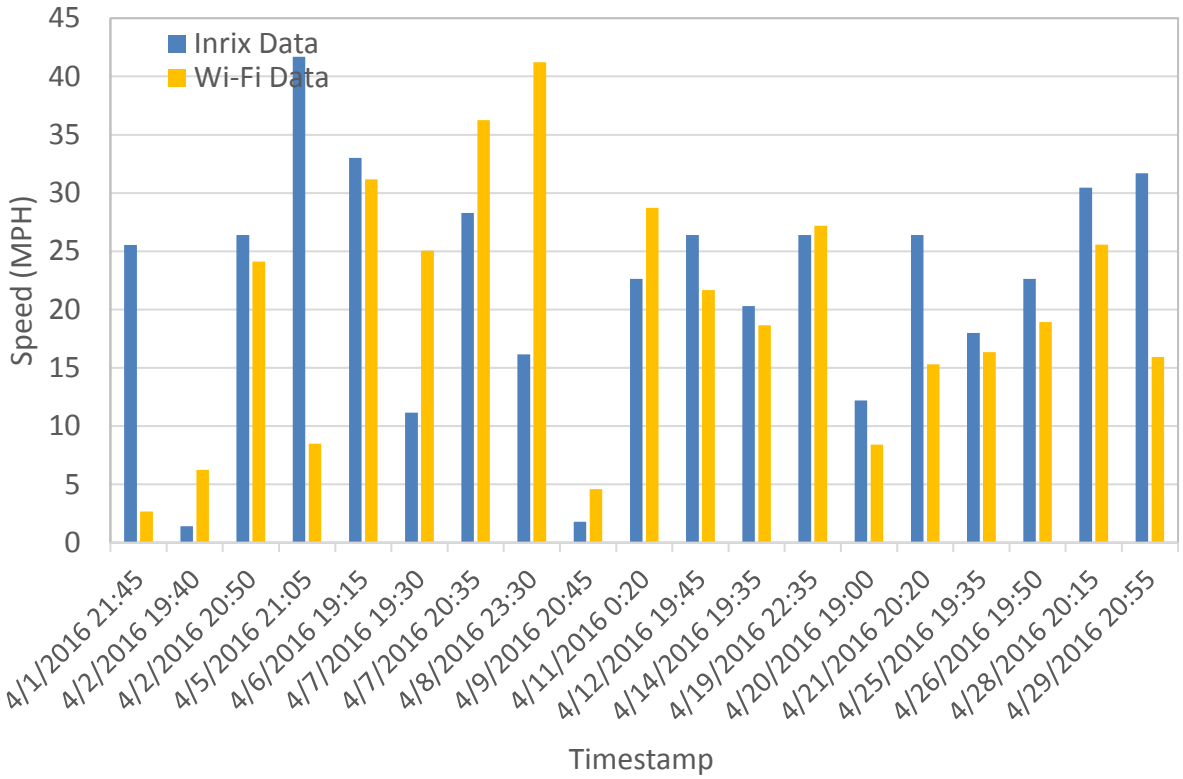

Figure A-49. Comparison of speed for northbound right turn movement during the night and early morning period.

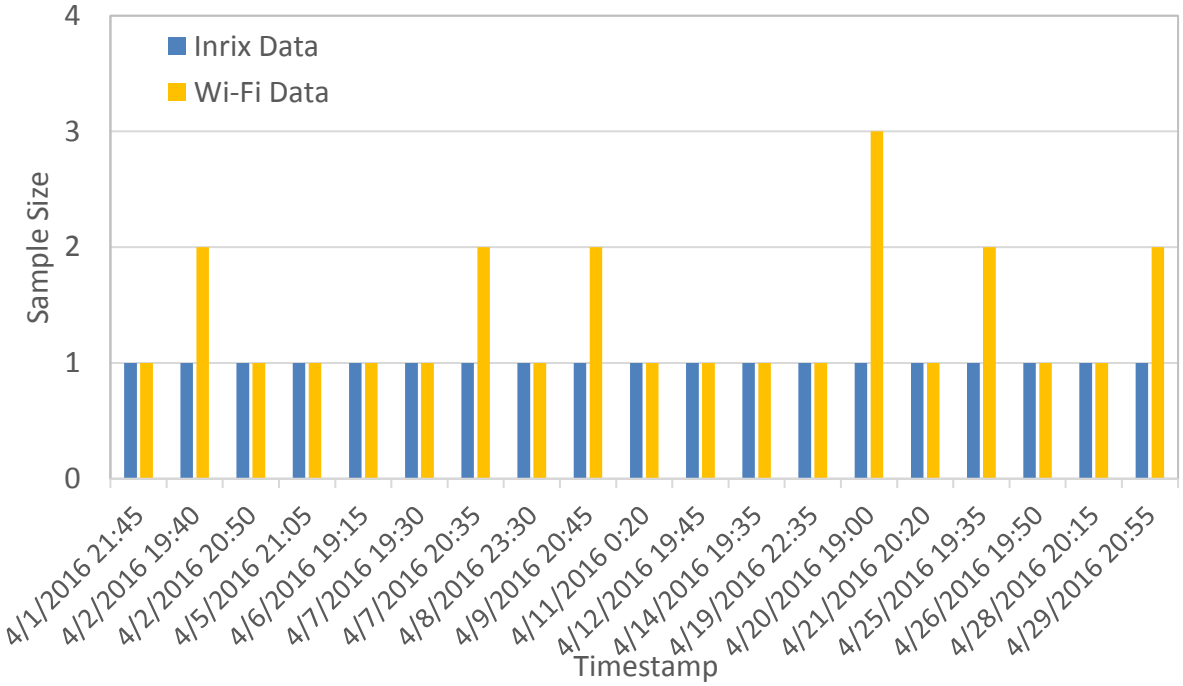

Figure A-50. Comparison of sample size for northbound right turn movement during the night and early morning period.

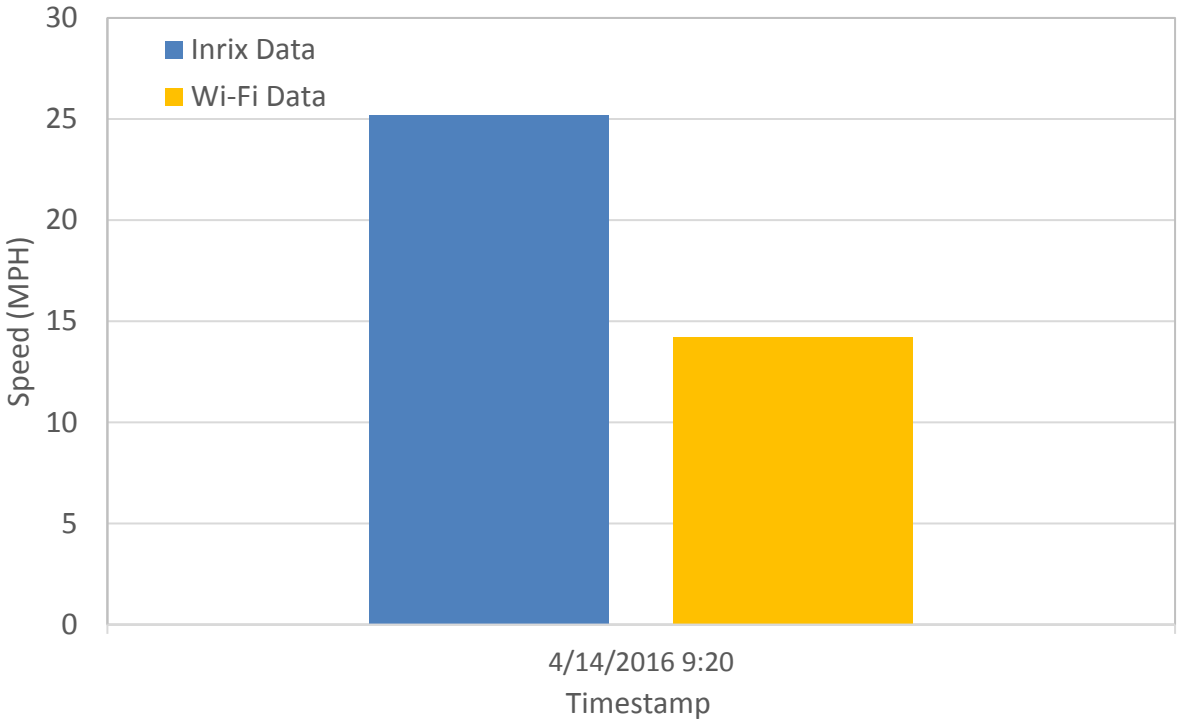

Figure A-51. Comparison of speed for southbound left turn movement during the AM peak period.

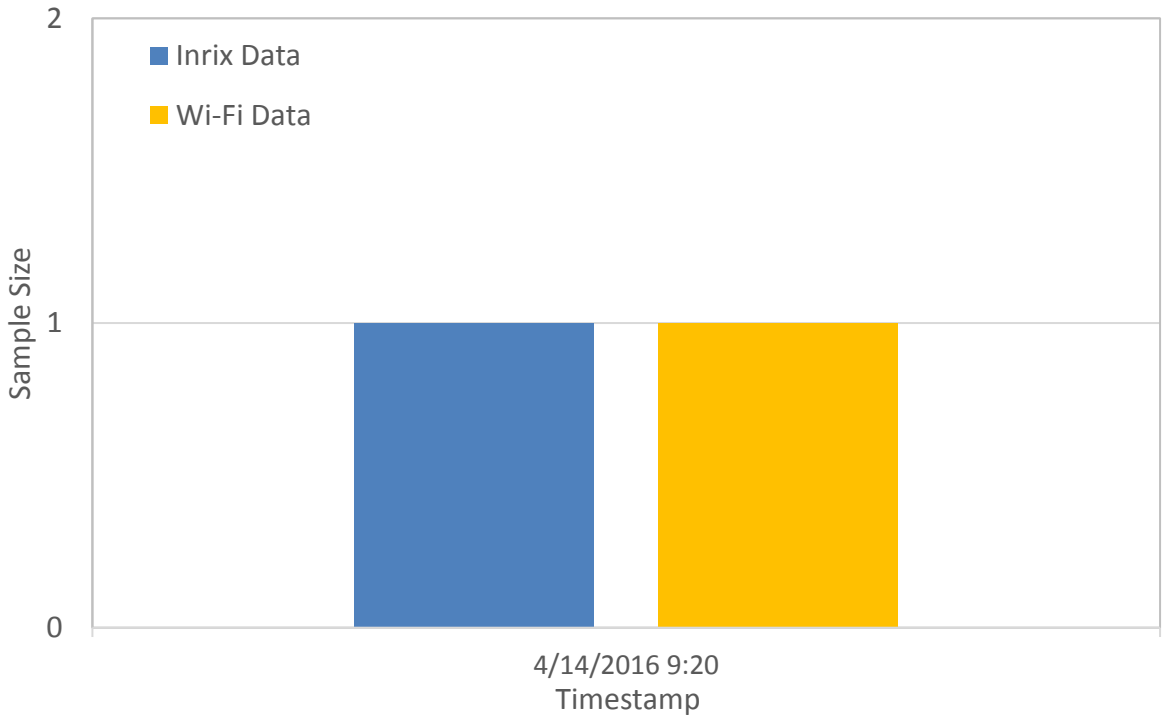

Figure A-52. Comparison of sample size for southbound left turn movement during the AM peak period.

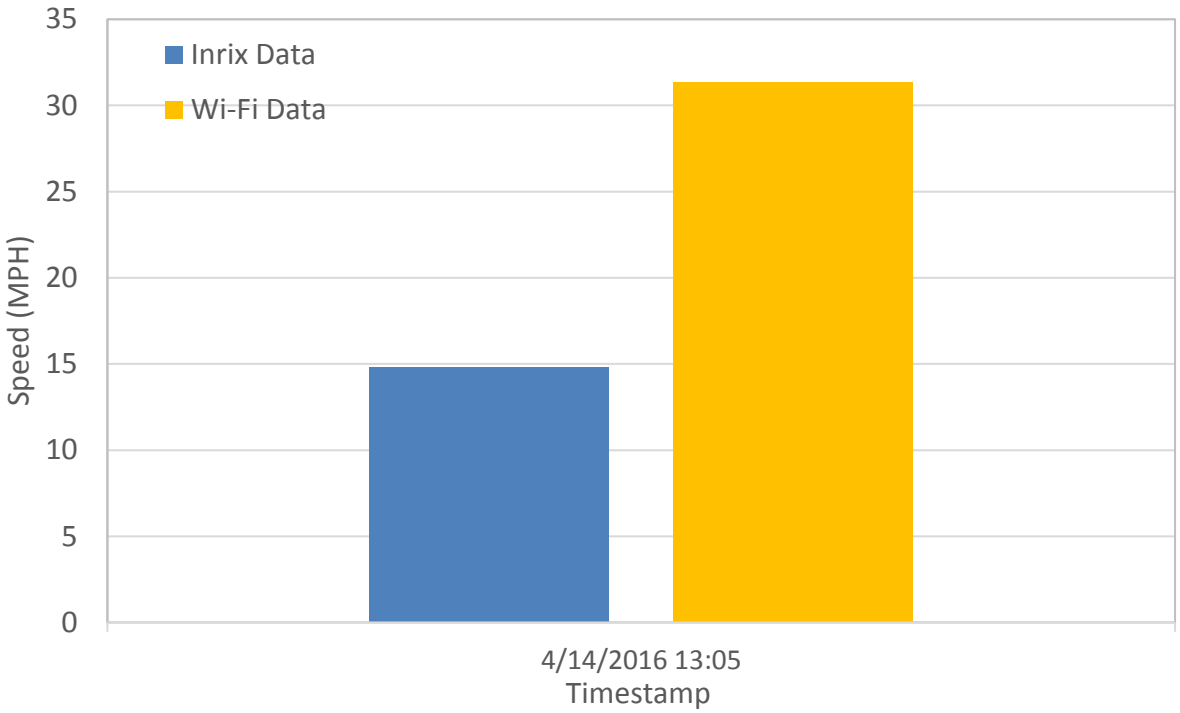

Figure A-53. Comparison of speed for southbound left turn movement during the midday.

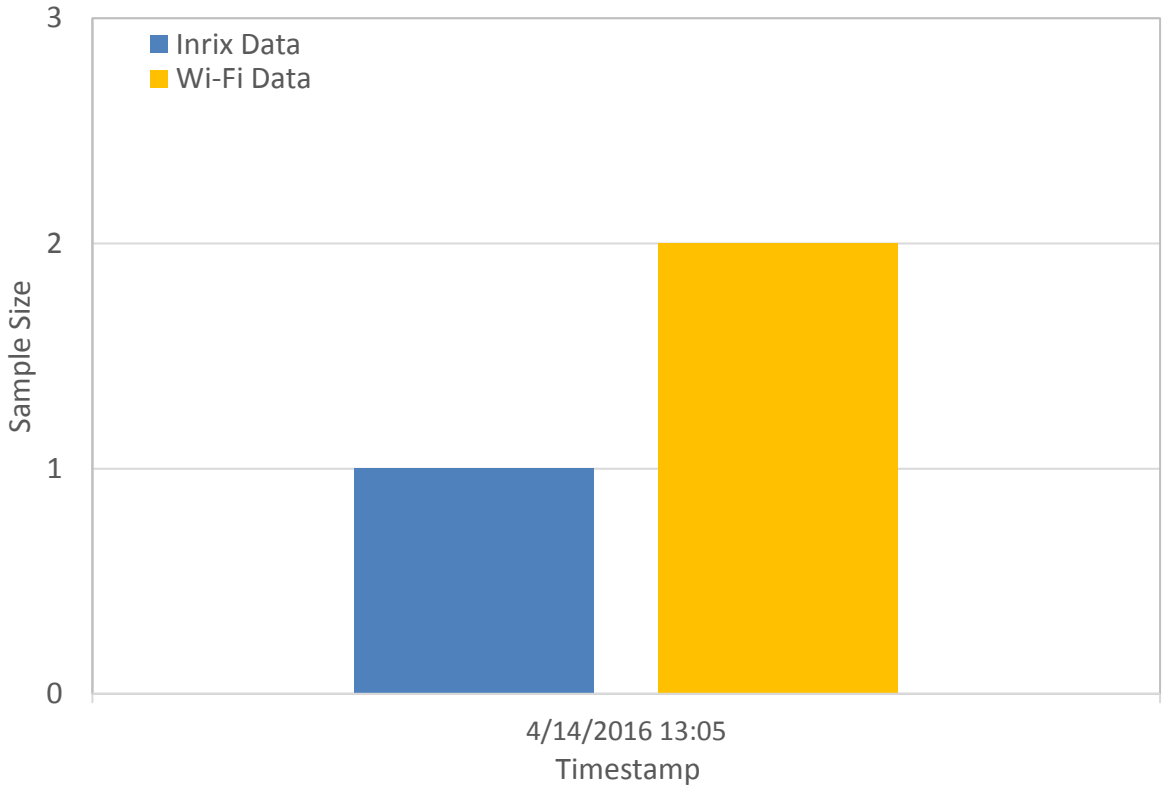

Figure A-54. Comparison of sample size for southbound left turn movement during the midday.

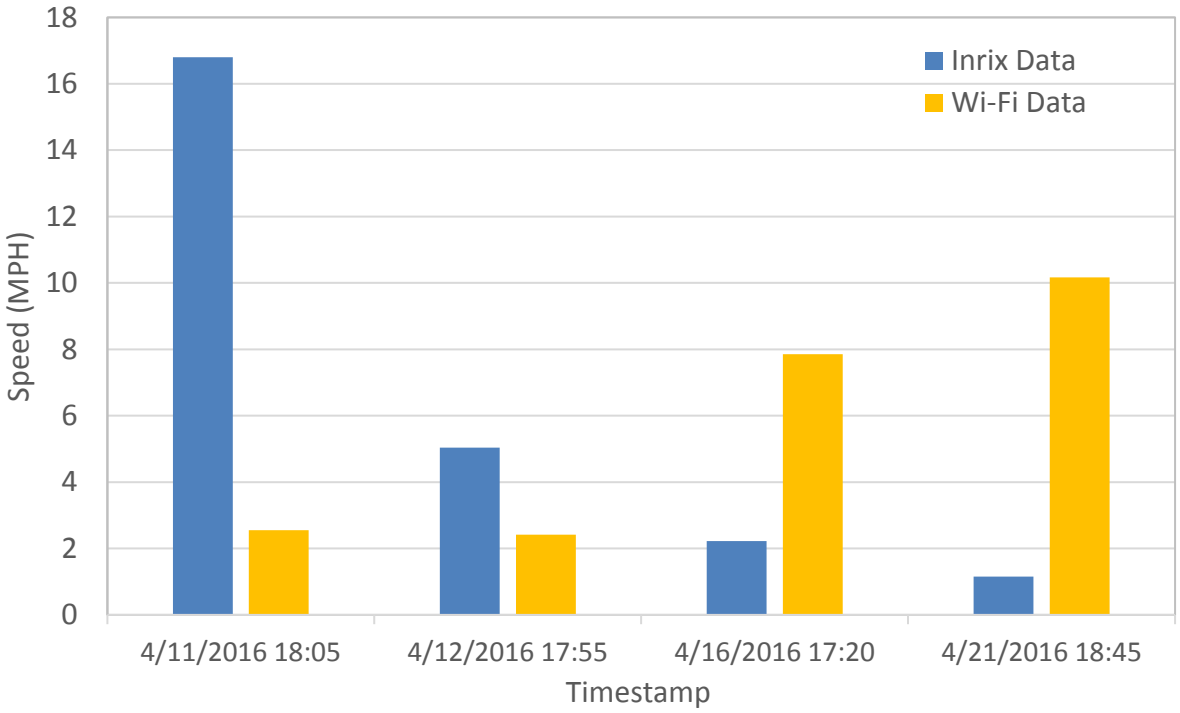

Figure A-55. Comparison of speed for southbound left turn movement during the PM peak period.

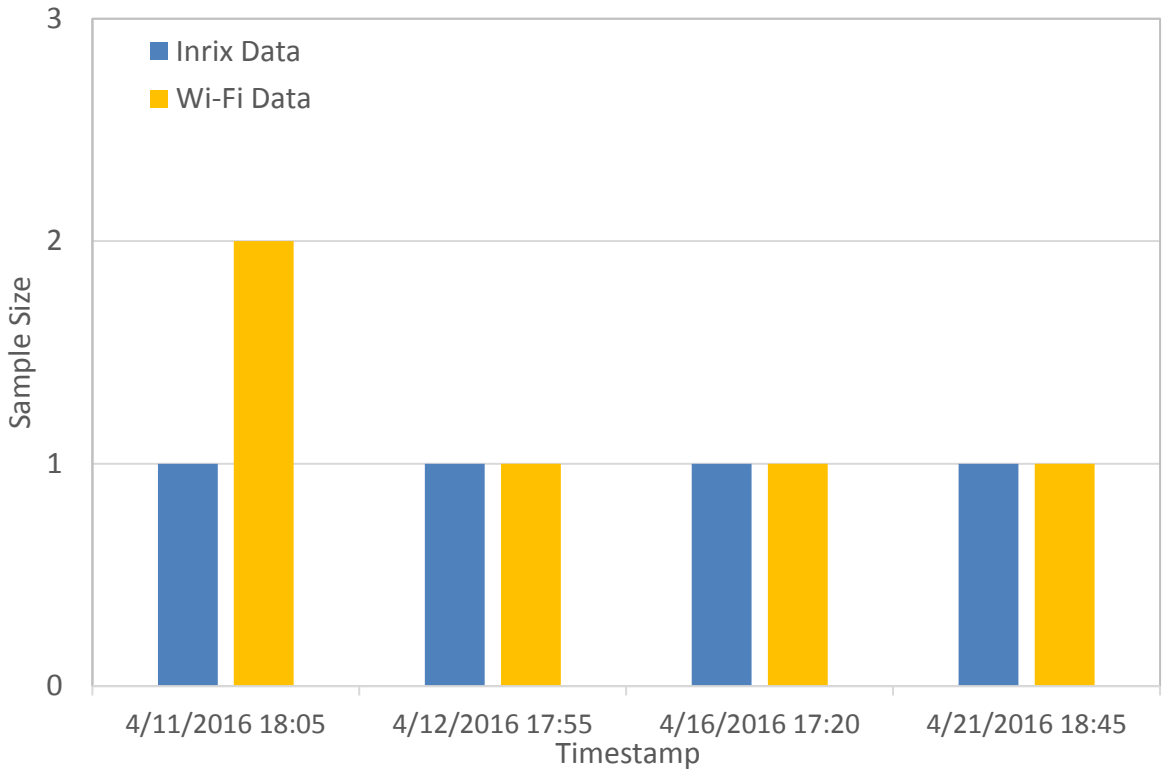

Figure A-56. Comparison of sample size for southbound left turn movement during the PM peak period.

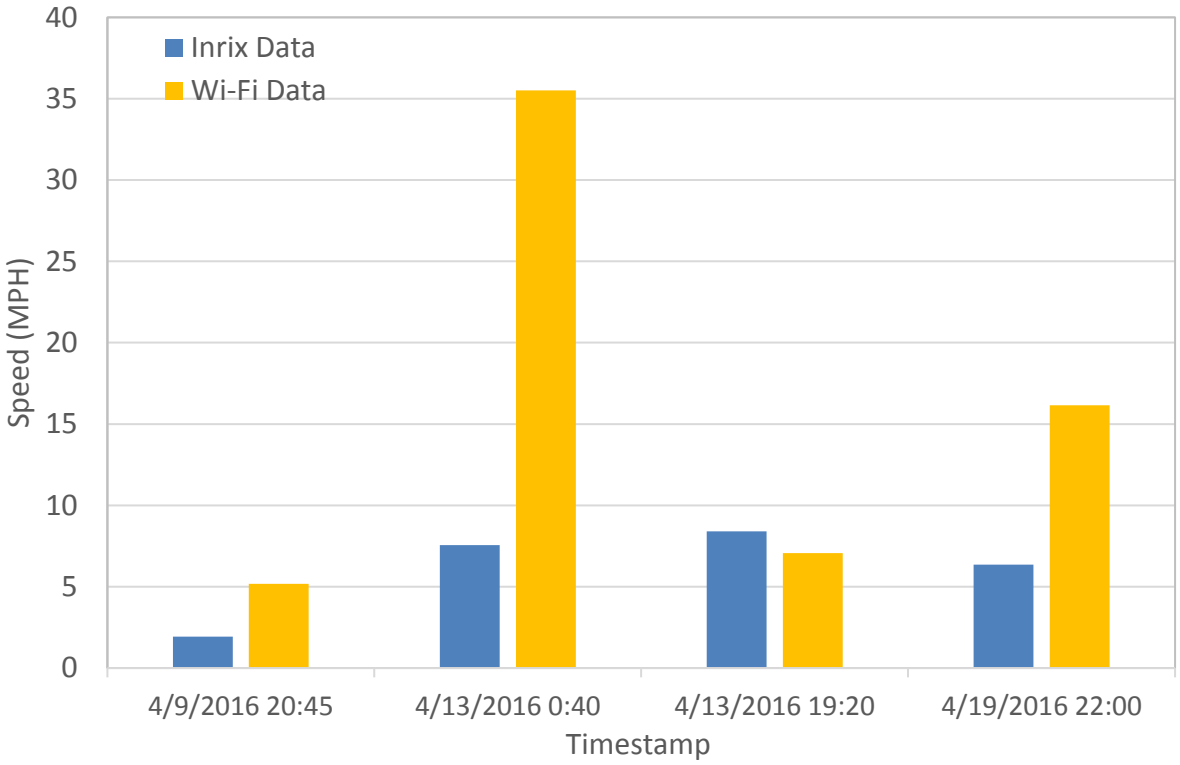

Figure A-57. Comparison of speed for southbound left turn movement during the night and early morning period.

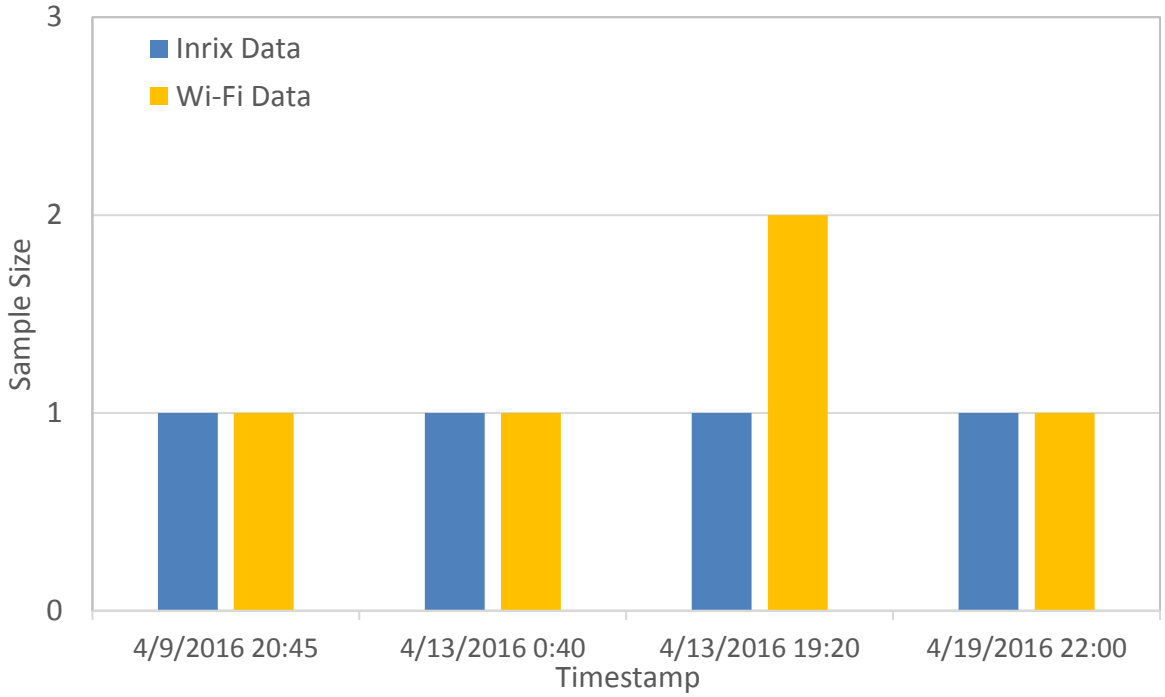

Figure A-58. Comparison of sample size for southbound left turn movement during the night and early morning period.

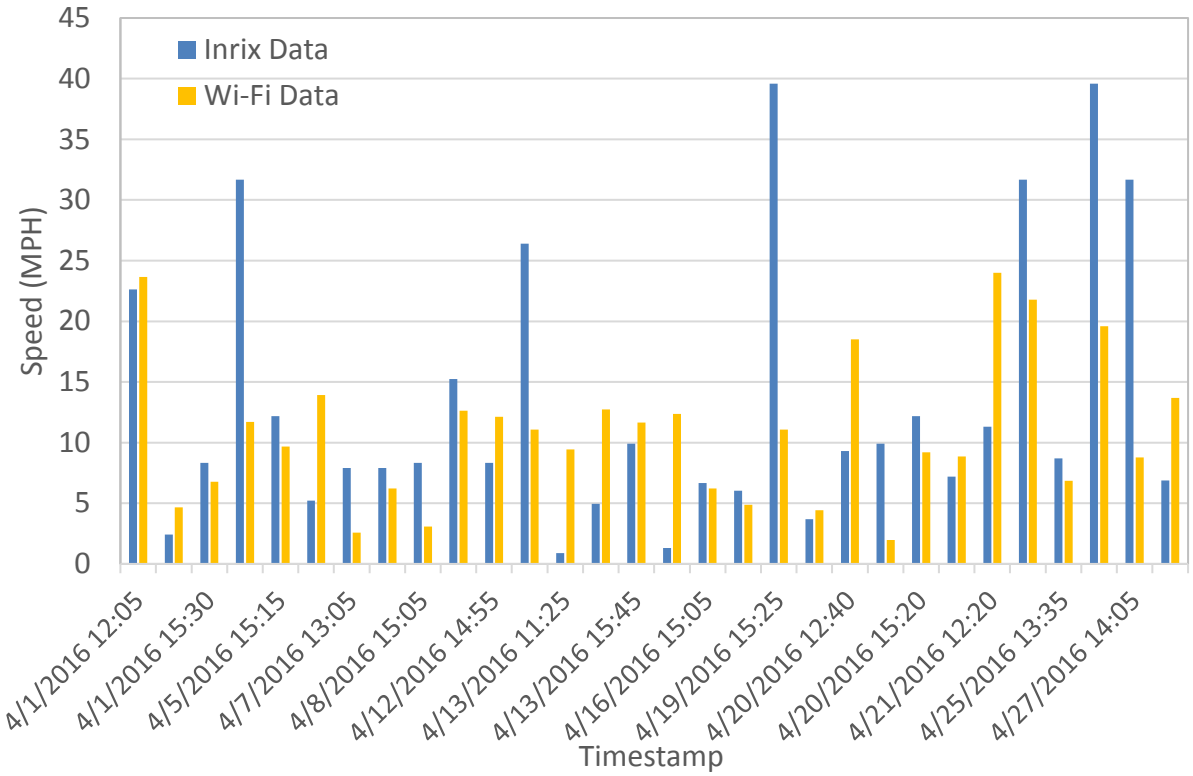

Figure A-59. Comparison of speed for southbound through movement during the midday.

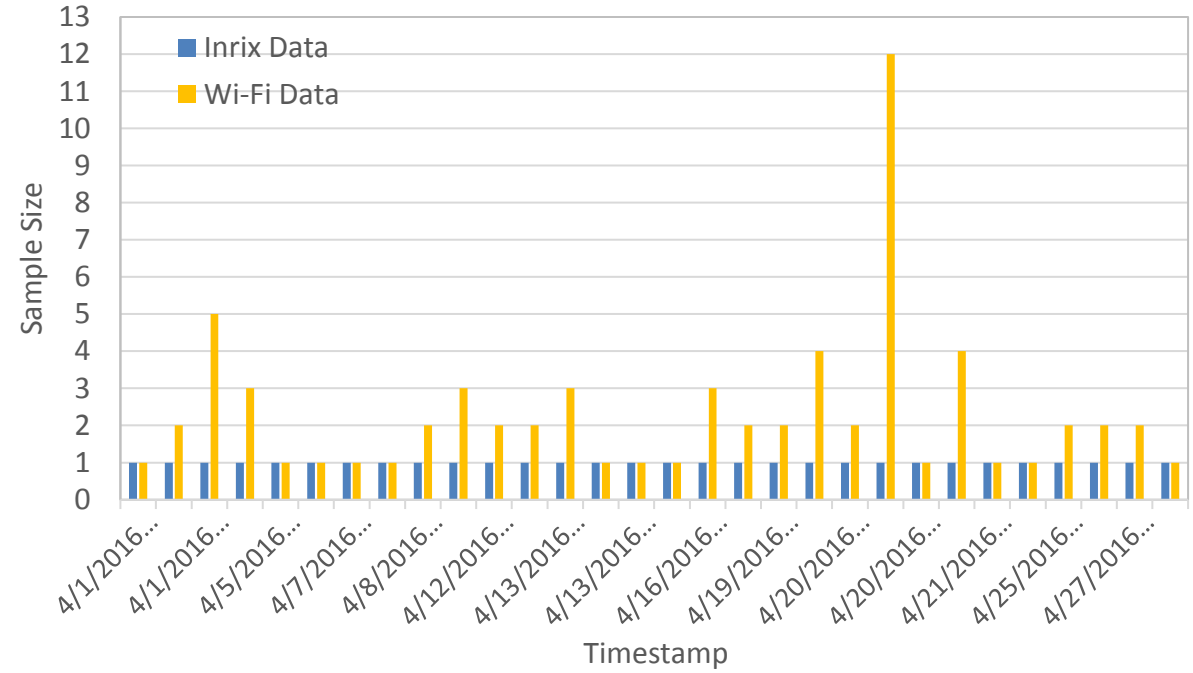

Figure A-60. Comparison of sample size for southbound through movement during the midday.

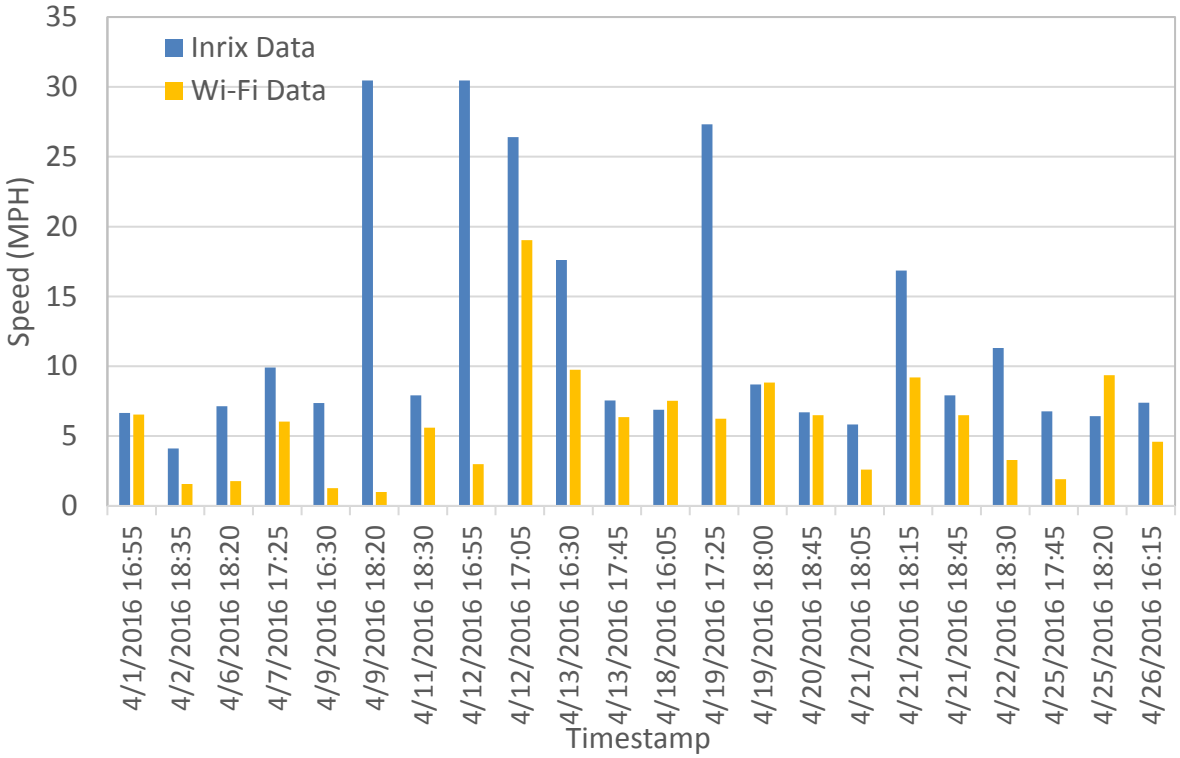

Figure A-61. Comparison of speed for southbound through movement during the PM peak period.

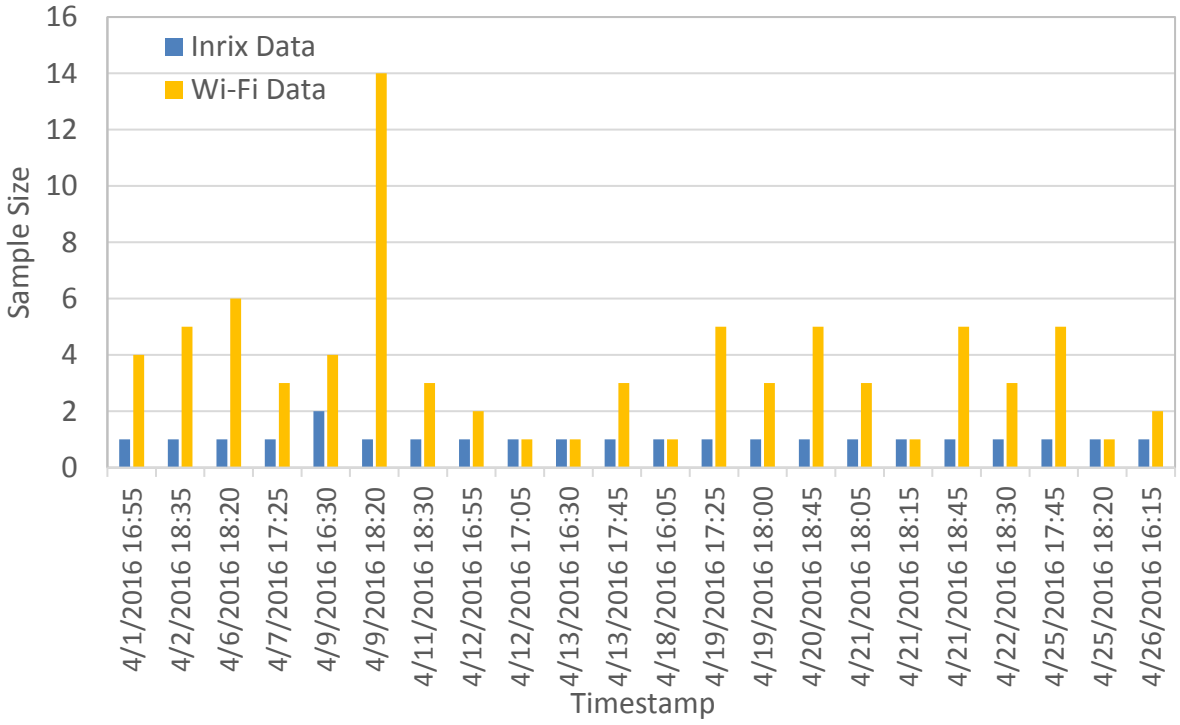

Figure A-62. Comparison of sample size for southbound through movement during the PM peak period.

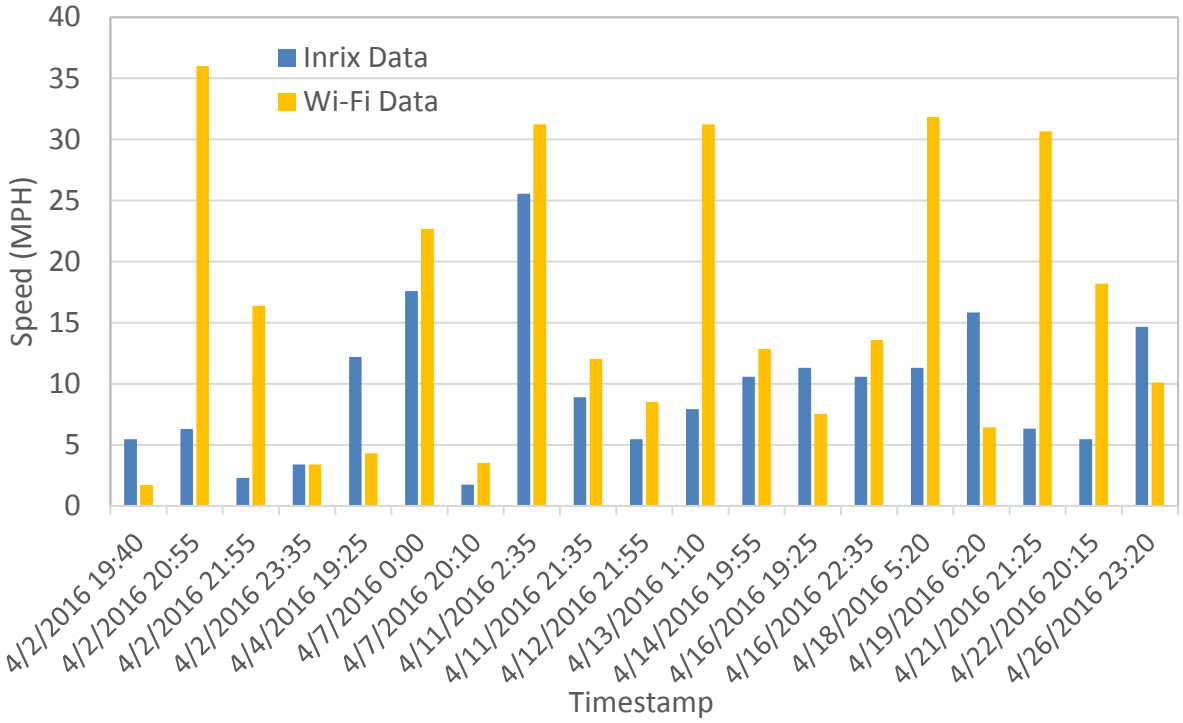

Figure A-63. Comparison of speed for southbound through movement during the night and early morning period.

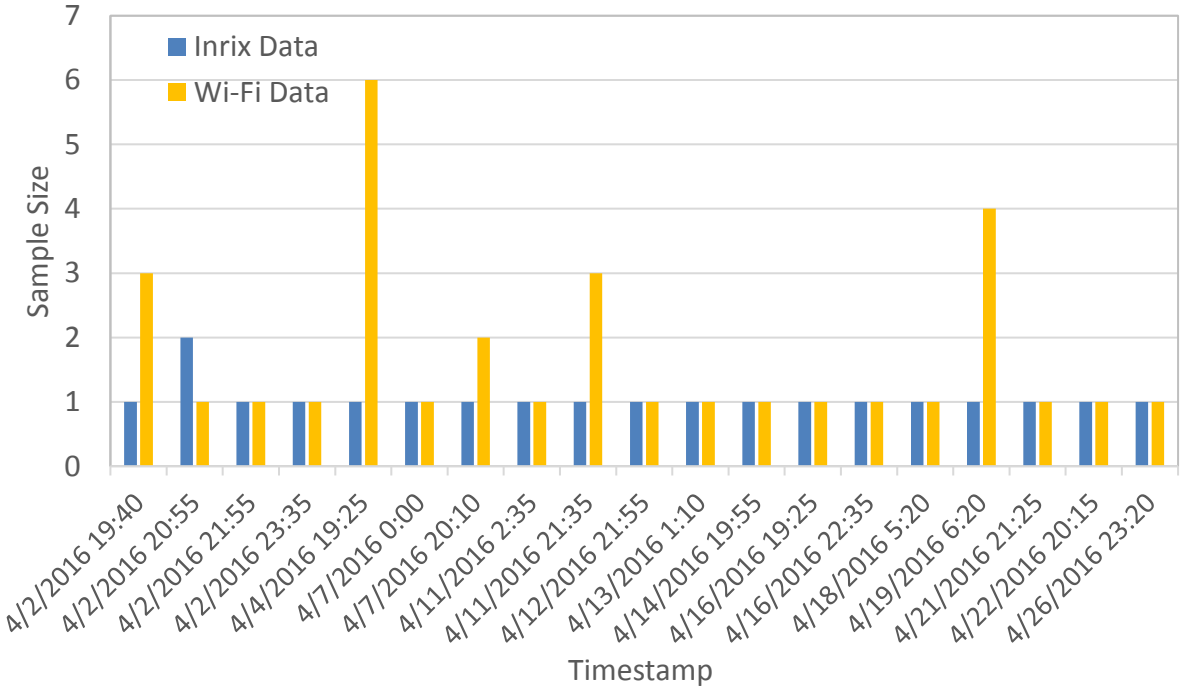

Figure A-64. Comparison of sample size for southbound through movement during the night and early morning period.

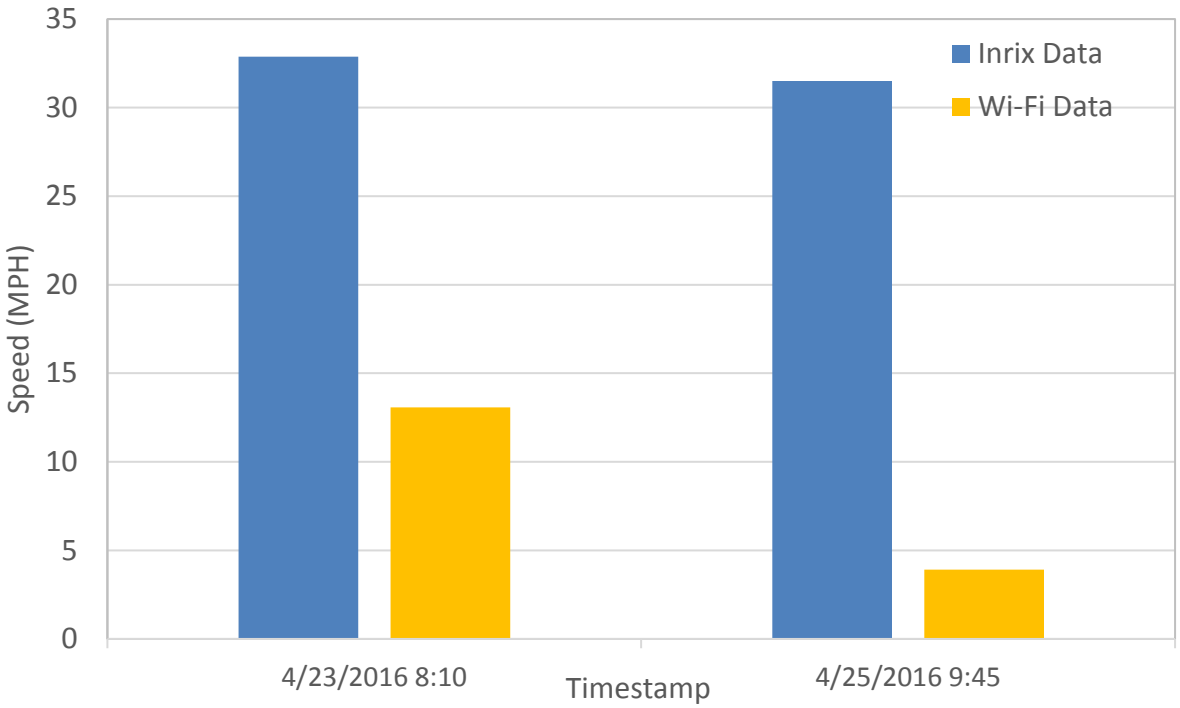

Figure A-65. Comparison of speed for southbound right turn movement during the AM peak period.

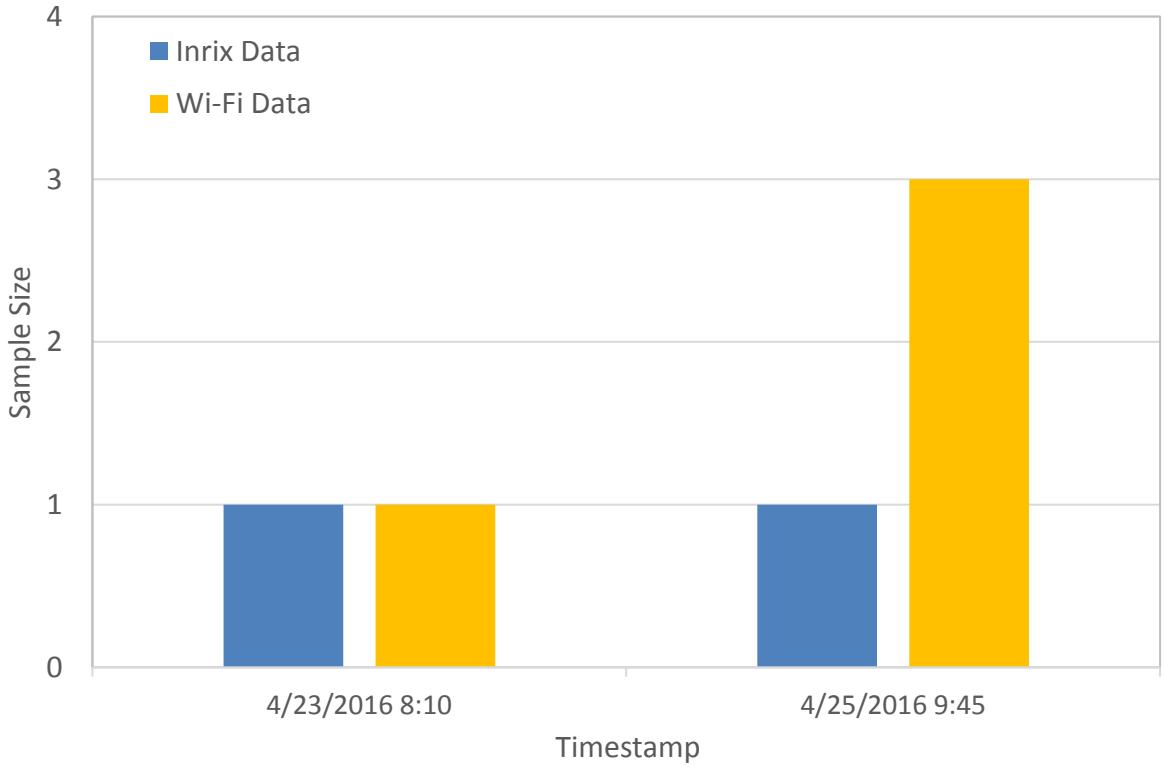

Figure A-66. Comparison of sample size for southbound right turn movement during the AM peak period.

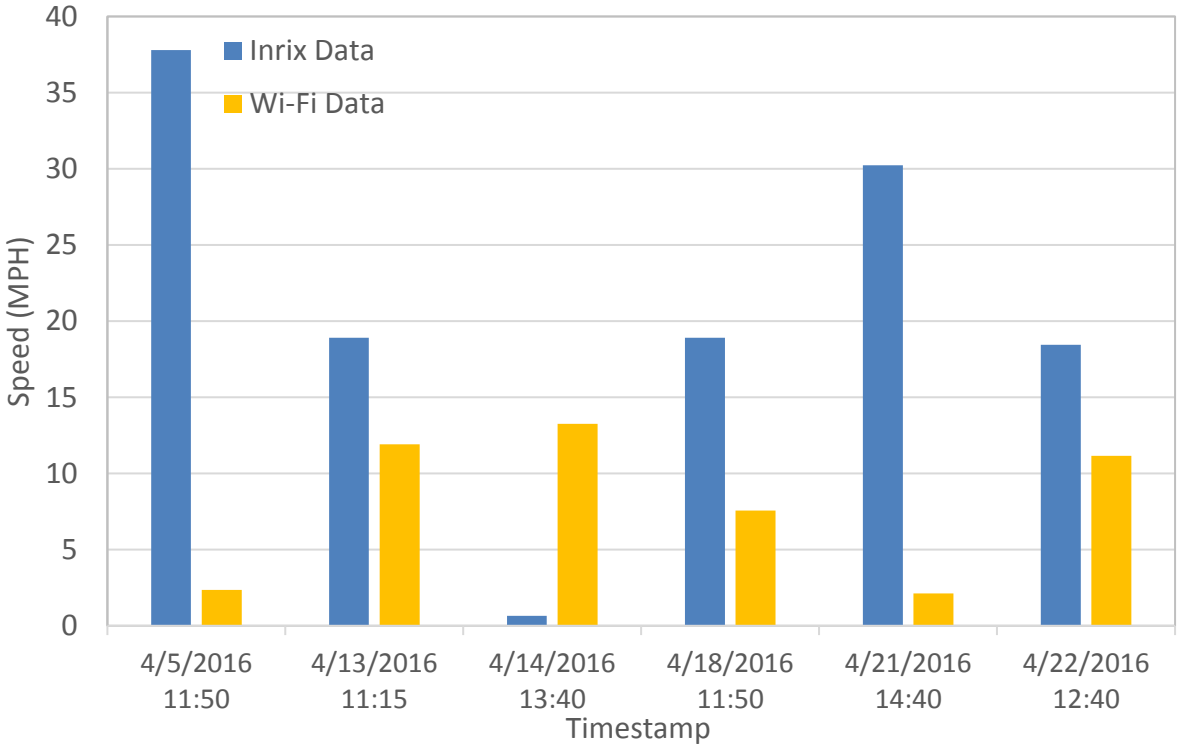

Figure A-67. Comparison of speed for southbound right turn movement during the midday.

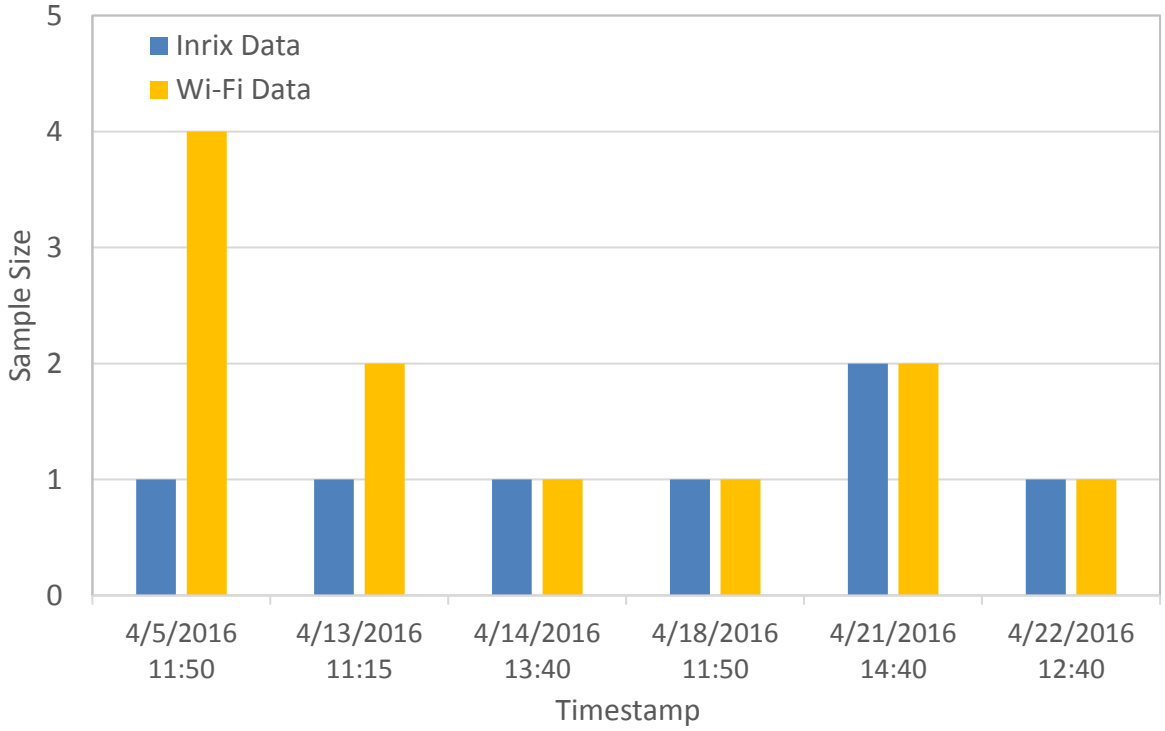

Figure A-68. Comparison of sample size for southbound right turn movement during the midday.

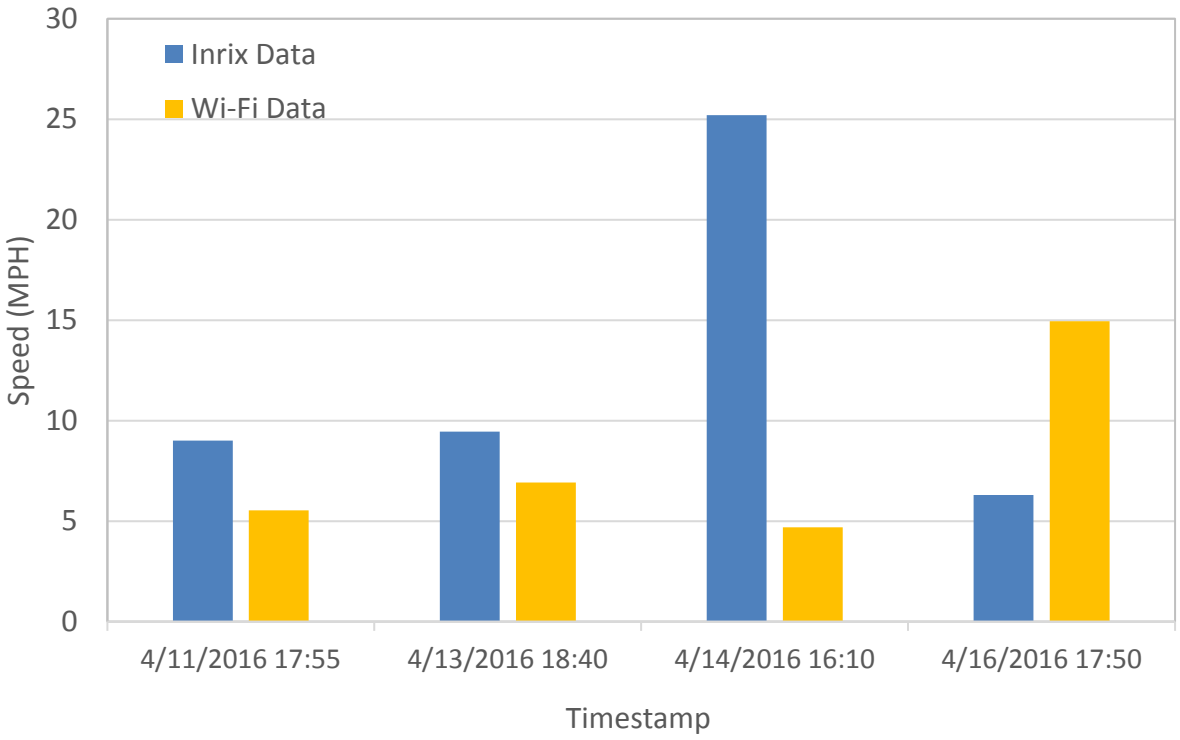

Figure A-69. Comparison of speed for southbound right turn movement during the PM peak period.

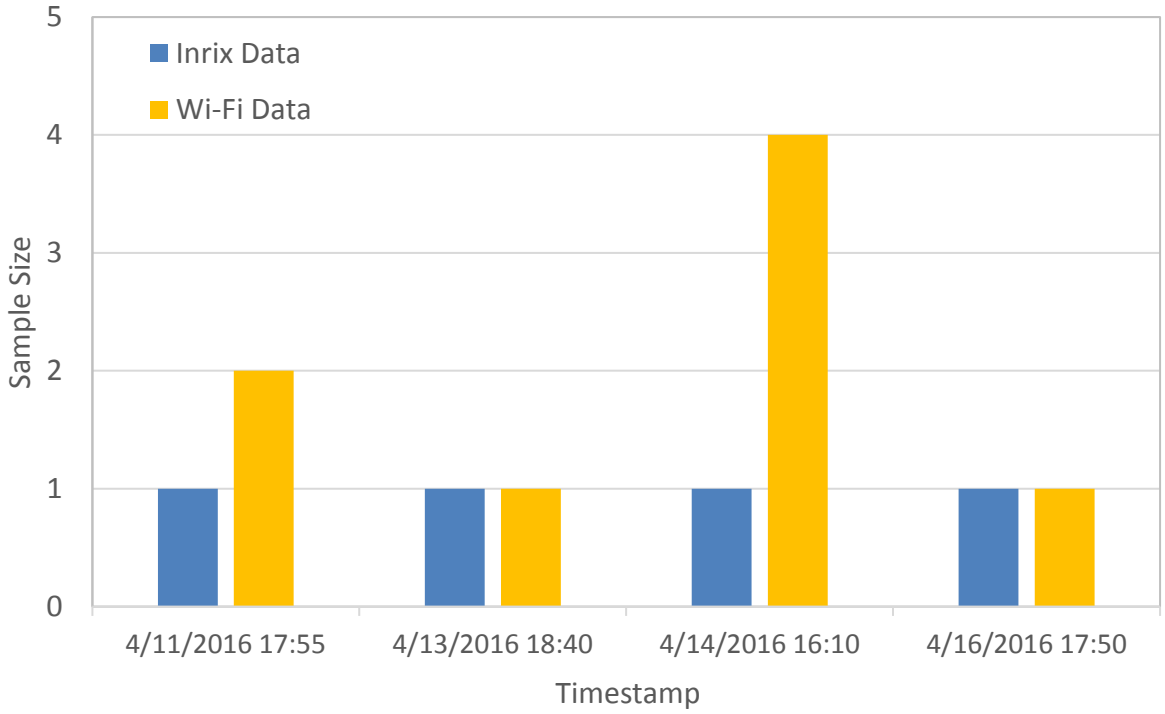

Figure A-70. Comparison of sample size for southbound right turn movement during the PM peak period.

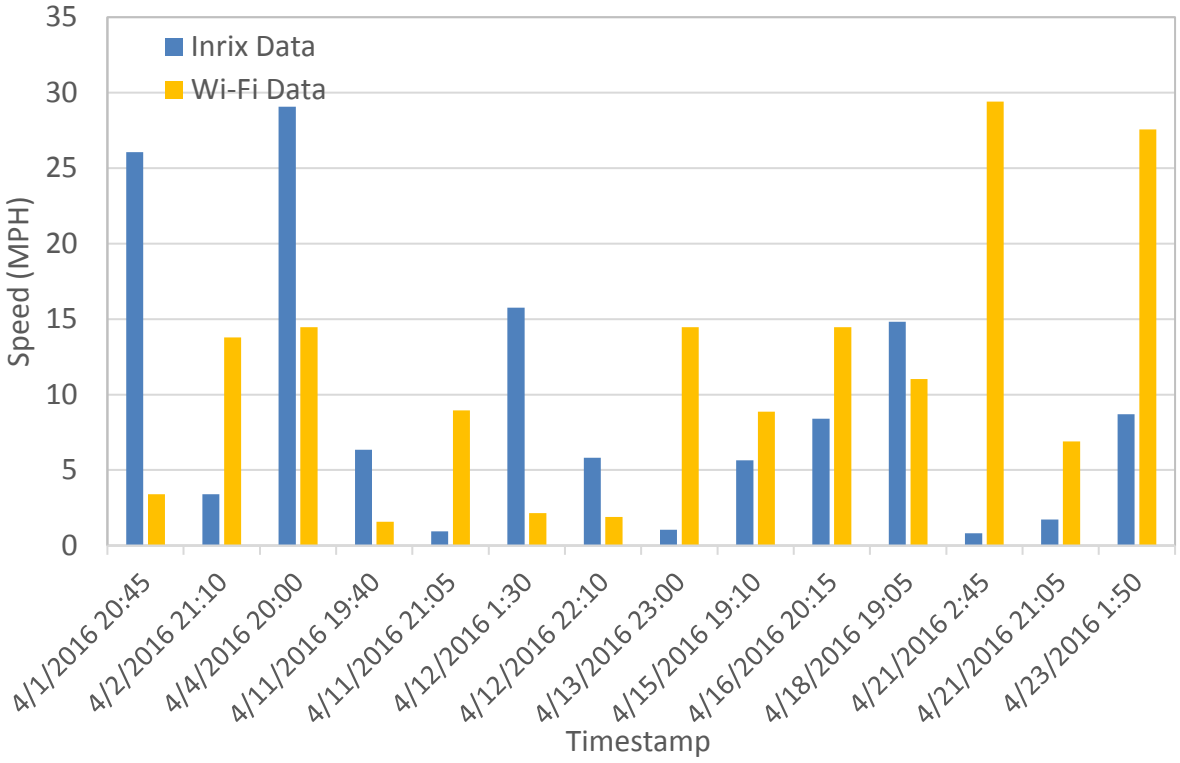

Figure A-71. Comparison of speed for southbound right turn movement during the night and early morning period.

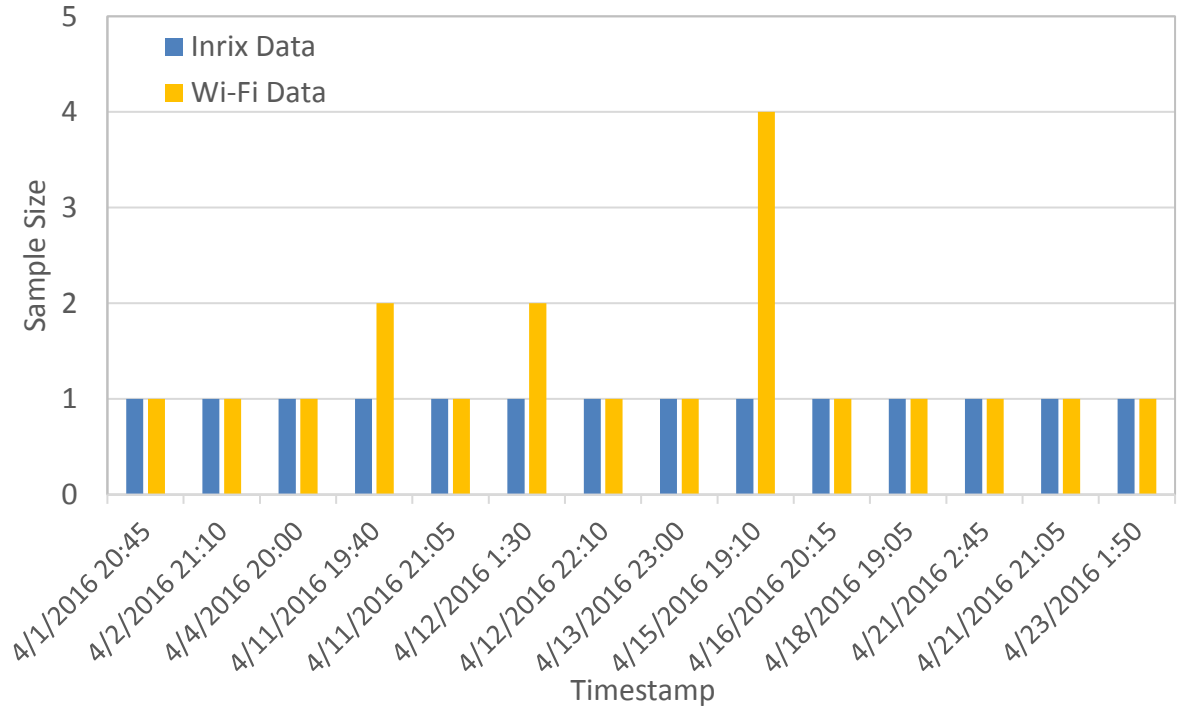

Figure A-72. Comparison of sample size for southbound right turn movement during the night and early morning period.

This page left intentionally blank.